ASSESSMENT OF NATURALLY OCCURRING RADIOACTIVE MATERIALS AND TRACE ELEMENTS IN PLAYGROUNDS OF SELECTED BASIC SCHOOLS IN THE GA EAST MUNICIPAL DISTRICT, ACCRA, GHANA

ERASTUS EIGHT TAAPOPI

(10444957)

Bachelor of Science in Physics, Geology (University of Namibia, 2012)

This thesis is submitted to the University of Ghana, Legon, in partial fulfillment of the requirements of the award of

MPhil Nuclear Science and Technology

JULY, 2015

DECLARATION

This is to certify that this thesis is the result of research work undertaken by Erastus Eight Taapopi towards the Degree of Master of Philosophy in Nuclear Science and Technology in the Department of Medical Physics, School of Nuclear and Allied Sciences (SNAS), University of Ghana, under the supervision of Prof. S.B. Dampare and Dr. A. Faanu.

…… Date: …….

Erastus Eight Taapopi

(Student)

…… Date: ……

Prof. S.B. Dampare

(Principal Supervisor)

…… Date: ……...

Dr. A. Faanu

(Co-Supervisor)

ABSTRACT

The ^{235}U, ^{232}Th series and natural ^{40}K are the main source of natural radioactivity in soil and have long half-lives up to 10^{10} years. Therefore their presence in soils and rocks is simply considered as permanent. Also due to rapid urbanization, most of Basic School playgrounds in Accra are built close to major roads or industrial areas for which they are subject to many potential pollution sources, including vehicle exhaust and industrial emissions.. A study has been carried out on playgrounds of basic schools in the Ga East municipal district in order to determine the exposure of the school children to naturally occurring radioactive materials (^{238}U, ^{232}Th and ^{40}K) and trace elements [aluminum (Al), cadmium (Cd), cobalt (Co), chromium (Cr), copper (Cu), mercury (Hg), potassium (K), lanthanum (La), manganese (Mn), sodium (Na), nickel (Ni), lead (Pb), titanium (Ti), vanadium (V), zinc (Zn)]. The activity concentrations were determined using high-purity germanium (HPGe) detector. The average activity concentrations of ^{238}U, ^{232}Th and ^{40}K determined were 19.8 ± 8.7, 29.1 ± 16.3 and 119.4 ± 97.9 $Bq.kg^{-1}$ respectively. The average annual effective dose was 0.039 ± 0.021 mSv and it is below the dose limit of 1 mSv/year recommended by International Commission on Radiological Protection (ICRP) for public exposure control. Radiological hazard assessments arising from the natural radionuclides were carried out. The average concentration of ^{222}Rn and exhalation rate were estimated to be 32.13 $kBq.m^{-3}$ and 0.016 $Bq.m^{-2}.s^{-1}$ respectively, which compared well with the world average values [78 $kBq.m^{-3}$ and 0.033 $Bq.m^{-2}.s^{-1}$ reported by (UNSCEAR, 2000)]. Soil samples were also analyzed for trace elements by Instrumental Neutron Activation Analysis and Atomic Absorption Spectrometry in order to assess the potential adverse health effects of the exposure of children to trace elements during their

games at school. Doses incurred via ingestion and inhalation and the dose absorbed through the skin were calculated using the United States Environmental Protection Agency's hourly exposure parameters for children. The toxicity values considered in this study were adapted from the Risk Assessment Information System (RAIS) compilation of United States Department of Energy (USoDE). The results of the risk assessment showed that the highest risk pathway of exposure was associated with ingestion of soil particles. It was found that the trace element of concern was As and its estimated cancer risk was found to be 3.48E-06. This can be considered insignificant since it is below the recommended trivial cancer risk value of 1.00E-05. The total hazard index was found to be 0.17, below the threshold value of 1.0. The concentrations of trace elements were also used to evaluate the level of contamination. Soil pollution evaluation was carried out by enrichment factor (EF), geo-accumulation index (I_{geo}) and contamination factor. The enrichment factor (EF) for the trace elements (As, Cd, Cr, Mn, Ni, Pb, Ti and Zn) show that the soils in the study area are uncontaminated to moderately contaminated (Zn). This indicates that some of these elements are derived from both natural and anthropogenic sources. The overall I_{geo} values have revealed that the playground soils are practically uncontaminated to moderately contaminated, whilst contamination factors indicate that the study areas are none to medium polluted. Multivariate Statistical Analyses, Principal Component and Cluster Analyses, suggest that Al, K, La, Mn and Ti are derived from crustal origin, As, Hg and Ni which are identified as a result of atmospheric pollution, Cd, Co and Na which previously identified as a result of particulate matters emitted from the geologic media. Cr, Fe and Zn are derived from both natural sources (Cu, Fe) and traffic sources (Cr, Zn) since some of the playgrounds were found to be close to the road.

Whilst Chromium (Cr) and Zinc (Zn) may have resulted from emissions of chromium-based automotive catalytic converters, cement and high Zn content in the soils may also come from traffic sources, particularly vehicle tyres.

DEDICATION

I dedicate my work to the Almighty **God** for the Gift of Life, his Blessings, and his Protection during my studies in Ghana. If it was not for Him, this project could not have been possible. I would like to dedicate this work to my parents Madam Monika Taapopi and Mr. ulius Aukongo Taapopi, as well as my great grandmothers Hileni Angula and Monika Taapopi for their words of encouragements and for keeping me in their daily prayers. To my siblings and entire family, I say thank you for inducing moral in me, thank you for having faith in me and for always believing in what I do.

To God be the Glory

ACKNOWLEDGEMENTS

First and foremost, I would like to gratefully acknowledge the International Atomic Energy Agency (IAEA), the Government of the Republic of Namibia (GRN) and University of Namibia (UNAM) for the opportunity to pursue this Master of Philosophy Degree in Nuclear Science and Technology. Their financial support/sponsorship is very much appreciated. I thank the School of Nuclear and Allied Sciences (SNAS), University of Ghana (UG) for equipping me with the requisite skills and knowledge, and for general assistance and intellectual support.

My sincere thanks goes to my experienced and trusted supervisors, Prof. S.B. Dampare and Dr. A. Faanu as well as Prof. A.W.K. Kyere (Head of Department of Medical Physics at SNAS) for all their supports, assistance, guidance and inspiration.

Thanks to Mr. David Okoh Kpeglo, a Research Scientist of the Radiation Protection Institute (RPI) of Ghana Atomic Energy Commission (GAEC), for offering me a helpful training on gamma spectrometric analysis. My sincere gratitude goes to the entire staff of the Radiation Protection Institute (RPI) Laboratory, and Neutron Activation Analysis and Atomic Absoption Spectrometry Laboratories of the National Nuclear Research Institute of the Ghana Atomic Energy Commission (GAEC) for their assistance during sample analyses.

I would like to thank Ms. Florence Esi Damali (Municipal Director of Ga East – Abokobi) and Mr. Rowland Ayisa (Personel Officer, Ga East – Abokobi) for assisting me with necessary information required for my work. I do not want to forget Mr. Emmanuel

Kwabena Owusu of SNAS for his assistance during soil sampling and my fellow students of SNAS for the knowledge shared among ourselves.

TABLE OF CONTENTS

LIST OF FIGURES

Figure **Description** **Page**

LIST OF TABLES

Table **Description** **Page**

LIST OF ABBREVIATIONS

AAS	Atomic Absorption Spectroscopy
ABS	Dermal Absorption Factor
AEDE	Annual Effective Dose Equivalent
AG	Agbogba Anglican
AH	Atomic Hills
AM	Akporman Model
AMA	Accra Metropolitan Assembly
AP	Abokobi Presby
AS	Ashongman M/A
AT	Average Time
BW	Average Body Weight
CA	Cluster Analysis
CF	Contamination Factor
CRM	Certified Reference Material
D	Absorbed dose rate in air
DA	Dome Anglican
DDREF	Dose and dose rate effectiveness factor
DNA	Deoxyribonucleic Acid
EC	Electron capture
ED	Exposure Duration
EF	Exposure Frequency also Enrichment Factor
FA	Factor Analysis
FWHM	Full Width at Half Maximum
GA	Greater Accra
GAEC	Ghana Atomic Energy Commission
GHRR-1	Ghana Research Reactor
GP	GAEC playground
GPS	Global Positioning Satellite

GRN	Government Republic of Namibia
GS	GAEC basic school
HC	Haatso calvary presby
HCA	Hierarchical agglomerative clustering
HM	Hillview Montessori
HPGe	High Purity Germanium
IAEA	International Atomic Energy Agency
ICP-AAS	Inductively Coupled Plasma Atomic Absorption Spectroscopy
ICP-MS	Inductively Coupled Plasma-Mass Spectrometry
ICRP	International Commission on Radiological Protection
I_{geo}	Geo-accumulation index
INAA	Instrumental Neutron Activation Analysis
IngR	Ingestion Rate
InhR	Inhalation Rate
IPCS	International Programme on Chemical Safety
KA	Kwabenya Atomic
KW	Kwabenya M/A
LEPS	Low-Energy Photon Spectrometers
LET	Linear Energy Transfer
LN_2	Liquid Nitrogen
LNT	Linear-Non-Threshold
MATLAB	Mathematics laboratory
MCA	Multi-Channel Analyzer
NORMs	Naturally Occurring Radioactive Materials
PCA	Principal Component analysis
PEF	Particle Emission Factor
RAIS	Risk Assessment Information System
RM	Reference Material
RPI	Radiation Protection Institute
SA	Exposured skin area

SL	Skin adherence factor
SNAS	School of Nuclear and Allied Science
SPSS	Scientific package for the social sciences
TC	Taifa Community
TD	Taifa St Dominic
TEs	Trace Elements
UG	University of Ghana
UNAM	University of Namibia
UNSCEAR	United Nations Scientific Committee on the Effect of Atomic Radiation
USDoE	United States Department of Energy
USEPA	United States Environmental Protection Agency
VF	Volatilization Factor
VGA	Vapor Generation Accessory
WHO	World Health Organization
WNA	World Nuclear Association

CHAPTER 1

INTRODUCTION

This chapter gives an overview of exposure of natural ionizing radiation, and briefly discusses the statement of the problem, objectives of the study, justification/relevance as well as scope and limitation of the study.

1.1. Background

Radionuclides are present everywhere in the natural environment (Aguko, 2013). The main natural contributors to external exposure from gamma-radiation are the uranium and thorium series, together with potassium-40 (^{40}K) which may be present in small quantities on the surface of the earth (Aguko, 2013; Faanu et al., 2012). Long-lived radioactive elements such as uranium, thorium and potassium and their decay products, such as radium and radon are examples of Naturally Occurring Radioactive Materials (NORMs). These elements have always been present in the earth's crust and atmosphere since the beginning of creation.

The ^{238}U and its daughters rather than ^{226}Ra and its daughter products are responsible for the major fraction of the internal dose received by humans from naturally occurring radionuclides. Even though the concentrations of these radionuclides are widely distributed in nature, they have been found to depend on the local geological conditions and as a result vary from place to place (Faanu et al., 2011; Baba et al., 2004). This is because the specific levels are related to the type of rocks from which the soil originates. Throughout the history of life on earth, organisms have been continuously exposed to radiation mainly from cosmic rays in the atmosphere, and from naturally occurring radionuclides which are ubiquitously distributed in all living and non-living

components of the biosphere . A wide range of activity concentrations in a wide variety of materials is reported (IAEA, 2011).

Also, trace elements such as As, Cd, Co, Cr, Cu, Hg, Pb and Zn that are found in soil are known persistent environmental pollutants. The presence of these elements in the environment could be as a result of pollution from different sources in urban areas. It has been identified that vehicular and atmospheric pollution is a major contributor to trace elements contamination (Baba et al., 2004). Although some trace metals such as Cu and Zn at small amounts are harmless, others notably Pb, Hg and Cd could be extremely harmful at low concentrations. These toxic elements are potential co-factors, and known as initiators or promoters of many diseases including cardiovascular diseases and cancer (Meza-Figueroa, 2007).

Others sources of pollution of environment from these elements are particulate matter emitted from the geologic media and may pose threats to human health and the environment (Meza-Figueroa, 2007). Anthropogenic particles derived from road construction (asphalt, concrete and road paint), automobiles (tire dust, brake dust), industrial inputs or atmospheric depositions are potential sources of pollution. All these anthropogenic activities tend to have introduced contaminants in topsoil from atmospheric deposition by sedimentation, impaction and interception (Baba et al., 2004). And as time goes by, dust can be carried by wind into sensitive environments. Lead (Pb) and a variety of other metals from automobile exhaust have been found to contaminate roadways (Baba et al., 2004). This is particularly of concern for schools along the roads with bare playgrounds since children whilst playing inhale dust which could be polluted with significant levels of trace metals including radionuclides. As a result of poor waste

management practices and poor observance of environmental regulations, environmental pollutants [such as lead (Pb) from paints, buning of plastics and paper, mercury (Hg) from electronics, plastic waste, pesticides, pharmaceutical and dental waste, cadmium (Cd) from electronics, plastics and batteries waste] could be littered all around. All these could eventually find their way into these bare playgrounds for the children in these schools and could pose serious health hazards in the long term. In the Ga East Municipal of the Greater Accra Region, there are thirty one (31) public Basic Schools in total that are registered within their respective five (5) circuits. Preliminary survey of the schools shows that there are fourteen (14) schools with bare lands, and children population in these schools range from 48 to 560 pipils.

A large body of knowledge has been developed over the last decades on the exposure of children to particulate materials such as soil and street dust. This is driven by the realization that children are the most sensitive segment of the population to anthropogenic contamination. Also by the strong indication that toxic trace elements may reach concentrations of potential concern for human health in the environments (De Miguel et al., 2007). Specifically, some researchers have looked at the chemical composition of playground soil and dust (De Miguel et al., 2007). According to De Miguel et al, (2007), the exposure of children to trace elements is particularly high relative to the kind of activities in the surroundings and types of games they play.

1.2. Statement of the Problem

Trace elements and naturally occurring radioactive materials (NORMs) are commonly found in soil at varying concentrations. Their levels in soil are largely controlled by geological factors and potential pollution from different sources. In most developing

countries, including Ghana, it is very common to find schools with very large population with bare playgrounds with no or very little knowledge of the extent of pollution of the soil of these playgrounds. However, because in our society the issues of environmental quality is sometimes relegated to the background, impact assessment of these school compounds are not carried out to ascertain the radiation levels as well as trace element contents by the authorities concerned before school enrollments. This is particularly of concern where the ground of the school compound is bare and there is constant inhalation of dust.

Meanwhile, the radiological and trace elements hazards of these playgrounds have not been investigated and as a result, the levels of exposure are unknown. Consequently, this study is being conducted to assess the levels of [aluminum (Al), cadmium (Cd), cobalt (Co), chromium (Cr), copper (Cu), mercury (Hg), potassium (K), lanthanum (La), manganese (Mn), sodium (Na), nickel (Ni), lead (Pb), titanium (Ti), vanadium (V), zinc (Zn)] and health risk associated with their exposure levels. This is because the exposure to children may lead to development of potential health consequences such as cancer. Generally, children are more susceptible to air pollutants than adults because children breathe higher volumes of air relative to their body weights and their tissue and organs are still growing. Small particles are associated with higher pollutant concentrations and these are the particles that children are most likely to inhale or ingest while playing outdoors. It is a known fact that young children are more likely to ingest significant quantities of dust than adults because of the behavior of mouthing non-food objects and repetitive hand/finger sucking. Besides, children have a much higher absorption rate of

heavy metals from digestion system and higher hemoglobin sensitivity to trace elements than adults.

1.3. Objectives

1.3.1. Primary Objectives

The purpose of this study is to assess naturally occurring radioactive materials (^{40}K and radionuclides from the ^{238}U and ^{232}Th decay series) and trace metals in soil from selected school playgrounds in the Ga East Municipal of Ghana in order to appraise their potential exposure to school children.

1.3.2. Specific Objectives

- To assess activity concentrations of natural radionuclides in selected basic schools play grounds.
- Develop a model for prediction of future exposure due to NORMs
- To evaluate soil pollution using enrichment factor (EF), geo-accumulation index (I_{geo}), contamination factor (CF)
- To embark on risk-based evaluation of the exposure of school children to trace elements in the playgrounds

1.4. Relevance and Justifications

The data from this study will serve as baseline research/data for monitoring natural radionuclides and trace elements levels in school playgrounds in Ghana and Ga East district in particular. The research data can be used for development of control and environmental protection strategy by providing information on the degree and spatial

distribution of trace elements pollution of the school playgrounds. This will serve as reference for authorities' regulation purposes in Ghana, and help develop management strategy for protecting children's health. The study also demonstrates the importance of multivariate statistical tools in routine monitoring of trace elements pollution of playgrounds of basic schools.

1.5. Scope of the study

The work is limited to assessment of NORMs and trace elements in playgrounds of selected basic schools. This was achieved by determining the levels and distribution of the naturally occurring radionuclides ^{40}K as well as ^{238}U and ^{232}Th decay series radionuclides. Soil samples were collected from selected school playing grounds and analyzed by gamma spectrometry using a high purity germanium detector (HPGe detector) for NORMs. For trace elements, the analysis was done by using instrumental neutron activation analysis (INAA) and atomic absorption spectrometry (AAS). A short MATLAB script was written for the prediction of future exposures arising from external gamma radiation.

CHAPTER 2

LITERATURE REVIEW

This chapter gives a general review of natural radiation background in the terrestrial environment, radionuclides decay series, as well as a review of other research works that have been done in the subject area of naturally occurring radionuclides and trace elements in soils of basic schools play grounds. The detector system and setup and biological effects of ionizing radiation and trace elements are also briefly discussed.

2.1. Naturally Occurring Radiation and Man-made Radiation

Natural background radiation exists everywhere and every natural substance contains some amount of radioactive material. The natural radiation environment consists of cosmic rays and naturally radioactive materials (Gupta et al., 2010). Some of the materials are cosmogenic, others are primordial and others exist naturally because of the radioactive transformation of substances produced through these processes. The radiological significance of naturally occurring radioactive materials and radiation sources is closely linked to the physical behaviour of the materials in the source and how they change with time (James, 2006).

2.1.1. Cosmogenic Radiation

The cosmogenic radiation is the oldest source of radiation, which is believed to have originated at the birth of the universe, about 13–14 billion years ago (Cember, 2009). The earth is bombarded continuously by radiation originating from the sun, and from sources within and beyond the galaxy. This cosmic radiation slams into the earth's upper atmosphere which provides an effective shield for living things below (James, 2006). Cosmic irradiation of the atmosphere produces neutrons and protons which react with N_2,

O_2, Ar and other atoms resulting in the production of radioactive nuclides. These nuclides are produced at constant rates and brought to the earth surface by rain water. Though they are formed in very low concentrations, the global inventory is by no means small (Choppin, 2002). Equilibrium is assumed to be well-known between the production rate and the mean residence time of these radionuclides in terrestrial basins leading to constant specific radioactivities of the elements in each reservoir. If a reservoir is closed from the environment, its specific radioactivity declines. This can be used to determine exposure times of meteorites to cosmic radiation (Choppin et al., 2002). Table 2.1 contains some of the cosmogenic radionuclides produced as a result of the cosmic radiation interaction with the atmosphere.

Table 2.1: Long-lived cosmogenic radionuclides appearing in meteorites and rain water (Choppin et al., 2002)

Nuclide	Half-life (years)	Decay Mode & particle energy (MeV)	Atmospheric production rate (atoms $m^{-2}s^{-1}$)
^{3}H	12.32	β^- 0.0186	2500
^{10}Be	1.52×10^6	β^- 0.555	300
^{14}C	5715	β^- 0.1565	17000 – 25000
^{22}Na	2.605	β^+ 0.545	0.5
^{26}Al	7.1×10^5	β^+ 1.16	1.2
^{32}Si	160	β^- 0.213	1.6
^{35}S	0.239 (87.2 d)	β^- 0.167	14
^{36}Cl	3.01×10^5	β^- 0.709	60
^{36}Ar	268	β^- 0.565	56
^{53}Mn	3.7×10^6	EC (0.596)	
^{81}Kr	2.2×10^5	EC (0.28)	

Values within parenthesis after EC are decay energies.

2.1.2. Primordal Radionuclides

Many of the naturally occurring radioactive elements are participants of one of four long chains, or radioactive series, stretching through the last part of the chart of the nuclides.

There are four main radioactive decay series, namely the Uranium (4n+2), Thorium (4n), Actinium (4n+3), and Neptunium (4n+1) series. Th-232 is the most abundant (about 100%) of the naturally occurring radioisotopes. The identification numbers are based on the divisibility of the mass numbers of each of the series by 4 (Cember, 2009; James, 2006). With the exception of neptunium, each of the parent radionuclides is primordial in origin because they are so long lived that they still exist some 4.5 billion years after the solar system was formed (James, 2006).

Uranium consists of three different isotopes; about 99.3% of naturally occurring uranium is ^{238}U, about 0.7% is ^{235}U, and a trace quantity (about 5×10^{-3} %) is ^{234}U. The ^{238}U and ^{234}U belong to one family, the uranium series, while the ^{235}U isotope of uranium is the first member of another series called the actinium series(Herman Cember & Johnson, 2009; Choppin et al., 2002). Uranium is ever-present in the natural environment and is found in the soil at average concentrations of about 3 ppm (parts per million) by weight, which corresponds to~2 pCi or ~74 mBq/g soil (Cember, 2009).

The first series is the thorium decay series, consisting of radionuclides going through the decay in which all the mass numbers are divisible by four (the 4n series). It has its natural origin in^{232}Th which occurs with 100 % isotopic abundance. Natural thorium has a specific activity of 4.06 MBq/kg, as its half-life through a-decay is 1.41 x 1010 y (Choppin et al., 2002). The final nuclide in this decay series is the stable species. The breakdown from the original parent to the final product requires 6 alpha and 4 beta decays. The longest-lived intermediate is 5.76 y ^{228}Ra (Cember & Johnson, 2009; Choppin et al., 2002). The uranium decay series consist of nuclides that, when their mass number is divided by 4, have a remainder of 2 (the 4n + 2 series). The parent of this

series is ^{238}U with a natural abundance of 99.3 % it undergoes a-decay with a half-life of 4.46 x 109 y. The stable end product of the uranium series is ^{206}Pb which is reached after 8 alpha and 6 beta decay steps (Choppin et al., 2002).

Table 1.2: Thorium series (4n) (Cember & Johnson, 2009)

		ENERGY (MEV)		
NUCLIDE	**HALF-LIFE**	**ALPHA[a]**	**BETA**	**GAMMA (PHOTONS/TRANS.)[b]**
$^{232}_{90}Th$	1.39 x 10^{10} years	3.98		
$^{228}_{88}Ra$ (MsTh1)	6.7 yrs		0.01	
$^{228}_{89}Ac$ (MsTh2)	6.13 h		Complex decay scheme Most intense beta group is 1.11 MeV	1.59 (n.v) 0.966 (0.2) 0.908 (0.25)
$^{228}_{90}Th$ (RdTh)	1.91 yrs	5.421		0.084 (0.016)
$^{224}_{88}Ra$ (ThX)	3.64 yrs	5.681		0.241 (0.038)
$^{220}_{86}Rn$ (Tn)	52 s	6.278		0.542 (0.0002)
$^{216}_{82}Po$ (ThA)	0.158 s	6.774		
$^{212}_{82}Pb$ (ThB)	10.64 h		0.35, 0.59	0.239 (0.40)
$^{212}_{83}Bi$ (ThC)	60.5 min	6.086 (33.7%)	2.25 (66.3%)[c]	0.04 (0.034 branch)
$^{212}_{84}Po$ (ThC')	3.04 x 10^{-7} s	8.776		
$^{208}_{81}TI$ (ThC")	3.1 min		1.80, 1.29, 1.52	2.615 (0.997)
$^{208}_{82}Pb$ (ThD)	Stable			

Table 2.3: Neptunium series (4n +1) (Herman Cember & Johnson, 2009)

NUCLIDE	HALF-LIFE	ENERGY (MEV)		
		ALPHA[a]	BETA	GAMMA (PHOTONS/TRANS.)[b]
$^{241}_{94}Pu$	13.2 yrs		0.02	
$^{241}_{95}Am$	462 yrs	5.496		0.060 (0.4)
$^{237}_{93}Np$	2.2 x 10^6 yrs	4.77		
$^{233}_{91}Pa$	27.4 d		0.26, 0.15, 0.57	0.31 (very strong)[c]
$^{233}_{92}U$	1.62 x 10^5yrs	4.823		0.09 (0.02) 0.056 (0.02) 0.042 (0.15)
$^{229}_{90}Th$	7.34 x 10^3 yrs	5.02		
$^{225}_{88}Ra$	14.8 d		0.32	
$^{225}_{89}Ac$	10.0 d	5.80		
$^{221}_{87}Fr$	4.8 min	6.30		0.216 (1)
$^{217}_{85}At$	0.018 s	7.02		
$^{213}_{83}Bi$	47 min	5.86 (2%)[d]	1.39 (98%)[d]	
$^{213}_{84}Po$	4.2 x 10^{-6} s	8.336		
$^{209}_{81}TI$	2.2 min		2.3	0.12 (weak)[c]
$^{209}_{82}Pb$	3.32 h		0.635	
$^{209}_{83}Bi$	Stable			

Table 2.4: Uranium series (4n+2) (Cember & Johnson, 2009)

		ENERGY (MEV)		
NUCLIDE	**HALF-LIFE**	**ALPHA[a]**	**BETA**	**GAMMA (PHOTONS/TRANS.)[b]**
$^{238}_{92}U$	4.51 x 10^9 yrs	4.18		
$^{434}_{90}Th$ (U X_1)	24.10 d		0.193, 0.103	0.092 (0.040) 0.063 (0.03)
$^{234}_{91}Pa$ (U X_2)	1.175 min		2.31	1.0 (0.015) 0.76 (0.0063), I.T.
$^{234}_{91}Pa$ (UZ)	6.66 h		0.5	Many (weak)
$^{234}_{92}U$ (UII)	2.48 x 10^5 yrs	4.763		
$^{230}_{90}Th$ (I_0)	8.0 x 10^4 yrs	4.685		0.068 (0.0059)
$^{230}_{90}Ra$	1.622 yrs	4.777		
$^{222}_{86}Em$ (Rn)	3.825 d	5.486		0.51 (very weak)
$^{218}_{84}Po$ (RaA)	3.05 min	5.998 (99.978%)[c]	Energy not known (0.022%)[c]	0.186 (0.030)
$^{218}_{85}At$ (RaA')	2 s	6.63 (99.9%)[c]	Energy not known (0.15)[c]	
$^{218}_{86}Em$ (RaA")	0.019 s	7.127		
$^{214}_{82}Pb$ (RaB)	26.8 min		0.65	0.352 (0.036) 0.295 (0.020) 0.242 (0.07)
$^{214}_{83}Bi$ (RaC)	19.7 min	5.505 (0.04%)[c]	1.65, 3.7 (99.96%)[c]	0.609 (0.295) 1.12 (0.131)
$^{214}_{84}Po$ (RaC')	1.64 x 10^{-4} s	7.680		
$^{210}_{81}TI$ (RaC")	1.32 min		1.96	2.36 (1) 0.783 (1) 0.297 (1)
$^{210}_{82}Pb$ (RaD)	19.4 yrs		0.017	0.0467 (0.045)
$^{210}_{83}Bi$ (RaE)	5.00 d		1.17	
$^{210}_{84}Po$ (RaF)	138.40 d	5.298		0.802 (0.000012)
$^{206}_{82}Pb$ (RaG)	Stable			

Table 2.4: Actinium series (4n +3) (Cember & Johnson, 2009)

NUCLIDE	HALF-LIFE	ENERGY (MEV)		
		ALPHA[a]	BETA	GAMMA (PHOTONS/TRANS.)[b]
$^{235}_{92}U$	7.13 x 10^8 yrs	4.39		0.18 (0.7)
$^{231}_{90}Th$ (U Y)	25.64 h		0.094, 0.302, 0.216	0.022 (0.7) 0.0085 (0.4) 0.061 (0.16)
$^{231}_{91}Pa$	3.43 x 10^4 yrs	5.049		0.33 (0.05) 0.027 (0.05) 0.012 (0.01)
$^{227}_{89}Ac$	21.8 yrs	4.94 (1.2%)[a]	0.0455 (98.8%)[c]	
$^{227}_{90}Th$ (RdAc)	18.4 d	6.03		0.24 (0.2) 0.05 (0.015)
$^{223}_{87}Fr$ (AcK)	21 min		1.15	0.05 (0.40) 0.08 (0.24)
$^{223}_{88}Ra$ (AcX)	11.68 d	5.750		0.270 (0.10) 0.155 (0.055)
$^{219}_{86}Em$ (An)	3.92 s	6.824		0.267 (0.086) 0.392 (0.048)
$^{215}_{84}Po$ (AcA)	1.83 x 10^{-3} s	7.635		
$^{211}_{82}Pb$ (AcB)	36.1 min		1.14, 0.5	Complex spectrum, 0.065-0.829 MeV
$^{211}_{83}Bi$ (AcC)	2.16 min	6.619 (99.68)[c]	Energy not known (0.32)[c]	0.35 (0.14)
$^{211}_{84}Po$ (AcC')	0.52 s	7.434	0.65	0.88 (0.005) 0.56 (0.005)
$^{207}_{81}TI$ (AcC")	4.78 min		1.47	0.87 (0.005)
$^{207}_{82}Pb$	Stable			

2.1.3. Radon

Radon is a gas with three natural isotopes of the radioactive element: actinon, (^{219}Rn) emitted from the ^{235}U decay series, thoron (^{220}Rn) emitted from the ^{232}Th decay series, and radon (^{222}Rn) which is emitted from the ^{238}U decay series (UNSCEAR, 1993).

Since the activity concentration of ^{235}U is low and the half-life of ^{219}Rn is short (3.96 s), the radiation exposure from ^{219}Rn is considered not to be significant for human exposure. Whilst ^{220}Rn with a half-life of 55.6 s is of concern only when the concentration of ^{232}Th is high, the ^{222}Rn with a half-life of 3.82 days is the isotope of concern in terms of human radiation exposure. It is a noble gas with slightly chance to form compounds under laboratory conditions. The density of ^{222}Rn is 9.73 g/L at 0 ^{o}C and the solubility in water at 0 ^{o}C is 510 cm^3/L, decreasing to 220 cm^3/L at 25 ^{o}C and 130 cm^3/L at 50 ^{o}C (Faanu, 2011; UNSCEAR, 2000).

The production of ^{220}Rn and ^{222}Rn in terrestrial materials is based on the activity concentrations of ^{228}Ra and ^{226}Ra present and these are predominantly alpha emitters. Radon is the most significant element of human irradiation by natural sources through inhalation of its short-lived products of ^{210}Pb and ^{210}Po (UNSCEAR, 1993, 2000).

The concentrations of ^{222}Rn in surface air vary with time-average concentrations in the range of 2-30 Bq/m^3 (UNSCEAR, 1993). In the soil, radon concentrations may be higher by a factor of about 1000 than in the open air, and the average concentration varies widely depending on the composition of the soil and the bedrock (UNSCEAR, 1993). For soil with an average ^{226}Ra concentration of 40 $Bq.kg^{-1}$, the average ^{222}Rn concentration in the soil water would be about 60 Bq/m^3. The action level of radon recommended by the ICRP for which intervention is necessary is 1000 Bq $/m^3$. This value is based on an assumed occupancy of 2000 hours per year and this is equivalent to an effective dose of 6 mSv per year. This value is also the midpoint of a range of 500-1500 Bq/m^3 (Faanu, 2011). Radon generation and transport in porous materials involves solid, liquid and gaseous phases through the process of emanation,

diffusion, advection, absorption in the liquid phase and adsorption in the solid phase (Faanu, 2011). The main mechanism for radon entry into the atmosphere is molecular diffusion.

Some factors that may influence the levels of ^{222}Rn concentration in soil, water and air include the following (Faanu, 2011):

- Grain or particle and shape determine the emanation of radon from the soil. The emanation factor is inversely proportional to the grain size.
- Soil moistures control the emanation of radon and diffusion in soil by capturing the radon recoils from the solid matrix.
- Advection caused by wind and changes in barometric pressure between the building shield and the ground around the foundation.
- Temperature, the solubility of radon in water decreases with temperature.
- The geology, which determines the ^{226}Ra concentration and climatic conditions.
- The distribution and concentrations of the parent radium radionuclides in the bedrock and overburden and permeability of the soil.
- Seasonal variation because ^{222}Rn in soil gas vary over many orders of magnitude from place to place and also show a significant time variations at any given site.

2.2. Anthropogenic Radioactivity

As far as the analysis of a sample is concerned for its content of natural radioactivity, it is necessary to have a look at the possibility that the sample may be contaminated by non-natural radioactivities. Radionuclides may be added to the environment by human

activities, and these are called anthropogenic sources. The cases of nuclear weapons tests, nuclear satellites burnt-up in the atmosphere, and nuclear power accidents have released significant amounts of activities into the environment. The nuclear power industry is permitted by health authorities to continually release small, controlled amounts of specified radionuclides into the atmosphere and into open waters (Choppin et al., 2002). Usually, one distinguishes between near field and far field effects of radioactivity releases. Near field effects are observed close to the release source, with examples being the nuclear power plant or nuclear waste storage facility. The dissolution of nuclear waste by rain or ground water is a typical near field problem. Since the source is known, it can be controlled and the environment can be monitored. If the radioactivity exceeds permitted levels, access to the contaminated area is restricted. Far field effects involve the behaviour of radionuclides which have spread out of such a restricted area, caused either by nuclear power accidents and weapons tests or by leakage from nuclear power plants (Choppin et al., 2002). However, some of these cases are sometimes known and contaminated areas are regulated.

Table 2.6: Events leading to large injection of radionuclides into the atmosphere (Choppin et al., 2002)

SOURCE	COUNTRY	TIME	RADIOACTIVITY (Bq)	IMPORTANT NUCLIDES
Hiroshima &Nagasaki	Japan	1945	4×10^{16}	Fission production. Actinides
Atmospheric weapon tests	USA USSR	-1963	2×10^{20}	Fission production. Actinides
Windscale	Uk	1957	1×10^{15}	^{131}I
Chelyabinsk (Kysthym)	USSR	1957	8×10^{16}	Fission production. ^{90}Sr, ^{137}Cs
Harrisburg	USA	1979	1×10^{12}	^{137}Cs
Chernobyl	USSR	1986	2×10^{18}	^{137}Cs
Fukushima	Japan	March, 2011	1×10^{18}	^{137}Cs, ^{131}I

2.3. External Exposure (outdoors)

External exposures outdoors arise from terrestrial radionuclides present at trace levels in all soils (Faanu et al., 2012; UNSCEAR, 2000). Higher radiation levels are associated with igneous rocks, such as granite, and lower levels with sedimentary rocks. There are exceptions, however, as some shales and phosphate rocks have relatively high content of radionuclides. There have been many surveys to determine the background levels of radionuclides in soils, which can in turn be related to the absorbed dose rates in air (UNSCEAR, 2000). The latter can easily be measured directly, and these results provide an even more extensive evaluation of the background exposure levels in different countries. Table 2.7 provides information regarding the abundance of radionuclides in different natural materials (IAEA, 2003), which is a summary of typical concentrations of radionuclides in different geological media. The radionuclides in the uranium and

thorium decay chains cannot be assumed to be in radioactive equilibrium. The isotopes ^{238}U and ^{234}U are in approximate equilibrium, as they are separated by two much shorter-lived nuclides, ^{234}Th and ^{234}Pa. The decay process itself may, however, allow some dissociation of the decayed radionuclide from the source material, facilitating subsequent environmental transfer.

Table 2.7: Abundance of major radionuclides in different rock types and soils (IAEA, 2003)

Rock type	40K		232Th		238U	
	Total K (%)	Bq/kg	ppm	Bq/kg	Ppm	Bq/kg
Igneous rocks						
Basalt, crustal average	0.8	300	3 to 4	10 to 15	0.5 to 1	7 to 10
Mafic	0.3 to 1.1	70 to 400	1.6, 2.7	7, 10	0.5, 0.9	7, 10
Salic	4.5	1100 to 1500	16, 20	60, 83	3.9, 4.7	50, 60
Granite, crustal average	> 4	> 1000	17	70	3	40
Sediment rocks						
Shale, sandstones	2.7	800	12	50	3.7	40
Clean quartz	< 1	< 300	< 2	< 8	< 1	< 10
Dirty quartz	2?	400?	3 to 6?	10 to 25?	2 to 3?	40?
Arkose (unconsolidated)	2 to 3	600 to 900	2?	< 8	1 to 2?	10 to 25?
Beach sands (unconsolidated)	< 1	< 300?	6	25	3	40
carbon rocks	0.3	70	2	8	2	25
Continental upper crust (average)	2.8	850	10.7	44	2.8	36
Soils	1.5	400	9	37	1 to 8	66

Note: Question marks indicate estimates in the absence of measured values.

Hence, ^{234}U may be somewhat deficient relative to ^{238}U in soils (UNSCEAR, 2000; Vanmarcke, 2002). The radionuclide ^{226}Ra in this chain may have slightly different concentrations as compared to ^{238}U, because separation may occur between its parent ^{230}Th and uranium and because radium has greater mobility in the environment (UNSCEAR, 2000). The decay products of ^{226}Ra include the gaseous element radon, and it diffuses out of the soil, reducing the exposure rate from the parent radionuclide ^{238}U. The radon radionuclide in this series, ^{222}Rn, has a half-life of only a few days, but it has two longer-lived decay products, ^{210}Pb and ^{210}Po which are important in dose evaluations.

2.4. Hazards Associated with NORMs

The exposure to ionizing radiation depends on the magnitude of dose absorbed, the time period, the dose rate as well as the specific organ that is exposed. The inhalation of short-lived decay products of ^{222}Rn, and the decay products of ^{220}Rn, and their successive deposition along the walls of the various airways of the bronchial tree provide the main pathway for radiation exposure of the lungs. This exposure is mostly produced by the alpha particles emitted by several of these radionuclides, although some beta particles and gamma radiation are also emitted.

Biological effects of ionizing radiation in humans, due to physical and chemical processes, occur immediately following the passage of radiation through living matter. These processes will involve successive changes at the molecular, cellular, tissue and whole organism levels. For acute whole-body exposures above a few gray from radiation of low linear energy transfer (LET), damage occurs principally as a result of cell killing. This can cause damage to organ and tissue and even death. These effects, termed early or

deterministic, occur principally above a threshold dose that must not be exceeded (UNSCEAR, 2000). A second type of damage can occur at late times after exposure (stochastic effects). This damage consists primarily of damage to the nuclear material in the cell, causing radiation-induced cancer to develop in a proportion of exposed persons or hereditary disease in their offspring.

2.5. Trace Elements (TEs)

The trace elements that have been studied most extensively in soils are those that are essential for the nutrition of higher plants such as B, Cu, Fe, Mn, Mo, and Zn (Domy, 2001). Similarly, those extensively studied in plants and foodstuffs because of their essentiality for animal nutrition are such as As, Cu, Co, Fe, Mn, Mo, Zn, Cr, F, Ni, Se, Sn, and V. Conversely, this study intends to observe a wide range of all trace metals (carcinogenic and non-carcinogenic) in the soils of basic school playgrounds.

The term trace element used in the literature has different meanings in various scientific disciplines. Often it designates a group of elements that occur in natural systems in minute concentrations (Adriano et al., 1986 ; Domy, 2001). Also, it is defined as those elements used by organisms in small quantities but believed to be essential to their nutrition. According to Kabata (2010), trace element concentrations significantly differ among both soil groups and geographic regions. This indicates that parent material and climatic conditions have predominated impact on the trace elements status of soils. In this study, trace elements are referred to elements that occur both in natural and by human activities and perturbed environments in small amounts, but when present in adequate bioavailable concentrations, they become toxic to living organisms. Other terms such as trace metals, heavy metals, micronutrients, microelements, and minor elements are

commonly used as synonyms for trace elements. The trace elements considered in this study are: arsenic (As), cadmium (Cd), cobalt (Co), chromium (Cr), copper (Cu), mercury (Hg), manganese (Mn), nickel (Ni), lead (Pb), vanadium (V), lanthanum (La), potassium (K), Alminium (Al), Titanium (Ti), sodium (Na), iron (Fe) and zinc (Zn). Moreover, the term heavy metals usually refers to elements having densities greater than 5.0 $g.cm^{-3}$ and signifies metals and metalloids that are associated with pollution and toxicity but also includes elements that are required by organisms at rather low concentrations (Domy, 2001).

2.5.1. Sources of Trace Elements

Natural sources of trace elements are found in both mineral and in the form of organic chelates (Shakeri et al., 2009). Most raw minerals (such as rock phosphate, greensand, granite dust and basalt) are rich in trace elements. Organic sources include composts, manures and green manures, but the trace mineral content of these sources will vary, depending on how much of these elements were in the environment where the sources were originally formed.

Besides, trace metals may also come from many different sources especially in urbanized areas (Li, Poon, & Liu, 2001; Shakeri et al., 2009). These anthropogenic inputs include waste disposal, waste incineration, urban effluent, traffic emissions (Shakeri et al., 2009). Atmospheric pollution is one of the major sources of trace elements contamination and can accumulate in top soil. It is believed that Cd, Cu, Pb and Zn are good indicators of contamination in soils because they appear in gasoline, car components, oil lubricants, industrial and incinerator emissions (Li et al., 2001).

2.6. Hazards Associated with Trace Elements

Potential hazards associated with trace elements are related to their accumulation in soils (Hagedorn et al., 1999). The elements of primary concern are arsenic, cadmium, copper, mercury, nickel, lead and zinc. Acute inhalation exposure to high levels of trace elements in humans may have effects on the lung, such as bronchial and pulmonary irritation and can even result in long-lasting impairment of lung function (IPCS, 2002; US EPA.). Children are known to be more vulnerable to these effects as they undergo cell divisions through their growth processes (Almeida et al., 2011; De Miguel et al., 2007; Wong & Mak, 1997).

2.7. Review of NORMs and TEs in Soils

The average dose received by all human from background radiation is around 2.4 mSv/yr, that varies depending on the geology and altitude where people live and it ranges between 1 and 10 mSv/yr, but can be more than 50 mSv/yr (UNSCEAR, 1993, 2000). The highest recorded level of background radiation affecting a substantial population is in Kerala and Madras States in India where some 140,000 people received doses which averaged over 15 millisievert per year from gamma radiation, in addition to a similar dose from radon (WNA, 2011). Comparable levels occur in Brazil and Sudan, with average exposures up to about 40 mSv/yr to many people. Also , another highest level of natural background radiation recorded is on a Brazilian beach: 800 mSv/yr, although people do not live there (WNA, 2011).

Other places in Iran, India and Europe (WNA, 2011) are noted for the natural background radiation that gives an annual dose of more than 100 mSv to people and up to 260 mSv (at Ramsar in Iran, where some 200,000 people are exposed to more than 10 mSv/yr). Lifetime doses from natural radiation range up to several thousand millisievert. Nevertheless, there is no evidence of increased cancers or other health risks arising from these high natural levels.

The study performed in Ghana (Faanu et al., 2012) shows that activity concentrations of natural radionuclides ^{226}Ra, ^{232}Th and ^{40}K in soil, rock, waste and tailing samples were measured by gamma spectrometry using high-purity germanium detector. In addition, radiological hazard assessments due to these natural radionuclides were carried out. The average activity concentrations of ^{226}Ra, ^{232}Th and ^{40}K determined were 13.61 $\pm$ 5.39 Bq/kg, 24.22 $\pm$ 17.25 Bq/kg and 162.08 $\pm$ 63.69 Bq/kg, respectively and the average annual effective dose was 0.17 + 0.09 mSv. The activity concentrations of NORMs from this study are expected to be lower that obtained by Faanu et al. (2012) since he conducted his research at the mining site where the existing exposure is likely to be elevated.

A similar study performed in Qatar (Al-Kinani et al., 2012) revealed that the soil activity concentrations ranged from 25.01- 40.31 for ^{226}Ra, 12.37- 4.99 for ^{232}Th and 133.8 - 250.1 for ^{40}K with mean values of 57, 87 and 207 Bq/kg, respectively. The corresponding outdoor annual effective doses ranged from 49.5 to 20.146 µSv with an average value of 136.95 µSv. Whereas the world wide average annual effective dose is approximately 460 µSv. Al-Kinani et al. (2012) collected soil samples from urban areas of Qatar.

Therefore, it is necessary to compare his result with the result of this study since the soil samples were also collected from playgrounds within the urban area of Accra, Ghana.

Moreover, studies on the level of trace metals in samples have been performed worldwide (Almeida et al., 2011; Baba et al., 2004; De Miguel et al., 2007, 2007; Kabata et al., 2010; Wong et al., 1997; Meza-Figueroa et al., 2007; Almeida et al., 2011) . De Miguel et al. (2007) carried out a study on children's playgrounds in Spain. The results of the risk assessment indicated that the highest risk was associated with ingestion of soil particles and that the trace element of most concern was arsenic, the exposure to which resulted in a cancer risk value of $4.19 \cdot 10 \times 10^{-6}$ close to the $1 \cdot 10 \times 10^{-5}$ probability level deemed unacceptable by most regulatory agencies. Regarding non-cancer effects, exposure to playground substrate yielded an aggregate Hazard Index of 0.28, below the threshold value of 1 (with As, again, as the largest single contributor, followed by Pb, Cr, Al and Mn). According to De Miguel et al. (2007), the work was done for two consecutive years (2002 – 2003) considering seasonal variations. In this study, trace elements were determined using INAA and AAS whereas De Miguel et al. (2007) used inductively coupled plasma-mass spectrometry (ICP-MS).

2.8. Gamma Spectrometry Analytical Techniques

In this study, two techniques were used for the analysis of gamma emitting naturally occurring radionuclides and trace metals in soil samples. These are High Purity Germanium (HPGe) detector and the Instrumental Neutron Activation Analysis (INAA). In this section, I will briefly discuss these techniques. In addition to INAA, AAS was also used for the analysis of some trace elements

2.8.1. Instrumental Neutron Activation Analysis (INAA)

Neutron Activation Analysis is a quantitative and qualitative analytical method with high high efficiency employed in the determination of trace elements in different kinds of samples. NAA involves nuclear reactions between neutrons and target nuclei. It can simultaneously determine about 25-30 major, minor, trace and rare elements of geological, environmental, biological samples in ppb-ppm range without or with chemical separation (Win, 2004). NAA was discovered in 1936 (Win, 2004). The initial step in neutron activation analysis is irradiating a sample with neutrons in a nuclear reactor or sometimes in other neutron sources. During irradiation the stable naturally occurring isotopes that constitute a sample are converted into radioactive isotopes by neutron capture. The activated nucleus is allowed to decay according to its half-life. Since nuclides contained in a sample will emit particles or gamma-quanta with specific energies, the quantity of radioactive nuclides is determined by measuring the intensity of the characteristic gamma-ray lines in the spectra. To perform these measurements, a gamma-ray detector is used. The irradiated samples consist of radionuclides of different half-lives and different isotopes can be determined at their respective time intervals. Nuclear reactors with high fluxes of neutrons produced from uranium fission yield the highest sensitivities for most elements contained in a sample compared to other sources of neutron.

A high-resolution gamma-ray spectrometer is used to detect the delayed gamma rays in the presence of the artificially induced radioactivity in the sample for both qualitative and quantitative analysis. The incident neutron hits the target nucleus, which captures the neutron and is converted into a compound nucleus (Figure 2.1). The last immediately

emits radiation called prompt gamma radiation and forms the radionuclide, which then excites out a beta particle and emits the delayed gamma radiation (emitted after sometime delay), forming the product nucleus (Win, 2004). The qualitative characteristics are the energy of the emitted gamma lines and the half-life of the nuclide. Whereas the quantitative characteristic is the intensity (the number of gamma quanta of energy measured per unit time).

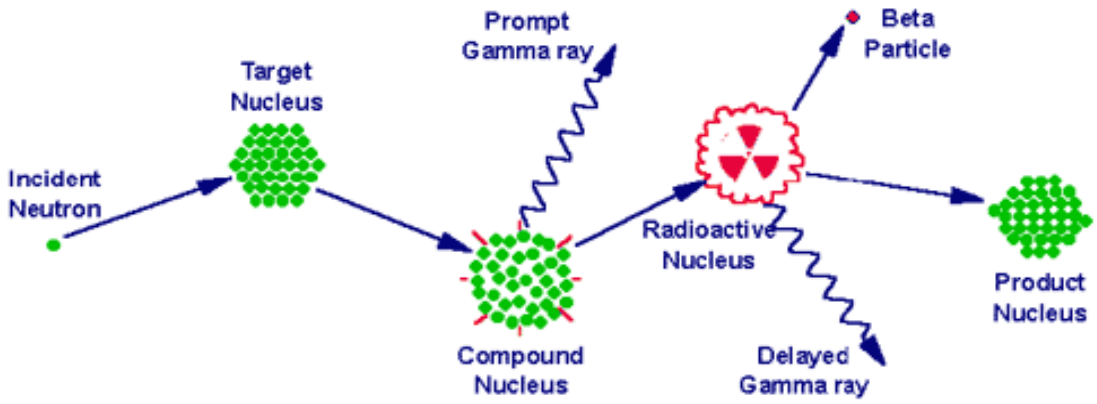

Figure 2.1: The process of neutron capture followed by the emission of gamma rays during activation analysis (Win, 2004)

NAA is chosen as an analytical technique in this study as it is competitive in many areas and for its advantage that it has high sensitivity and accuracy in respect of some trace elements. The method is of a multi element character and it simultaneously determine many elements without chemical separation. The samples preparation involves only pulverization or homogenization and this decreases the threat of contamination to a least and help accelerates the whole analytical process.

2.8.2. HPGe Detector

Germanium detectors are semiconductor diodes with a p-i-n structure in which the intrinsic region is sensitive to ionizing radiation, especially gamma rays (Knoll, 2010). When a gamma photon enters a detector, it interacts with the detector material by ionization process and generates an electric signal which is converted to a pulse by a pre-amplifier electronics connected to the detector (Knoll, 2010). The pulse is then amplified in amplifier electronics. Further amplification is done to the pulse to shape it and reduces electronic noise and sent to the multi-channel analyzer (MCA). The MCA sorts the pulses into full energy peaks. The main characteristic of a nuclear detector in activation analysis is its resolution which is expressed as full width at half maximum of the peak (FWHM). It is believed that, the narrower the peak, the lower the FWHM, the better the ability of the detector to resolve and separate close peaks or interference. Hence, the detector is said to have the better resolution.

Since germanium has a low band gap, these detectors are cooled in order to reduce the thermal generation of charge carriers. Also, leakage current produce noise that destroys the energy resolution of the detector (Knoll, 2010). Liquid nitrogen, which has a temperature of -196.15 ^{o}C, is the commonly to cool such detectors.

The detector is put on a vacuum chamber which is attached and inserted into a LN_2 dewar (Knoll, 2010). The sensitive detector surfaces are thus protected from moisture and condensable contaminants. The energy resolution of these detectors is very high, but because of their small volume, their sensitivity is low and it may take several minutes to record a spectrum. Arrangement of p-type and n-type semiconductor detectors is shown in the Figure 2.2.

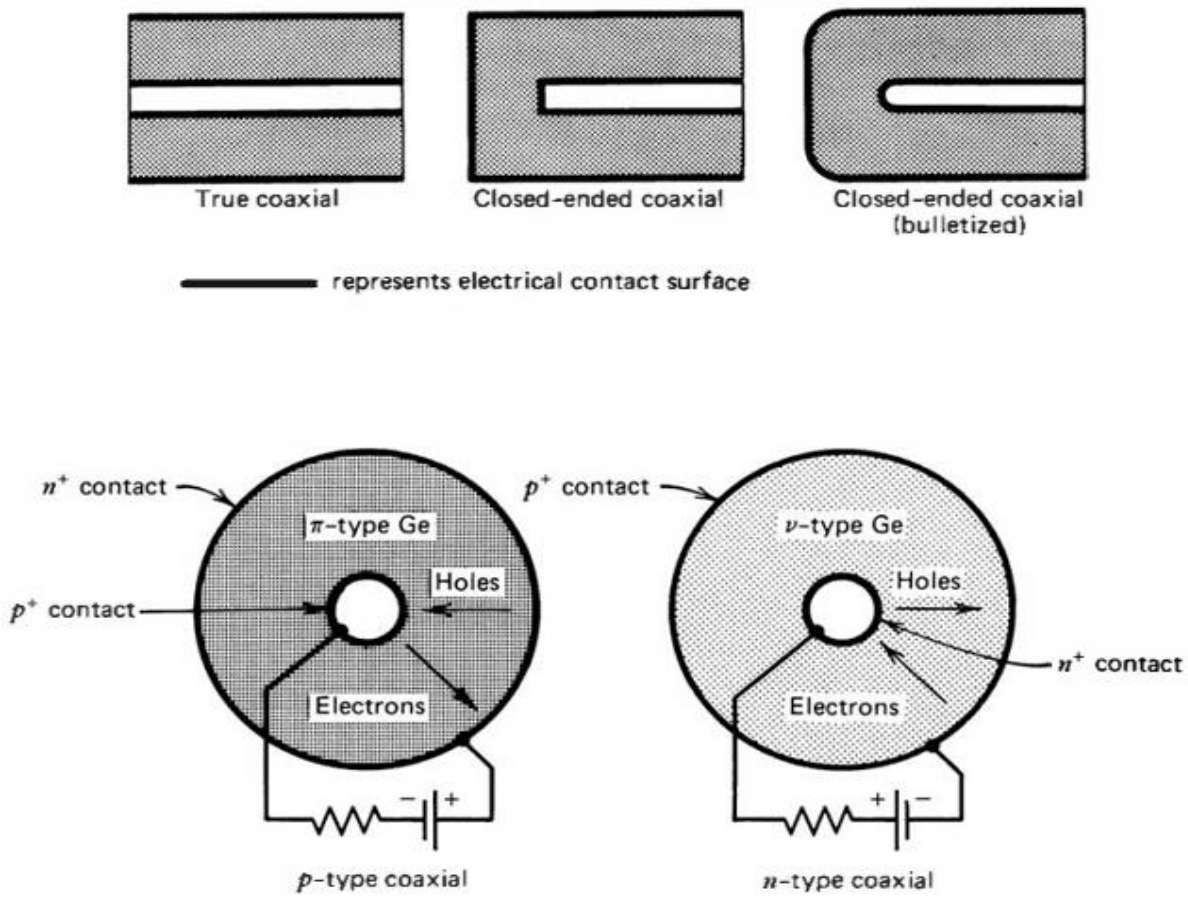

Figure 1.2: Configuration of closed end coaxial n-type and p-type semiconductor detectors and Cross sections perpendicular to the cylindrical axis of the high-purity germanium p or n type crystal and corresponding electrode configuration for each type (Knoll, 2010)

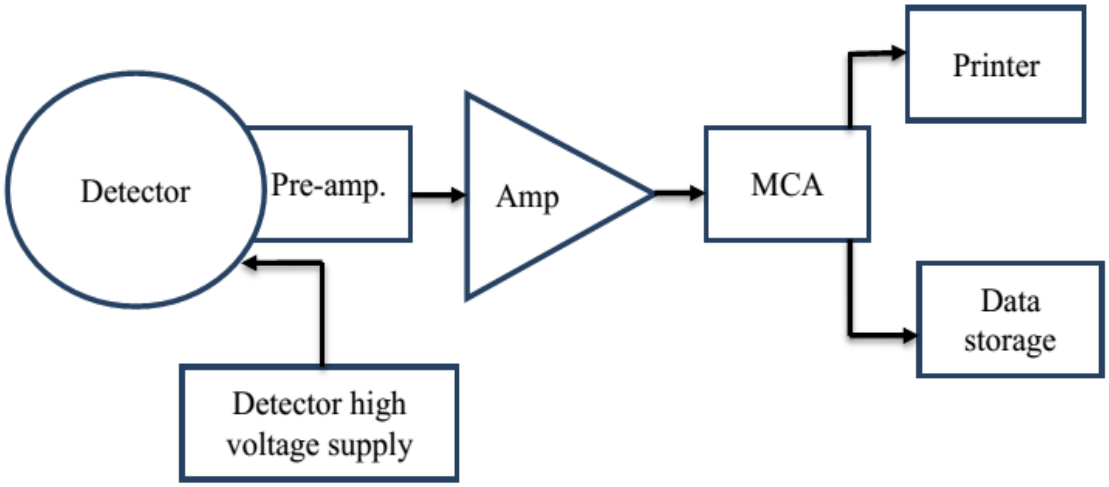

Figure 2.3: Block diagram of a particular gamma spectroscopic system (Shimboyo, 2012).

HPGe detectors that are in use come in two geometries. These are the planar and the co-axial HPGe detectors. Coaxial detectors have large active volume that makes them most appropriate for detection of high energy gamma radiation (300 – 2000 KeV). Planar detectors are widely used to measure lower energy gamma photons (60 – 300 KeV) and X-rays (Khandaker, 2011). Planar detectors are also known as low-energy photon spectrometers (LEPS). In this study, the co-axial Ge detector was used.

Gamma-ray detection is based on the effect of a γ-ray interacting with matter (Khandaker, 2011). There are only three important types of interaction of a γ-ray with matter. These are namely, the photoelectric effect, the Compton Effect, and the pair-production. The characteristics of these effects are important in detector design.

In the photoelectric process, the gamma ray contributes all of its energy to the withdrawn electron. The recoil electron ejected from the shell of atoms and hence yields the

electron-hole pairs in the detector that produces the output pulse. This output pulse is proportional to the energy of the gamma ray that made the interaction. In the spectrum, these events will appear as full-energy photo-peaks. The Photo electric effect is significant for the incident gamma energy of 0-150 keV.

The Compton cross section is the dominant one for all energies except the very lowest ($E_\gamma \leq 150$ keV) and the very highest ($E_\gamma = 8.5$ MeV). The Compton Effect too contributes strongly to the full energy peak by multiple Compton scattering under the condition that the last interaction is a photoelectric one and that all the preceding Compton interactions take place in the Ge crystal. In large-volume detectors the probability of multiple Compton scattering increases. If the last interaction does not occur by the photoelectric effect or if one of the multiple Compton interactions takes place outside the sensitive volume of the detector, the pulse will contribute to the Compton continuum

The pair-production process also provides a total absorption of the γ-ray energy. The gamma ray interacts in the detector and creates an electron positron pair. By the law of conservation of mass and energy, the initial gamma must have energy of at least 1.02 MeV since it takes that energy to initiate both the negative and positive electrons.

The positron will yield a pulse proportional to E_{e+} and because these two pulses are produced simultaneously, the resulting pulse from the detector would be the totality of the two pulses. When the positron enters the detector, the annihilation radiation γ_1 and γ_2 are produced. If both γ_1 and γ_2 goes beyond the boundaries of the detector without making additional interactions, the energy of exactly 1.02 MeV also escapes from the detector and this is subtracted from the initial total energy that entered the detector. In

most cases, only one of the gammas creates a photoelectric interaction in the detector as others escapes. In such cases, the total energy absorbed by the detector is 0.511 MeV less than the original incident gamma-energy. It is possible that both gammas cause photoelectric interactions without escaping and the incident γ-energy will be absorbed by the detector. Therefore, in the measured spectrum three peaks can be observed for each gamma-energy. These peaks are referred to as full-energy peak, single escape peak, and double-escape peak which can be distinguished by 0.511 MeV increments (Khandaker, 2011; Knoll, 2010).

2.9. Atomic Absorption Spectroscopy

Atomic absorption, coupled with atomic emission, was first used by Guystav Kirchhoff and Robert Bunsen in 1859 and 1860, for the qualitative identification of atoms. The atomic emission made progress and developed as an analytical technique. Atomic Absorption Spectroscopy (AAS) is the term used when the radiation absorbed by atoms is measured (Ebdon & Evans, 1998). The energy of the radiation absorbed or emitted is quantized according to Planck's equation as shown by equation (2.1). These quanta are known as photons, the energy of which is proportional to the frequency of the radiation.

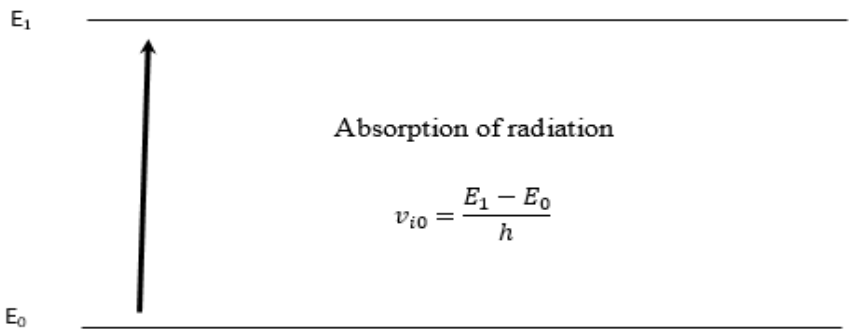

Figure 2.4: Diagram showing absorption of atomic radiation

$$h = h\nu = \frac{hc}{\lambda} \quad (2.1)$$

Where h is Plank's constant (6.62 x 10^{-34} J.s), v is velocity of light (3.0 x 10^{8} m.s^{-1}) and λ is the wave length (m) for the propagation of light.

The so called ground state atom absorbs light energy of a specific wavelength as it goes in the excited state. When the number of atoms in the light path increases, the quantity of light absorbed also increases. By considering the amount of light absorbed, a quantitative evaluation of the amount of analyte can be made. The use of special light sources and careful selection of wavelengths allow the specific determination of individual elements.

2.9.1. Atomic Absorption Instrumentation

There are five basic components of the atomic absorption instrument. These are namely, the light source that emits the light band of the element of interest, the absorption cell in which atoms of the samples are produced, a monochromator light dispersion, a detector that measure the light intensity and amplifies the signal and the display that indicated the reading after being processed by the instrument electronics. Atomic absorption spectrophotometers are designed to use either the single-beam or double-beam optics.

2.9.2. Single Beam Optics

In a single beam optics, the light source in the form of hollow cathode lamp or electrodeless discharge lamp produces a spectrum specific to the element of which it is made of, and which is concentrated through the sample cell into the monochromator (Harvey, 2000). The light source has be electronically structured to differentiate between the light coming from the source and the production from the sample cell. The monochromator separates the light and the definite wavelength of light isolated goes to a

photomultiplier tube that acts as detector (Ebdon & Evans, 1998; Harvey, 2000). The electrical current is formed based on the light concentration and managed by the electronics instrument. The electronics will quantity the light attenuation in the sample cell and transform the readings to the real sample concentration. In single-beam systems, a short warm up period is required to allow the source lamp to stabilize (Harvey, 2000).

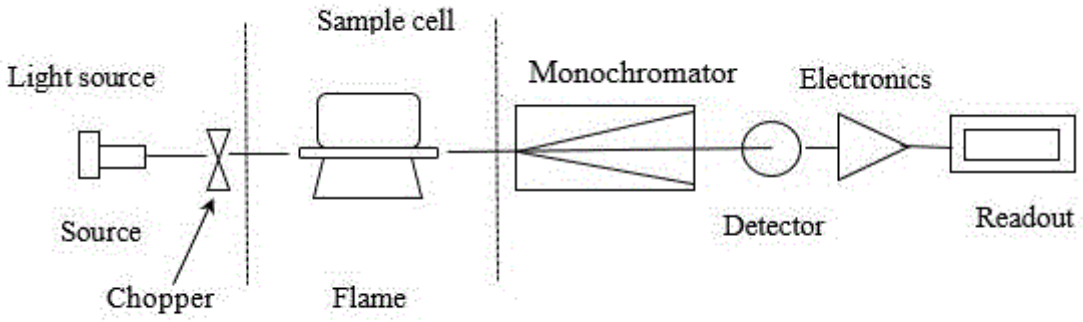

Figure 2.5: Block diagram showing single-beam atomic absorption spectrometer

2.9.3. Double Beam Optics

The light from the light source is split into a sample beam and is focused through the sample cell, and a reference beam, which is absorbed around the sample cell. In a double-beam arrangement, the display represents the ratio of the sample and reference beams. Therefore, an oscillation in source intensity does not influence the oscillations in instrument display, and stability is improved. Generally, analyses can be performed immediately with no lamp warm-up required (Ebdon & Evans, 1998; Harvey, 2000)

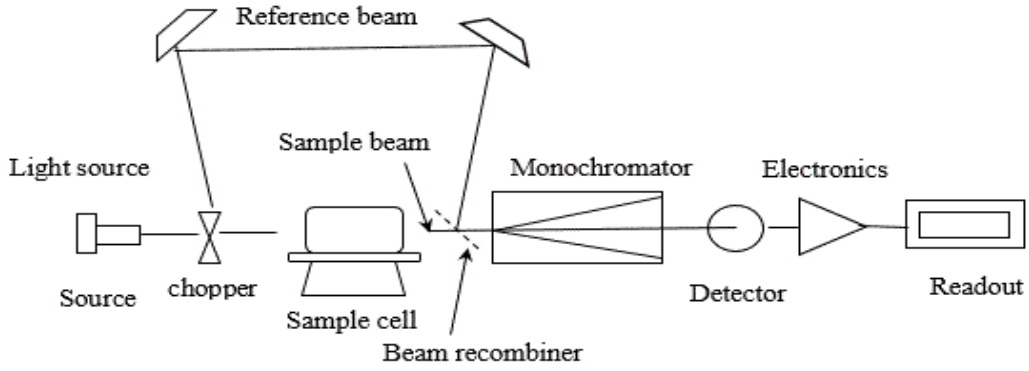

Figure 2.6: Block diagram showing double-beam atomic absorption spectrometer

2.9.4. Atomization

The most fundamental different between a spectrophotometer for atomic absorption and that of molecular absorption is the necessity to transform the analyte into a free atom (Harvey, 2000). The process of transforming an analyte in solid, liquid, or solution form into atomic state is referred to as atomization. Most of the time, the sample comprising the analyte undergoes some stages of sample preparation that causes the analyte in an organic or aqueous solution. Generally, two methods of atomization used are the flame atomization (used in this study) and electro thermal atomization. Whilst, elements such as As and Hg are atomized using Hydrode Generation (HG) and Cold Vapour (CV) respectively.

2.10. Multivariate Statistical Analysis

2.10.1. Principal Component Analysis (Factor Analysis)

Principal component analysis (PCA) is designed to convert original variables into, uncorrelated variables (axes) which are called principal components. This method decreases the dimension of data by a linear combination of original data to produce new

underlying variables that are orthogonal and uncorrelated to each other (Jolliffe, 2002). The new axes lie alongside the directions of maximum variance. According to (Bhuiyan et al., 2011), PCA offers an independent way of discovering indices of this type so that the deviation in the figures can be taken into account for as briefly as possible. The Principal Components (PC) which are linear combination of observable variables, account for information on the most significant parameters, which define the whole data set capable of data reduction with the least loss of original information (Bhuiyan et al., 2011).

The only difference between factor analysis (FA) and PCA is the preparation of the perceived correlation matrix for abstraction and the fundamental theory. FA helps reducing the involvement of less significant variables to make it easier for data construction from PCA. This is done by rotating the axis defined PCA based on well-established rules and fabricating new variables called VF (Bhuiyan et al., 2011). It can contain unobservable, hypothetical, underlying variables. PCA of the normalized variables is presented to extract significant principal components and to decrease the involvement of variables with less significance. These PCs are exposed to varimax rotation generating VFs (Bhuiyan et al., 2011; Jolliffe, 2002).

2.10.2. Cluster Analysis (CA)

Cluster analysis is defined as a group of multivariate systems that serve to accumulate objects depending on their characteristics (Bhuiyan et al., 2011). Cluster analysis categorizes objects, so that each object is matching to the others in the group based on a prearranged selection criterion. The subsequent clusters of objects are imaginary to show high internal homogeneity and high external (between clusters) heterogeneity. Thus, each

cluster defines the data composed, the class of which participants belong and this explanation may be preoccupied via use from the specific to the general class (Bhuiyan et al., 2011). Hierarchical agglomerative clustering (HCA) is the mutual approach, which presents perceptive similarity between a sample and the whole data set, and is ordinarily illustrated by a dendrogram or a tree diagram. The dendrogram presents a graphic summary of the clustering processes, by showing a picture of the groups and their closeness, with a dramatic decrease in the dimension of the initial data. The Euclidean space gives the likeness between two samples and a distance can be represented by the disparity between the obtained analytical values of the samples (Bhuiyan et al., 2011; Boamponsem et al., 2010)

CHAPTER 3

MATERIALS AND METHODS

In this chapter, the history, geographical location and the geology of the study area, the materials used as well as the methods used for sampling, sample preparation and measurements are discussed. Also, the dose and radiological risk assessments, level of trace elements are discussed in this section.

3.1. Description of the study area

3.1.1. History of Accra

Accra is the capital and largest city of Ghana, with an estimated urban population of 2,269.143 million as of 2012 ("Accra," 2015). The name *Accra* is believed to be derived from the Akan word *nkran*, meaning "ants", a reference to the numerous manner in which the natives of Accra kept re-appearing like army ants during a war with the Ashantis ("Accra," 2015). It is said to be the capital of the Greater Accra Region and of the Accra Metropolitan District. Furthermore, Accra provides stability and confidence for a larger metropolitan area, the Greater Accra Metropolitan Area (GAMA), which is inhabited by about 4 million people and this makes it the second largest metropolitan conglomeration in Ghana by population, and the eleventh-largest metropolitan area in Africa ("Accra," 2015).

3.1.2. Basic Education Statistics

Pre-school comprises nursery and kindergarten. In 2001, there were 7,923 children (3,893 girls and 4,030 boys) in pre-schools in Accra. In 2010, the enrollment rate at pre-school was 98 %. Pre-schools are regulated by the Ministry of Employment and Social Welfare, and are mostly privately owned and operated. In 2001, there were 62 government-owned pre-schools in the Accra metropolis. In primary school enrollment of girls is higher than that of boys. In 2010, the enrollment rate at primary school level was 95 % ("Accra," 2015).

The Junior High School is part of Ghana's basic education program. Its nationwide implementation began on 29 September 1987. In the 2001/2002 academic year, 61,080 pupils had enrolled in Accra, representing 57.17 % of the 129,467 school-age 12–to-14-year-olds. In 2010, the enrollment rate at Junior High School level was 95 %. The ratio of girls is also higher at this level ("Accra," 2015).

3.1.3. Climate of Accra

Accra features a tropical savanna climate that borders on a semi-arid climate. The average annual rainfall is about 730 mm, which falls primarily during Ghana's two rainy seasons. The major rainy season begins in April and ends in mid-July, whilst a minor second rainy season occurs in October ("Accra," 2015). Rain usually falls in short intensive storms and causes local flooding in which drainage channels are obstructed. There is very little variation in temperature throughout the year. The mean monthly temperature ranges from 24.7 °C (76.5 °F) in August (the coolest) to 28 °C (82.4 °F) in March (the hottest), with an annual average of 26.8 °C (80.2 °F). It should be noted, however, that the "cooler" months tend to be more humid than the warmer months.

As a result, during the warmer months and particularly during the windy harmattan season, the city experiences a breezy "dry heat" that feels less warm than the "cooler" but more humid rainy season (“Accra,” 2015). As Accra is close to the equator, the daylight hours are practically uniform during the year. Relative humidity is generally high, varying from 65% in the mid-afternoon to 95% at night. The predominant wind direction in Accra is from the WSW to NNE sectors. Wind speeds normally range between 8 to 16 km/h. High wind gusts occur with thunderstorms, which generally pass in squall along the coast (“Accra,” 2015).

The maximum wind speed record in Accra is 107.4 km/h (58 knots). Strong winds associated with thunderstorm activity often cause damage to property by removing roofing material. Several areas of Accra experience micro-climatic effects (“Accra,” 2015). Low-profile drainage basins with a north-south orientation are not as well ventilated as those orientated east-west. Air is often trapped in pockets over the city, and an insulation effect can give rise to a local increase in air temperature of several degrees. This occurs most notably in the Accra Newtown sports complex areas (“Accra,” 2015).

3.1.4. Geographical and Geological Description of the Study Area

Ga East Municipal District, located between 5° 33′ 00″ N and 0° 12′ 00″ W, is bordered on the north by the Akuapim South District in the Eastern Region of Ghana (“Accra,” 2015). It is bordered on its other three sides by other districts in the Greater Accra Region of Ghana. On its west is the Ga West District, south by Adentan municipal is the Accra Metropolis and in the east by La-Nkwantanang-Madina municipal is the Tema Metropolis (“Accra,” 2015). The geology of the Ga East district consists of Precambrian Dahomeyan schists, granodiorites, granites gneiss and amphibolites to late Precambrian

Togo Formation [comprising mainly quartzite, phyllites, and quartz breccias] ("Accra," 2015). The towns in Ga East District include Abokobi (the capital), Dome, Taifa, Ashongman, Haatso, Ayi Mensa, Bansa, Oyarifa, Pantag and Kwabenya. The Ghana Atomic Energy Commission (GAEC) is found in Kwabenya.

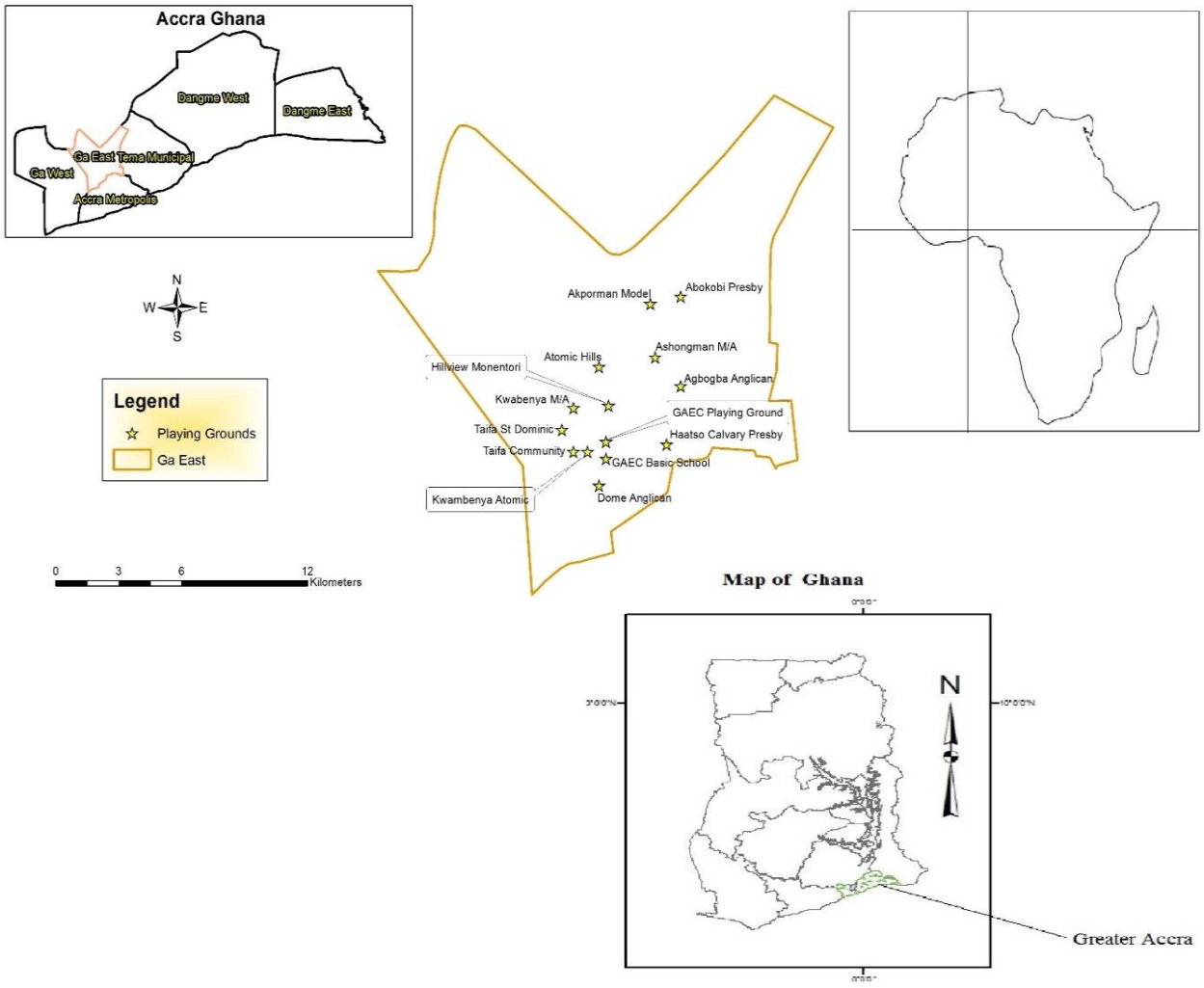

Figure 3.1: Layout of Ga East showing sampling points

3.2. Sample Collections

A total of 70 soil samples were collected from selected school playing grounds (Fig 3.1 and Fig 3.2) within Ga East District of Greater Accra Region during October and November 2014. For the soil samples, each playing ground of an area of (64 × 100) m^2 was marked and 5 samples were randomly taken at depth up to 5 cm using a plastic dust pan and brush and transferred into a clean polythene bag (Faanu et al., 2012). The samples were properly labeled catalogued and brought to the Radiation Laboratory at the Radiation Protection Institute (RPI), Ghana Atomic Energy Commission (GAEC).

At each location, 5 measurements of the ambient gamma dose rates were taken at 1 m above the ground using a digital environmental radiation survey meter (RADOS, RDS-200, manufactured in Finland). The dose rate meter was calibrated at the Secondary Standard Dosimetry Laboratory (SSDL) of the RPI. The average value was taken in $\mu Sv.h^{-1}$. At the same time, the geographical coordinates for each sampling location were recorded using a Global Positioning Satellite (GPS).

In the laboratory, each of the 5 soil samples collected from the same playing ground were mixed to obtain a composite sample that represents a particular school playing ground. The composite samples were air dried on trays for 7 days and then oven dried at a temperature of 105 ˚C for between 3 and 4 h, to remove all the moisture contents (Faanu et al., 2012).

3.3. Instrumentation and Calibration

In this study, two analytical techniques namely gamma spectrometry and INAA were used. The quantitative determination of NORMs in soil samples was done using HPGe

detector while determination of trace element in soil samples was carried out by INAA with Ghana Research Reactor – 1 (GHARR–1). The AAS analytical technique was also used for some trace elements that INAA could not analyze due to some unexpected challenges that occurred during the study.

3.3.1. HPGe Detector System Setup

Direct instrumental analysis without pre-treatment (non-destructive) was used for the measurement of gamma rays for the soil using a coaxial one open end, closed end facing down HPGe detector (detector model GX4020, cryostat model 7500SL and preamplifier model 2002CSL). The detector has a diameter of 60.5 mm, length of 61.5 mm and distance from window (outside) of 6 mm. The resolution of the detector is 2.0 keV and relative efficiency of 40 % for 1.33 MeV gamma energy of ^{60}Co. The output of the detector is connected to PC. The identification of individual radionuclides was performed using their gamma ray energies, and the quantitative analysis of radionuclides was performed using gamma ray spectrum analysis software package, "Gennie 2000". The detector was surrounded by a lead shield (100 m) on all sides to reduce the background radiation level of the system, and lined inside with copper, cadmium and plexiglass (3 mm each) sheets to minimize the X-rays emitted due to interaction of cosmic radiation with lead (Faanu et al., 2012).

The detector is cooled with liquid nitrogen at a temperature of -196 ˚C (77 k). In order to determine the background distribution in the environment around the detector, the empty Marinelli beakers were thoroughly cleaned and filled with distilled water and counted for 36,000 s at the same geometry as the samples. The background spectra were used to correct the net peak area of gamma rays of measured isotopes. The background spectra

were also used to determine the minimum detectable activities of ^{238}U, ^{232}Th and ^{40}K of the detector.

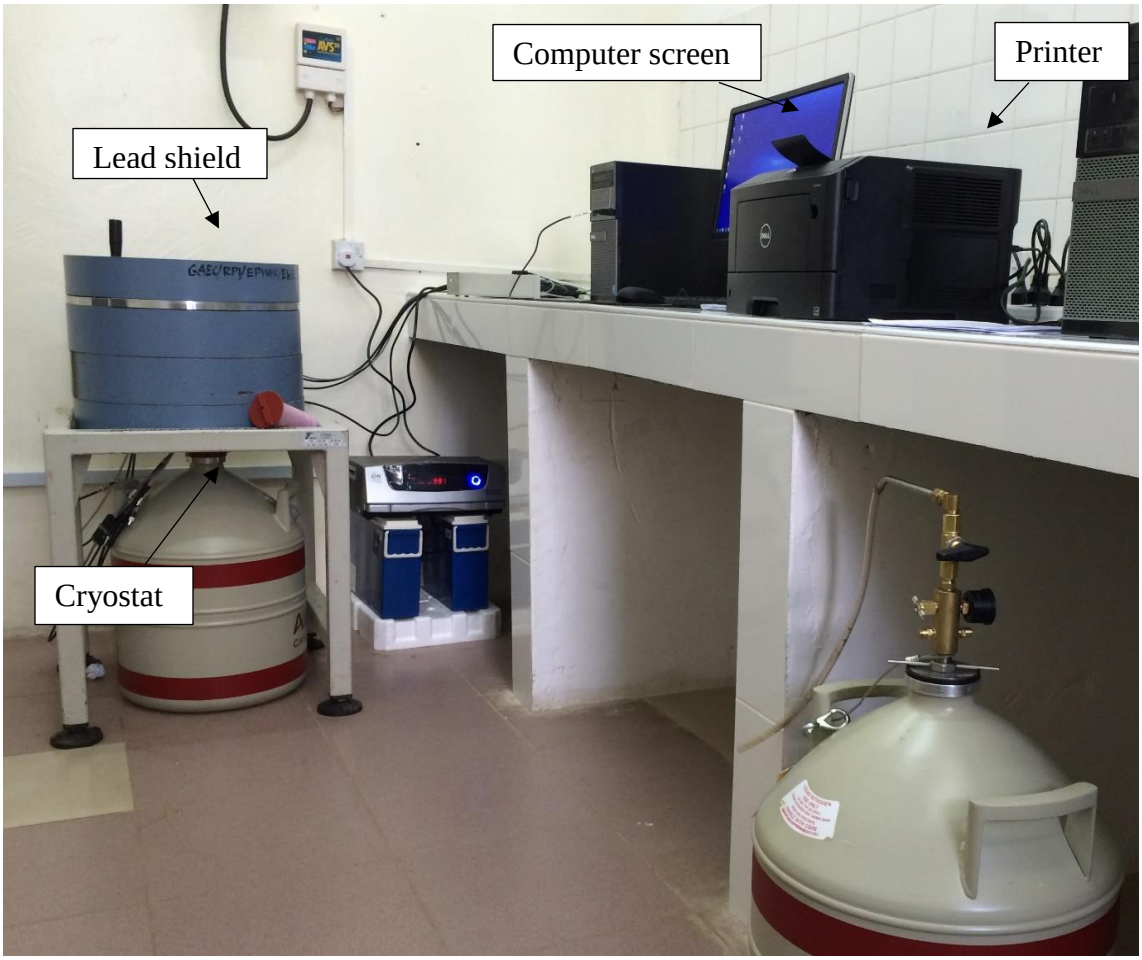

Figure 3.2: Gamma spectrometry set-up at Radiation Protection Institute (GAEC)

3.3.2. Energy Calibration

The relationship between the channel numbers corresponding to specific gamma-ray energies was determined before sample measurement (Faanu et al., 2012). The establishment of this relationship is known as energy calibration and the idea is to identify the radionuclides in a sample. The linearity of energy response is an essential feature for any γ-ray detector and the direct proportionality between the quality of energy

deposited in the detector by the incident radiation event and the height of the output pulse ensures that the system is working properly (Osvath et al., 2008). This is illustrated by fitting a straight line of incident photon energy of a number of known sources against the channel number of peak centroid in each spectrum. Accurate calibration involves a standard source with gamma ray energies that are not widely different from those to be measured in the unknown spectrum (Faanu et al., 2012).

The energy calibration was done by means of multi peaked and multi nuclide radioactive standard sources emitting gamma rays of precisely known energy, and the peak position in channels with this energy was identified. In this study, this was carried out by counting standard radionuclides (a mixture of ^{241}Am, ^{109}Cd, ^{139}Ce, ^{57}Co, ^{60}Co, ^{137}Cs, ^{113}Sn, ^{85}Sr and ^{88}Y) of known activities with well-defined energies in the energy range of 60 to ~2000 keV. The standard was counted on a detector for 10 hours or 36000 s. A certificate of the standard used is shown in Appendix I and the energy calibration curve is shown in Figure 3.3.

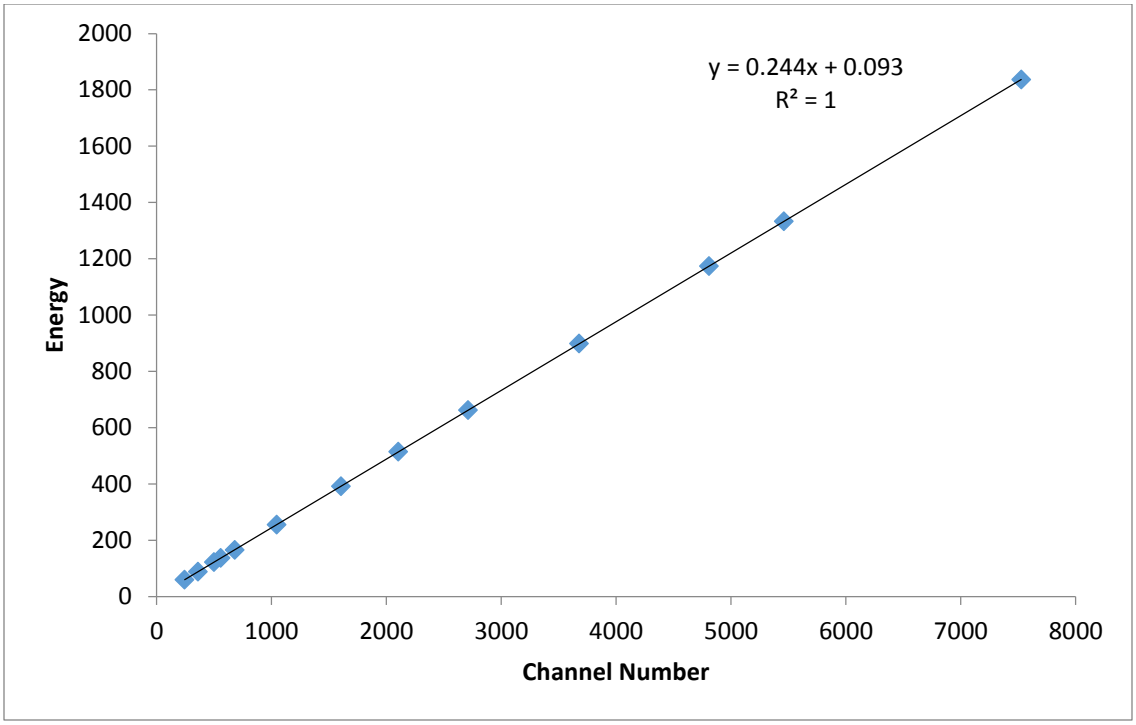

Figure 3.3: Energy calibration curve for standard

3.3.3. Efficiency Calibration

It is known for gamma-ray radiations that they can pass through relatively large distances before an interaction begins (Osvath et al., 2008). Therefore, the efficiency is said to be less than 100 %. Thus, it is important to accurately determine the counting efficiency of the detector in order to quantify the radionuclides in a sample. The efficiency of the detector is defined by the ratio of the pulses recorded under the photo peak to the total number of gamma rays emitted by the source (Osvath, 2008). The geometrical counting arrangement and detector characteristic influence the detector's efficiency. The standard was also counted on a detector for 10 hours or 36000 s, and the net counts for each of the full energy peak in the spectrum was determined and their corresponding energies used in the determination of the efficiency. The expression (3.1) used to determine efficiency is given below (Faanu et al., 2012).

$$Eff(E) = \frac{Net\ Area}{A_{std} \times P_{\gamma} \times T_{std}} \quad (3.1)$$

Where, $Eff(E)$ is the efficiency of the detector, A_{std} is the activity (Bq) of the radionuclide in the calibration standard at the time of calibration, P_{γ} is gamma emission probability for energy (E), and T_{std} is the counting time of the standard. The efficiency calibration curve is shown in Figure 3.4.

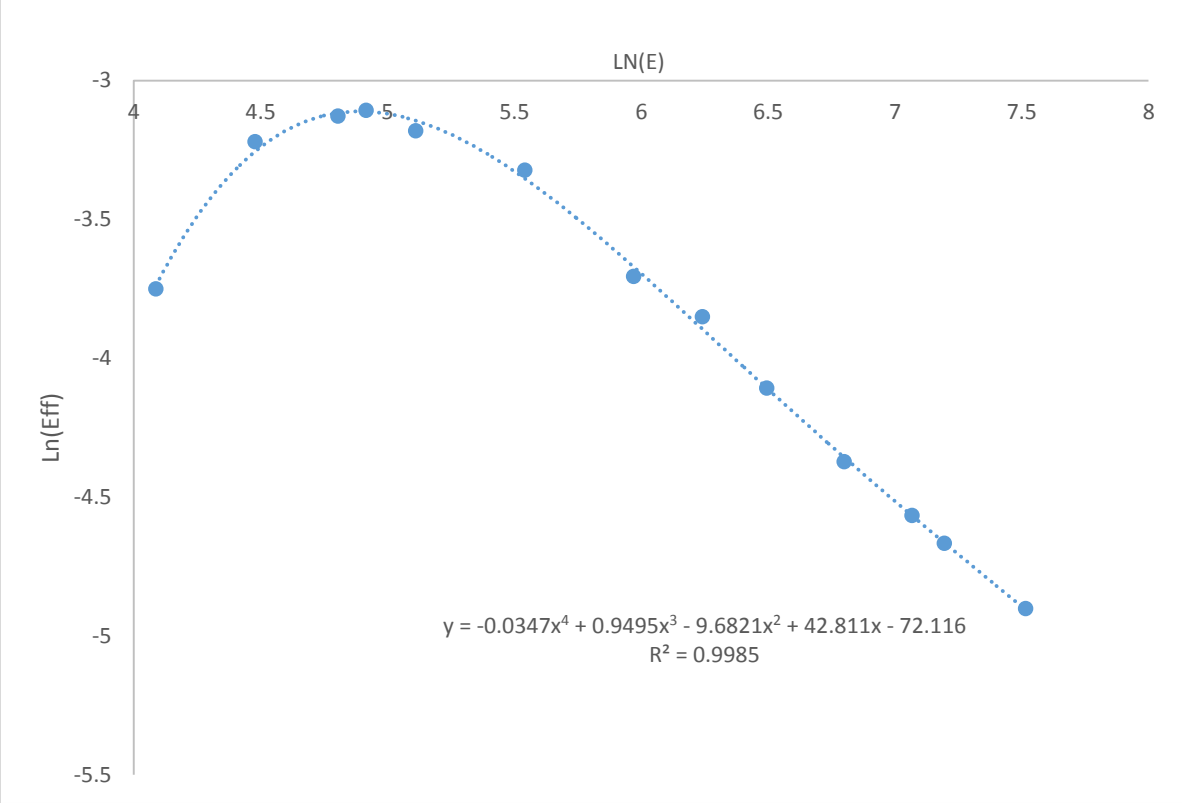

Figure 3.4: Absolute full-energy peak efficiency as function of energy for the HPGe detector

3.3.4. Detection Limit and Minimum Detectable Activity (MDA)

The MDA (Bq) is defined as the smallest quantity of radioactivity that could be distinguished from the blank under specified conditions (Cember & Thomas, 2009). Determination of MDA for each nuclide in a sample is required in order that a measurement can be expected to correctly imply the presence, and correctly quantitatively assess the activity with a predetermined degree of confidence. Therefore, the calculation of Minimum Detectable Activity for a given nuclide, at the 95 % confidence level, was determined based on Currie's derivation formula (3.2), given as below.

$$MDA = \left(\frac{2.71+4.65\sqrt{N_{TB}\left(\frac{t_T}{t_B}\right)+N_c}}{t_T.I.E} \right) \quad (3.2)$$

where N_{TB} is the background count, t_T is the sample counting time, t_B is background counting time, N_c is the integral count or the continuum, I is the gamma yield or gamma intensity or the emission probability and E is the efficiency (Faanu et al., 2012). The above formula takes into account both kinds of errors [i.e., false positive (deciding there is sample activity when there, in fact, there is none); and false negative (concluding there is no sample activity when there is some)]. It yields the smallest level of activity which can be detected with 95 % confidence, while also having 95 % confidence that activity is not detected falsely from a null sample. In this study, the gamma line energies that were used to calculate MDA were 1460 keV for ^{40}K; 609 keV for ^{214}B; 295 keV for ^{214}Pb and 911 keV for ^{228}Ac. The MDA values for ^{238}U, ^{232}Th and ^{40}K are tabulated in Table 3.1.

Table 3.1: Minimum detectable activities of 238U, 232Th and 40K

Radionuclide	MDA ($Bqkg^{-1}$)
^{238}U	0.13
^{232}Th	0.40
^{40}K	4.75

3.3.5. INAA system set-up

The reference materials (RM) SAMPLE 4 (114ISE4) of International Soil-analytical Exchange 2011 and SAMPLE 4 (131ISE4) of International Soil-analytical Exchange 2013 were used to validate the short-lived elemental concentration for quality control of the facility. Also, SAMPLE 2 (114ISE2) of International Soil-analytical Exchange 2011 was used in order to validate the medium lived elemental concentration. These were prepared by weighing 100 mg onto polyethylene film of about 6 mm by 4 mm in length and thickness. Three separate packaging were done; short and medium irradiation. For short irradiation, each sample was encapsulated in one container. Certified reference materials (CRM) were first irradiated, followed by separate irradiation of the samples and finally irradiation of the quality control materials. This allowed for pre-instrumentation calibrations and subsequent standardization for sample analysis. The packaging for medium irradiation was done in such a way that the samples were packed into one capsule with two RM and CRM arranged evenly amongst the samples. All the activations were performed at irradiation site B2 (using pneumatic transfer system B) under thermal neutron flux of $5.0\times 1011ncm^{-2}s\text{-}^{1}$ with the reactor operated at half power of 15 kW.

An irradiation time of 1 minute were applied for short-lived radionuclides (elements) determination and 2 – 6 hours for medium-lived radionuclides determination. After the short irradiation, the samples were allowed a delay time of about 4 minutes and measured

for 300 seconds each within the first 15 minutes and recounted. These were to ensure good selectivity and reduction of high background by Al and other short-lived radionuclides. The medium irradiations was allowed decay times of few day(s) (between 1 and 2) and weeks (spectrum acquired after 2 weeks) and their spectra acquired for 600 seconds and 10800 seconds respectively for identification of medium-lived elements. All the measurements were done at a source-detector distance of 50 mm and 10 mm respectively for short and medium counting. Gamma spectrometry measurements of induced radionuclide(s) were performed by a PC-based γ-ray spectrometry set-up. It consisted of an N-type, High purity Germanium detector (HPGe-coaxial type) coupled to a computer based multi-channel analyzer (MCA) via electronic modules. The relative efficiency of the detector is 40 %. Its energy resolution is 1.95 keV at a γ-ray energy of 1332 keV for ^{60}Co, Peak-to-Compton Ratio for ^{60}Co is 59:1.

The detector's dimensions were 63.0 mm in diameter, 65.0 mm in length with 4 mm End Cap to detector distance and an absorbing layers of 0.5 mm for beryllium, 0.3 μm inactive Germanium and 0.5 thin foil Aluminum top cap. The data acquisition and identification of γ-rays of product radionuclides were performed via ORTEC MAESTRO-32. The peak reduction and interpretation of gamma spectrum and elemental quantifications of samples and controls were done using multipurpose γ-ray spectrum analysis software; WinSPAN-2010 version 2.10 which works on the basis of relative comparator methodology.

3.3.6. AAS System Set-up

Figure 3.5 shows the Varian AA-240FS First Sequential Atomic Absorption Spectrometer. It consists of three major chambers in addition to the monitor and the compressor. These components are the lamp, spray and atomizing chambers indicated as a, b and c respectively on the diagram.

Figure 3.5: Set up of AAS equipment at Nuclear Chemistry and Environmental Research Center (GAEC)

The lamp chamber consists of a multi-cathode chamber that can accommodate four lamps at the same time. The spray chamber houses the burner head, spray block as well as the nebulizer. The atomizing chamber consists of the monochromator and detector lenses.

The function of the compressor labelled d in the figure is to supply compressed air that aids the flame during the burning process as well as creating pressure in the capillary tube that introduces the analyte into the system. Calibration of the instrument was done by aspiring into the flame samples of reference standard solutions containing known concentration of each element to be determined and then measuring absorption of each solution. The calibration curves for each element determined are shown in Appendix VII. After each reading, the instrument was reset to read zero % precision by aspiring into the flame with distilled water. This was done to completely remove trapped elemental ions from the previous reading that could give incorrect readings. For each element, the measured absorbance was plotted against the concentration. In this study, the reference standards were from Fluka Analytical Sigma Aldrich Chemie GmbH, product of Switzerland.

3.2.1. Determination of NORMs

The composite samples were ground into fine powder (pulverized) using a Retsch vibratory ball mill to increase the total emission area (Faweya, Alabi & Adewumi, 2014); and sieved through a

Figure 3.6: A typical bare playground of Taifa Community Basic School in Ga East District

500 µm mesh size pore so that particles may be homogenized and packed into 1 litre Marinelli beakers (Figure 3.7). The weights of empty Marinelli beakers and beakers with samples were measured using a mass balance (OHAUS Corp, Model: EP2102C, SNR: B0390772836, Mass range: 0.01 g – 2100 g, Temperature range: +10 ^{o}C – +40 ^{o}C, Power requirements: 12 V ~ 1 A, made in Switzerland). The Marinelli beakers with the samples were then sealed and left for at least a month in order to allow secular equilibrium between ^{226}Ra and its decay products before counting by gamma-ray spectrometry (Faanu

et al., 2012). Each sample was placed on a high purity germanium detector (HPGe) and activity of the naturally occurring radionuclides measured for 10 hours.

Figure 3.7: Sealed Marinelli beakers containing soil samples.

3.2.2. Determination of Trace Elements by NAA

Each composite sample was sieved through 250 µm, 100 µm and below 100 µm mesh size pore so that each sample was fractionated into different size particles. For each fraction, a mass of 0.1 g was weighed using a weighing balance and wrapped into a transparent sheet of polythene and labelled. When samples are packed into "rabbit capsules", they are sent into the reactor for irradiation with thermal neutrons and analyzed for trace elements by instrumental neutron activation analysis (INAA). The

reference materials SAMPLE 4 (114ISE4) of International Soil-analytical Exchange 2011, SAMPLE 4 (131ISE4) of International Soil-analytical Exchange 2013 and SAMPLE 2 (114ISE2) of International Soil-analytical Exchange 2011 were also prepared in the same manner for quality control and validation of data.

3.2.3. Determination of Trace Elements by AAS

A portion of each sample sieved through a 90 µm mesh screen was placed in air tight plastic bag and reserved for elemental analysis by AAS. The acid digestion method was used for soil samples according to the GAEC acid digestion protocol. Two grams (2 g) of sieved soil was weighed and transferred into a 100 mL borosilicate beaker. 25 mL of aqua regia [prepared in the ratio of 1 mL concentrated HCl (37%) to 3 mL of concentrated HNO_3 (65%)] was added to the beaker and covered with cling film and left overnight. The contents were then placed on a hot plate and digested for 3 hours and again left to cool at room temperature. The cooled suspension was filtered into a 100 mL measuring cylinder and 30 mL of distilled water was added to it. The filtrate was transferred to a plastic container ready to be analyzed. The two reference materials 114 ISE4 of International analytical soil exchange 2011 and NIST Standard Reference Material (SRM) 16469a (Estuarine sediment) were prepared and digested in the same way as that of the samples for the purpose of validating the results for samples measurements.

3.4. Determination of Concentrations in samples

In order to obtain the qualitative and quantitative elemental concentrations, the prepared samples were counted using the gamma-ray spectrometry system with HPGe for 36000 s. The spectra of each sample were analyzed and the identification of unkown radionuclides

was done by considering their peak centroid energies. The centroid energies of the peaks from the spectrum were compared with reference gamma-ray energies obtained from other nuclear data (Nichols et al., 2008). The radionuclides contained in the samples were identified and the areas under the peaks then activity concentrations of each nuclide was calculated (Diab et al., 2008; Hamdy et al., 2008). Typical photopeaks of ^{228}Ac, ^{214}Bi and ^{40}K analyzed using Genie 2000 are shown in Appendix II.

3.4.1. Radionuclides Activity Concentrations

The relation (3.3) was used in determining activity concentration (Bq/kg) of radionuclides in samples (Ebaid et al., 2010; Thabayneh et al., 2012; Darko et al., 2005).

$$A_{sp} = \frac{N_D.e^{\lambda_P t_d}}{p.T_c.\eta(E).m} \qquad (3.3)$$

where, N_D is the net counts of the radionuclide in the samples, t_d is the delay time between sampling and counting, p is the gamma ray emission probability (gamma ray yield), $\eta(E)$ is the absolute counting efficiency of the detector system, T_c is the sample counting time, m is the mass of the sample (kg) or volume (l), $exp^{(\lambda ptd)}$ is the decay correction factor for delay between time of sampling and counting, and λ_p is the decay constant of the parent radionuclide. The specific activities of the measured radionuclides are in good agreement with the reference values. The activity concentration of ^{232}Th was determined by the mean of the specific activities of ^{208}Tl, ^{212}Pb and ^{228}Ac. The activity concentration of ^{226}Ra was the mean specific activities due to gamma energies of ^{214}Pb and ^{214}Biand ^{40}K was measured directly using the 1460 KeV photo peak. Each sample was counted for 10 hrs in order to reach ± 5 % of analytical accuracy of measurements (Faweya et al., 2014).

3.4.2. Radon Concentration in Soil

The estimation of the concentration of radon in soil C_{Rn} in the absence of radon transport was determined using a proposal in UNSCEAR report from the activity concentrations of ^{226}Ra (Faanu, 2011; UNSCEAR, 2000). The equation (3.4) was employed in calculation.

$$C_{Rn} = C_{Ra}.f.\rho_s.\varepsilon^{-1}(1-\varepsilon)(m[k_T - 1] + 1)^{-1} \quad (3.4)$$

where C_{Ra} is the activity concentration of ^{226}Ra in soil (Bq.kg^{-1}), f is the radon emanation factor (0.2), ρ_s is the density of the soil grains (2700 kg.m^{-3}), ε is the total porosity (0.25), m is the fraction of the porosity that is water filled (0.95), m is zero if the soil is dry and k_T is the partition coefficient of radon between the water and air phases (0.23). In this study, soil samples were dried before activity concentration measurements; therefore, m is zero and the last term of the expression becomes one.

3.4.3. Radon Exhalation Rate

The major mechanism by which radon gets into the atmosphere is molecular diffusion. An expression to estimate the diffusive entry rate of radon into the atmosphere was used (UNSCEAR, 2000). It is suggested that for a porous mass of homogeneous material semi-infinite in extent, the flux density of radon at the surface of dry soil J_D (Bq.m^{-2}.s^{-1}) is given by equation (3.5).

$$J_D = C_{Ra}.\lambda_{Rn}.f.\rho_s(1-\varepsilon)L \quad (3.5)$$

where C_{Ra} is the activity concentration of ^{226}Ra in earth material (Bq.kg^{-1}), f is the emanation fraction for earth material (0.2), ρ_s is the soil grain density (2700 kg.m^{-3}), and ε is the porosity. This equation is said to be valid only for dry soil and all the parameters

were previously discussed in equation (3.4), except λ_{Rn} and L which are the respectively decay constant of ^{222}Rn (2.1 x 10 s^{-1}) and diffusion length [which equals $\left(D_e/\lambda_{Rn}\right)^{1/2}$ respectively, where $D_e = 2 \times 10^{-6} m^2.s^{-1}$].

3.4.4. Trace Elements Concentration by NAA

In order to determine elemental concentration of element of interest, the equation (3.6) was used by the comparator method using the same geometry, equal weights of both sample and standard, with the same irradiation, decay and counting times (Landsberger, 1994).

$$C_{sam} = C_{std}\left(\frac{A_{sam}}{A_{std}}\right) \quad (3.6)$$

Where C_{sam} is the unknown concentration of the element in the sample, C_{std} is the known elemental concentration of the element in the standard, A_{sam} is the activity concentration of the sample and A_{std} is the activity concentration of the standard. By introducing the terms D and C and also normalizing the weights between standards and unknowns, the overall equation becomes equation (3.7) in ppm or mg.kg^{-1}(Landsberger, 1994).

$$C_{sam} = C_{std}\left(\frac{A_{sam}}{A_{std}}\right)\left(\frac{D_{std}}{D_{sam}}\right)\left(\frac{C_{std}}{C_{sam}}\right)\left(\frac{W_{std}}{W_{sam}}\right) \quad (3.7)$$

Where W_{sam} and W_{std} are the weights of the sample and the standard respectively. The product is required to be radioactive and capable of emitting at least one gamma-ray photon. The gamma ray photon emitted was counted on a gamma ray detector using HPGE. The duration of irradiation of the sample depends on the characteristics of the sample and element of interest. The duration of the irradiation

also depends on the neutron flux density, mass of the sample and the efficiency of the gamma detector. The samples were sealed in capsules and transferred to the reactor core and irradiated with high flux neutrons. The activated components were then analyzed to identify and determine quantitatively the concentration of each radionuclide applying gamma spectrometry technique.

3.4.5. Trace Elements Concentration by AAS

A Varian AA-240FS First Sequential Atomic Absorption Spectrometer was used to determine the concentration levels of all the elements of interest. Replicate analyses were carried out for each determination to ascertain reproducibility and quality assurance. After every five real sample measurements for all the elements of interest, both the standard and blank were re-read to detect any drift in the instrument as soon as possible. Arsenic has short-wavelength and primary resonance lines; therefore, different equipment was used for generating its hydride before being atomized in the AAS equipment. The equipment is called Vapour Generation Accessory (VGA) that makes use of a gas-liquid separator to separate the gaseous hydrides from the liquid reagents prior to introduction into the atom cell. The cold vapour generation was used for mercury as it is the only analyte that has an appreciable atomic vapour pressure at room temperature (Evans et al., 1998)

3.5. Dose Assessment

The digital environmental radiation survey meter (RADOS, RDS-200, manufactured in Finland) was used to measure five outdoor external gamma dose rates at 1 m above the ground from each sampling location. The radiation survey meter was calibrated at Secondary Dosimetry Laboratory (SSDL) of RPI at GAEC with a provided calibration

factor. The absorbed dose rate in air and the annual effective dose were estimated from activity concentrations measured in the soil samples.

3.5.1. Absorbed Dose Rate in Air (D) from Activity Concentration

A direct relationship between radioactivity concentrations of natural radionuclides and their exposure is referred to as absorbed dose rate in air at 1 m above the ground. This is calculated from the activity concentrations using the equation (3.8) (Faanu et al., 2012; Oyedele, 2006; Oyedele & Shimboyo, 2013; Oyedele, Sitoka, & Davids, 2008).

$$D_\gamma(nGyh^{-1} = DCF_K \times A_K + DCF_U \times A_U + DCF_{Th} \times A_{Th} \quad (3.8)$$

where DCF_K= 0.0417, DCF_U= 0.462 and DCF_{Th}= 0.604 are the absorbed dose rate conversion factors for ^{40}K, ^{238}U and ^{232}Th in $nGy.h^{-1}/Bq.kg^{-1}$ and A_K, A_U and A_{Th} are the activity concentrations for ^{40}K, ^{238}U and ^{232}Th, respectively.

3.5.3. Annual Effective Dose Equivalent (AEDE)

In order to provide the radiological risk to which the public is exposed, the absorbed dose is considered in terms of annual effective dose equivalent from terrestrial gamma radiation taking into account the conversion coefficients from absorbed dose in air to effective dose which is estimated to be 0.7 Sv/Gy and the outdoor occupation factor of 0.2. Therefore, the outdoor annual effective dose equivalent was estimated by using the following equation (3.9) (Darko et al., 2008; Faanu et al., 2012; Gbadago et al., 2011).

$$E_\gamma = D_\gamma \times 0.2 \times 8760 \times 0.7 \quad (3.9)$$

Where E_γ is the average annual effective dose and D_r is the absorbed dose rate in air.

3.6. Cancer Risk Assessment

3.6.1. Radiological cancer risk assessment

Table 3.2: Detriment adjusted nominal risk coefficients for stochastic effects after exposure to radiation at low dose rate (ICRP, 2007).

Exposed population	Cancer fatality		Heritable effects		Total	
ICRP publication	103	60	103	60	103	60
Whole	5.5	6	0.2	1.3	5.7	7.3
Adults	4.1	4.8	0.1	0.8	4.2	5.6

Note: Detriment-adjusted nominal risk coefficients (1E-02 Sv^{-1}) for stochastic effects after exposure to radiation at low dose rate.

The radiological fatality cancer risks and the severe hereditable effects due to exposure to NORMs were assessed from the playgrounds of Basic Schools. This was done by using the ICRP recommended risk assessment technique and the use of appropriate nominal probability coefficients for stochastic effects (ICRP, 2007). The ICRP recommended nominal risk coefficients for stochastic effects are shown in Table 3.2 (ICRP, 2007). The risk to fatality cancer and hereditary effect were estimated as shown below:

Fatality cancer risk = [Annual effective dose (Sv)] x [cancer nominal risk factor]

Hereditary effects risk = [Annual effective dose (Sv)] x [hereditary nominal risk factor]

3.6.2. Elemental Risk-based Assessment

Exposure of children playing in school playgrounds to trace elements can occur via three main pathways: (a) direct ingestion of substrate particles; (b) inhalation of re-suspended particles through the mouth and nose; and (c) dermal absorption of trace elements in particles adhered to exposed skin (De Miguel et al., 2007). The dose received through

each of the three pathways considered has been calculated using the following four equations:

$$D_{ingestion} = C \times \frac{IngR \times EF \times ED}{BW \times AT} \times 10^{-6} \quad (3.10)$$

$$D_{inhalation} = C \times \frac{InhR \times EF \times ED}{PEF \times BW \times AT} \quad (3.11)$$

$$D_{dermal} = C \times \frac{SA \times SL \times ABS \times EF \times ED}{BW \times AT} \times 10^{-6} \quad (3.12)$$

$$D_{vapour} = C \times \frac{InhR \times EF \times ED}{VF \times BW \times AT} \quad (3.13)$$

where D ($mg.kg^{-1}.day^{-1}$) is dose contacted through ingestion ($D_{ingestion}$), and inhalation ($D_{inhalation}$) of substrate particles and dermal contact with the substrate particles (D_{dermal}), C ($g.kg^{-1}$) is the concentration of trace element in substrate ("exposure point concentration") (USEPA, 1997).

IngR: Ingestion rate; in this study, 20 $mg.h^{-1}$ (USEPA, 1997)

InhR: Inhalation rate,; in this study, 1.2 $m^3.h^{-1}$ (EPA, 2002)

EF: Exposure Frequency (site specific), in this study 990 h $year^{-1}$ is used

ED: Exposure Duration (site specific; in this study, 14 years is used

SA: Exposed skin area; in this study, 2800 cm^3 (De Miguel et al., 2007)

SL: Skin adherence factor; in this study, 0.07 $mg.cm^{-2}h^{-1}$ (EPA, 2002)

ABS: Dermal absorption factor (dimensionless); in this study, 0.001 for all elements except for arsenic which is 0.03

PEF: Particle emission factor; in this study, 6.8 x 10^8 $m^3.kg^{-1}$ (De Miguel et al., 2007)

VF: Volatilization factor; in this study, for elemental Hg, 32.376.4 m^3kg^{-1} (De Miguel et al., 2007).

BW: Average body weight; in this study, 15 kg (De Miguel et al., 2007)

AT: Average time, for non-carcinogens is (ED x 365 days) and carcinogens is (70 x 365 days)

The obtained data for particles with diameter below 100 µm were selected in order to perform the estimation of this risk-based assessment. This is because they can easily be inhaled faster through the nose and mouth. Exposure frequency was estimated based on the information obtained from the Municipal Education Office of Ga East Municipal District.

Children spend about 30 minutes on playgrounds during their 2 break times at school (A total of 1 hour a day). They are assumed to visit the playground from Monday to Friday (5 times a week). There are three school terms per year, and children vacate after every three months of school days. The duration of their vacation is four weeks (1 month), so they go to school for a period of 9 months in a year. The total exposure frequency is therefore estimated to be 990 hours/year $\left(5 \times \frac{1\ hour}{1\ day} \times \frac{22\ day}{1\ month} \times \frac{9\ month}{1\ year}\right)$. It should be noted that this estimation is strictly based on the children that are enrolled within their respective schools, and they graduate from their elementary school after 14 years from the day of their enrollment. So, the exposure duration is taken as 14 years. The remaining exposure factors used in this study are the USEPA's default exposure factors for children (De Miguel et al., 2007). Inhalation-specific toxicity data are available only for Al, As,

Cd, Cr, Hg, Mn and Ni. For the rest of elements included in the risk analysis, the toxicity values considered for the inhalation path are the corresponding oral reference doses and slope factors. And on the postulation that, after inhalation, the absorption of the particle-bound toxicants will result in similar health effects as if the particles had been ingested (De Miguel et al., 2007), especially for this extended particle size range.

The concentration term *C* which is the exposure point concentration in equations (3.10) – (3.13) combined with their corresponding exposure values shown above to give an approximation of the sensible maximum exposure. The concentration term C used is the upper limit of 95 % confidence interval for the mean (95 % UCL) which cater for the uncertainties associated with estimating the true average concentration at a site (US EPA, 2002). In this study, the 95 % UCL was calculated with Methods for Specific Distributions (UCLs for Normal Distributions) using Microsoft Excel 2013. A step by step method of calculating 95% UCL is shown in Appendix VIII (US EPA, 2002). The doses calculated with Equations (3.10) – (3.13) for each element and exposure pathway were subsequently divided by the corresponding Reference Dose to yield a Hazard Quotient, HQ (or non-cancer risk), whereas for carcinogens the dose was multiplied by the corresponding slope factor to produce a level of cancer risk

3.7. Quantification of Soil Pollution

3.7.1. Enrichment Factor (EF)

The enrichment factor for each metal was calculated using the relationship in equation (3.14). It is the quotient of the ratio of the normalizing element in a sample and the same ration established in the chosen baseline (Bhuiyan et al., 2010).

$$EF = \frac{\left(Metal/Fe\right)_{sample}}{\left(Metal/Fe\right)_{Background}} \quad (3.14)$$

Bhuiyan et al. (2010) recommended the use of concentration of metal in unaffected soils of the study area. Nevertheless, in this study, the world average shales background values were used (Ebenezer, 2011; Rubio et al, 2000). This is because shales integrate crustal material derived from different earth-surface environments. Therefore, their deposition and formation is an averaging process and shale soils are normalized enabling the elemental concentrations to be well distributed. The EF values close to unity indicate original crustal elemental concentration, those less than 1.0 show a possible mobilization or depletion of metals, whereas EF >1.0 is an indication that the element is a result of anthropogenic activities. EFs greater than 10 are considered to be non-crusted source (Bhuiyan et al., 2010). In this study, iron (Fe) was used as the reference element for geochemical normalization. Bhuiyan et al. (2010 justified this with three reasons that Fe is associated with fine solid surfaces, its geochemistry is similar to that of many trace metals and its natural concentration tends to be uniform.

3.7.3. Geo-accumulation index (I_{geo})

The geo-accumulation index (I_{geo}) was originally expressed by Muller (1979) for metal concentrations in the < 2 µm fraction as follows (Rubio et al., 2000):

$$I_{geo} = log_2\left(\frac{C_n}{1.5 \times B_n}\right) \quad (3.15)$$

Where C_n is the measured concentration in the sediment for the metal n, B_n the background value for the metal n and the factor 1.5 is used to correct for possible variations of the background data due to lithological changes.

The Index of Geo-accumulation consists of seven grades (Table 3.3), with I_{geo} of 6 indicating almost a 100-fold enrichment above background values (Rubio et al., 2000; Yaqin et al., 2008).

Table 3.3: Six classes of the Geo-accumulation Index

Class	Value	Soil quality (pollution intensity)
0	$I_{geo} \leq 0$	Practically uncontaminated
1	$0 < I_{geo} < 1$	Uncontaminated to moderately contaminated
2	$1 < I_{geo} < 2$	Moderately contaminated
3	$2 < I_{geo} < 3$	Moderately to heavily contaminated
4	$3 < I_{geo} < 4$	Heavily contaminated
5	$4 < I_{geo} < 5$	Heavily to extremely contaminated
6	$5 < I_{geo}$	Extremely contaminated

3.7.3. Contamination Factor (CF)

The CF is the ratio obtained by dividing the concentration of each metal in the soil by the baseline or background value of concentration in unaffected soil (Bhuiyan et al., 2010). The expression is as follow:

$$CF = \frac{C_{metal}}{C_{background}} \tag{3.16}$$

The contamination levels are classified based on their intensities on a scale ranging from 1 to 6 [0 = none; 1 = none to medium; 2 = moderate; 3 = moderately to strong; 4 = strongly polluted; 5 = strong to very strong; 6 = very strong]. The highest number (6) indicates that the metal concentration is 100 times greater than what would be expected in the crust (Bhuiyan et al., 2010).

3.8. Computational Analysis (NORMs)

The activity concentrations of NORMs were reconstructed by using the Forward Different Interpolation Method. This was achieved by expressing the exponential term "$e^{-\lambda t}$" of the radionuclide decay equation "$A = A_0 e^{-\lambda t}$" into a 4th order Taylor polynomial form (Sey, 2014). The decay factor $e^{-\lambda t}$ was approximated to a polynomial form by the following analysis.

$$P_n(\lambda t) = P_n(x)$$

Since $P_n(x) = e^{-\lambda t} = e^{-x}$; this yields the polynomial of

$$e^{-x} = P_n(x) = a_0 + a_1(x - x_0) + a_2(x - x_0)(x - x_1) + a_3(x - x_0)(x - x_1)(x - x_2) + \cdots + a_n(x - x_0)(x - x_1)(x - x_2) \ldots (x - x_{n-1})$$

And the fourth order of this can be written as;

$$e^{-x} = P_n(x) = a_0 + a_1(x - x_0) + a_2(x - x_0)(x - x_1) + a_3(x - x_0)(x - x_1)(x - x_2) + a_4(x - x_0)(x - x_1)(x - x_2)(x - x_3)$$

Where $a_0 = y_0 = P_0(x_0)$

$$a_1 = \frac{y_1 - y_0}{h} = \frac{\Delta y_0}{h}$$

$$a_2 = \frac{y_2 - 2y_1 + y_0}{2h^2} = \frac{\Delta^2 y_0}{2h^2}$$

$$a_3 = \frac{y_3 - 3y_2 + 3y_1 - y_0}{2!\, h^3}$$

$$a_4 = \frac{y_4 - 4y_3 + 6y_2 - 4y_1 + y_0}{4!\,h^4}$$

So that,

$$P_n(x) = ax^4 + bx^3 + cx^2 + dx + e$$

And

$a = a_4$,

$b = a_3 - a_4(x_0 + x_1 + x_2 + x_3)$

$c = a_2 - a_3(x_0 + x_1 + x_2) + a_4(x_0x_1 + x_0x_2 + x_0x_3 + x_1x_2 + x_1x_3 + x_2x_3)$

$d = a_1 - a_2(x_0 + x_1) + a_3(x_0x_1 + x_0x_2 + x_1x_2) + a_4(x_0x_1x_2 + x_0x_1x_3 + x_0x_2x_3 + x_1x_2x_3)$.

$e = a_0 - a_1(x_0) + a_2(x_0x_1) - a_3(x_0x_1x_2) + a_4(x_0x_1x_2x_3)$

Microsoft Excel (2013 version) was used for the computation of these relations to obtain the coefficients *a*, *b*, *c*, *d* and *e*, and the polynomial (3.17) equals to e^{-x} was obtained (Sey, 2014).

$$e^{-x} \approx 0.0067x^4 - 0.0820x^3 + 0.3993x^2 - 0.9560x + 1 \qquad (3.17)$$

Based on the expression and an assumption that radionuclides activity concentrations in the soils are uniform, a MATLAB R2011b script (Appendix V) was written to approximate the naturally occurring radionuclides (^{238}U, ^{232}Th and ^{40}K) activity concentrations for the next 10 years as of 2015. The decay constants of ^{238}U, ^{232}Th and ^{40}K were calculated using the half-lives of ^{226}Ra, ^{228}Ra and ^{40}K respectively.

3.9. Statistical Analysis (Trace Elements)

The experimental data were treated statistically using SPSS software (version 20.0 for Windows). Principal Component Analysis (PCA) was used to deduce the hypothetical source of heavy metals whether natural or anthropogenic. Factor Analysis (FA) or the components of the PCA was done by Varimax Rotation. Varimax Rotation was used since Orthogonal Rotation minimizes the number of variables with a high loading on each component and therefore facilitates the interpretation of PCA results (Bhuiyan et al., 2010, 2011). Cluster Analysis (CA) was applied to classify different geochemical groups, clustering the samples with comparable trace metal contents. CA was expressed according to the Ward-algorithmic Method, and the squared Euclidean distance was employed for quantifying the distance between clusters of identical metal contents.

CHAPTER 4

RESULTS AND DISCUSSIONS

In this chapter, the activity concentrations of ^{238}U, ^{232}Th and ^{40}K measured in soil samples collected from selected sampling site in Ga East are presented. The absorbed dose rate in air, annual effective dose, cancer risk assessment due to effective dose, and the approximation of future doses are also presented. In addition, the elemental concentrations of trace metals determined in soil sample are presented as well as their risk assessments. The indices of pollution due to elemental concentrations and pollution source identification are also discussed.

4.1. Assessment of Natural Radioactivity

Table 4.1: Sample locations and coordinates

Sampling ID	School	Coordinates	
		Latitude	Longitude
AP	Abokobi Presby	5˚43'45"N	0˚12'4"W
AG	Agbogba Anglican	5˚41'31"N	0˚12'3"W
AM	Akporman Model	5˚43'35"N	0˚12'52"W
AS	Ashongman M/A	5˚42'13"N	0˚12'42"W
AH	Atomic Hills	5˚42'0"N	0˚14'8"W
DA	Dome Anglican	5˚39'4"N	0˚14'10"W
GS	GAEC Basic School	5˚39'39"N	0˚14'66"W
GP	GAEC Playing Ground	5˚40'7"N	0˚13'58"W
HC	Haatso Calvary Presby	5˚40'3"N	0˚12'25"W
HM	Hillview Montessori	5˚41'4"N	0˚13'55"W
KA	Kwabenya Atomic M/A	5˚39'54"N	0˚14'28"W
KW	Kwabenya M/A	5˚41'12"N	0˚14'48"W
TC	Taifa Community	5˚39'4"N	0˚14'10"W
TD	Taifa St Dominic	5˚40'26"N	0˚15'8"W

4.1.1. Ambient measurements

Table 4.2: Average absorbed dose rate in air at 1 m above the sampling points in the study area and calculated annual effective dose

Sampling ID	School	Absorbed dose rate ($nGyh^{-1}$)		Annual effective dose (mSv)
		Average ± σ	Range	
AP	Abokobi Presby	86 ± 18	60 – 110	0.105
AG	Agbogba Anglican	94 ± 13	80 – 100	0.115
AP	Akporman Model	74 ± 13	60 – 90	0.091
AS	Ashongman M/A	80 ± 20	60 – 100	0.098
AH	Atomic Hills	74 ± 15	60 – 90	0.091
DA	Dome Anglican	92 ± 30	60 – 140	0.113
GS	GAEC Basic School	76 ± 17	60 – 100	0.093
GP	GAEC Playing Ground	78 ± 18	60 – 100	0.096
HC	Haatso Calvary Presby	80 ± 20	60 – 100	0.098
HM	Hillview Montessori	74 ± 17	60 – 100	0.091
KA	Kwabenya Atomic M/A	96 ± 29	60 – 130	0.118
KW	Kwabenya M/A	90 ± 23	60 – 110	0.110
TC	Taifa Community	88 ± 29	60 – 130	0.108
TD	Taifa St. Dominic	66 ± 09	60 – 80	0.081
Average ± σ		82.0 ± 6.5		0.101 ± 0.011

Table 4.2 shows the absorbed dose rate measured in air at 1 m above the ground at the sampling points. The table indicates the average and range values of the absorbed dose as well as the calculated annual effective doses. The measured absorbed dose rates varied in a range of 60–140 $nGyh^{-1}$ with an average value of 82.0 ± 6.5 $nGyh^{-1}$. The corresponding average annual effective dose was calculated to be 101 ± 11 µSv (0.101 ± 0.011 mSv) in a range of 81 – 115 µSv (0.081 – 0.115 mSv). The results of the absorbed dose rates in this study compare well with the range of dose rates values reported for other countries (UNSCEAR, 2000). The highest absorbed dose rate value of 140 $nGyh^{-1}$ was measured at Dome Anglican School Playground. The high absorbed dose rate in this area could be

attributed to cosmic radiation and natural abundance of radionuclides in the soil of the area.

4.1.2. Activity Concentrations of NORMs in Soil

Figure 4.1 shows the Activity Concentrations of ^{238}U, ^{232}Th and ^{40}K. The activity concentrations of ^{238}U, ^{232}Th and ^{40}K are in the range of 9.7 – 40.3 $Bqkg^{-1}$, 9.2 – 66.4 $Bqkg^{-1}$ and 20.4 – 342.2 $Bqkg^{-1}$, respectively. The average activity concentrations of ^{238}U, ^{232}Th and ^{40}K are respectively 19.8 ± 8.7 $Bqkg^{-1}$, 29.1 ± 16.3 $Bqkg^{-1}$, and 119.4 ± 97.9 $Bqkg^{-1}$. These results are tabulated in Appendix II. The worldwide average activity concentrations of ^{238}U, ^{232}Th and ^{40}K in soil samples from similar studies are reported in the United Scientific Committee on Effect of Atomic Radiation (UNSCEAR) for individual member of public as 35, 30 and 400 $Bqkg^{-1}$, respectively (UNSCEAR, 2000).

In comparison to the average activity concentrations observed in this study, ^{238}U is about two times lower than the world average; ^{232}Th is nearly similar and compares well to the world average; whilst ^{40}K is about three times lower than values in normal continental soils (UNSCEAR, 2000). The average values in this study are lower than the worldwide average values. The activity concentrations are way far below the exemption values of 1000 $Bqkg^{-1}$ for ^{238}U and ^{232}Th, and 10000 $Bqkg^{-1}$ for ^{40}K in material that will warrant regulatory control (IAEA, 2011).

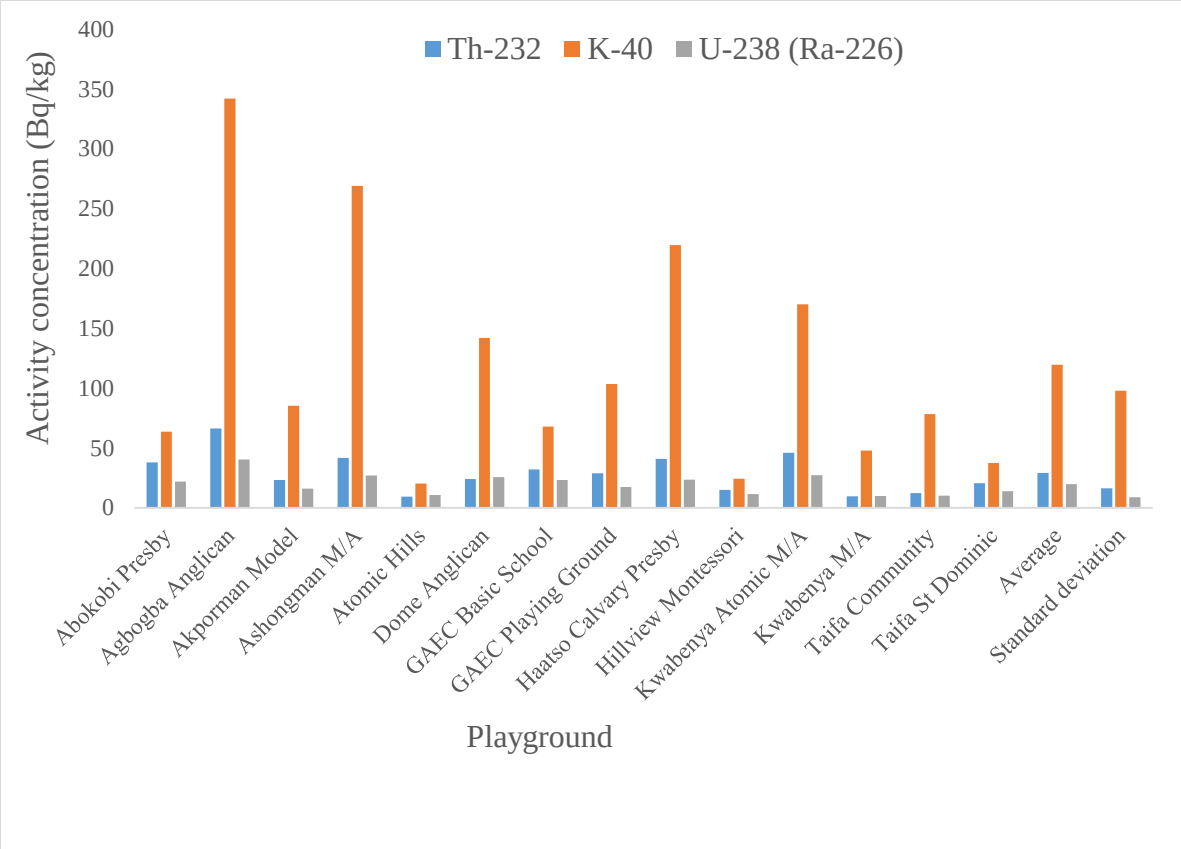

Figure 4.1: Activity concentrations of ^{238}U, ^{232}Th and ^{40}K in soil samples

4.1.3. Estimation of Radon Concentration in Soil

The activity concentration of ^{222}Radon in the soil matrix was calculated from the activity concentration of ^{226}Ra in the soil samples (Table 4.3). The range of activity concentrations of ^{222}Ra in the soil was 15.79–65.36 kBq.m^{-3} with a mean value of 32.13kBq.m^{-3}. These activity concentrations are below the value of 78 kBq.m^{-3} (UNSCEAR, 2000). The mean exhalation rate was 0.016 Bq.m^{-2}.s^{-1} (in a range of 0.008 – 0.033 Bq.m^{-2}.s^{-1}), and this compares well with the value of 0.033 Bq.m^{-2}.s^{-1} (UNSCEAR (2000). The observed measurements of exhalation rates of radon from soil indicate the unpredictability that reflects the variability of radon concentrations in near-surface pore spaces.

Table 4.3: Estimated concentration of ^{222}Rn and their corresponding exhalation rate

Sample Identity	School	C_{Ra} ($Bq.kg^{-1}$)	C_{Rn} ($kBq.m^{-3}$)	E_x rate ($Bq.m^{-2}.s^{-1}$)
AP	Abokobi Presby	21.89	35.46	0.018
AG	Agbogba Anglican	40.35	65.36	0.033
AP	Akporman Model	16.08	26.04	0.013
AS	Ashongman M/A	26.86	43.52	0.022
AH	Atomic Hills	10.55	17.09	0.009
DA	Dome Anglican	25.52	41.35	0.021
GS	GAEC Basic School	23.15	37.51	0.019
GP	GAEC Playing Ground	17.38	28.16	0.014
HC	Haatso Calvary Presby	23.48	38.03	0.019
HM	Hillview Montessori	11.52	18.67	0.010
KA	Kwabenya Atomic M/A	27.20	44.06	0.023
KW	Kwabenya M/A	9.75	15.79	0.008
TC	Taifa Community	10.18	16.50	0.008
TD	Taifa St Dominic	13.74	22.27	0.011
Mean		19.83	32.13	0.016
St.dev		8.74	32.13	0.007
Min		9.75	15.79	0.008
Max		40.35	65.36	0.033

This is because the concentrations of ^{222}Rn in soil gas vary over many orders of magnitude from place to place and show significant time variations at any given site.

4.1.4. Estimation of Absorbed Dose (D) and Annual effective Dose Equivalent (AEDE)

The average gamma dose rate and annual effective dose from terrestrial gamma rays calculated from soil activity concentrations are shown in Appendix IV. The average absorbed dose rate is found to be 31.7 ± 17.4 $nGyh^{-1}$ in a range of 11.3 – 73.0 $nGyh^{-1}$, which is by a factor of three lower than the dose rate measured in air at 1 m above the ground. The average absorbed dose rate due to the soil concentrations is observed to be

about two times lower than the worldwide average value of 60 $nGyh^{-1}$ (UNSCEAR, 2000).

This difference could be attributed to differences in the geology and geochemical state of the sampling sites. The corresponding average annual effective dose estimated from the soil concentrations is 0.039 ± 0.021 mSv in a range of 0.014 – 0.090 mSv.

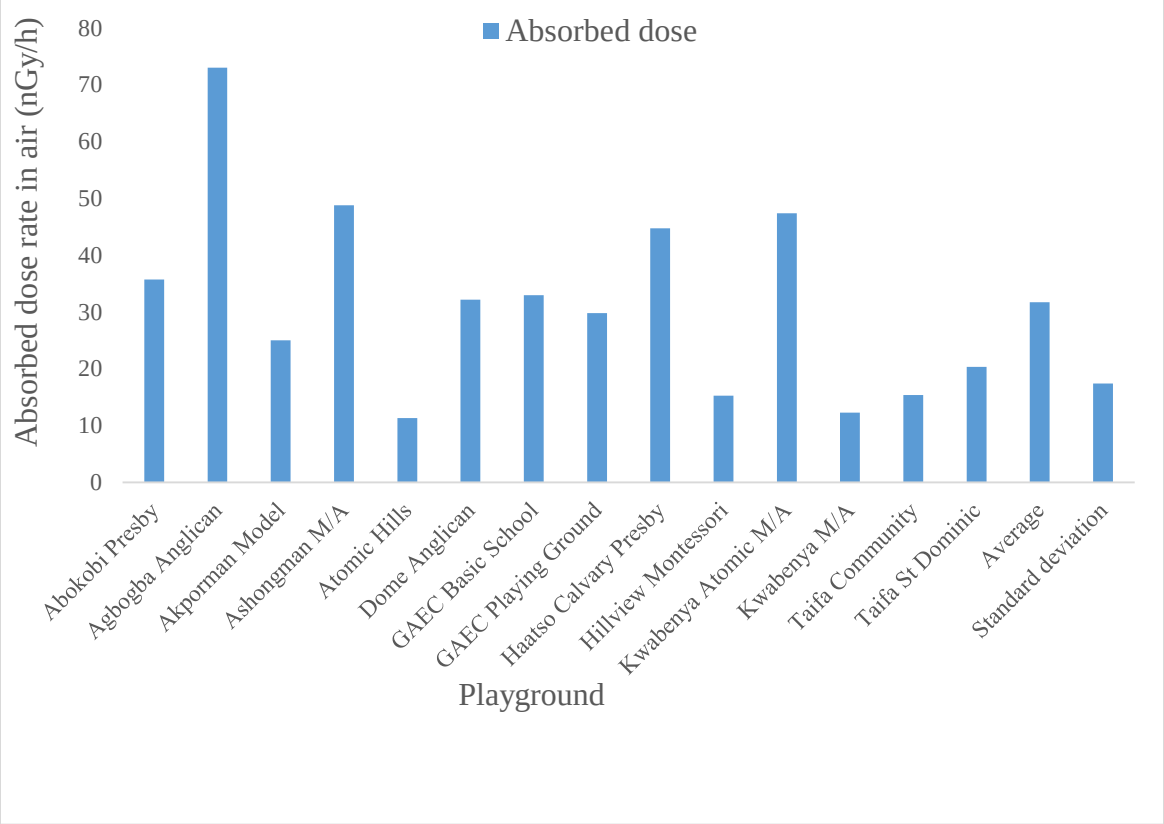

Figure 4.2: Comparison of Absorbed dose rate in different playing grounds

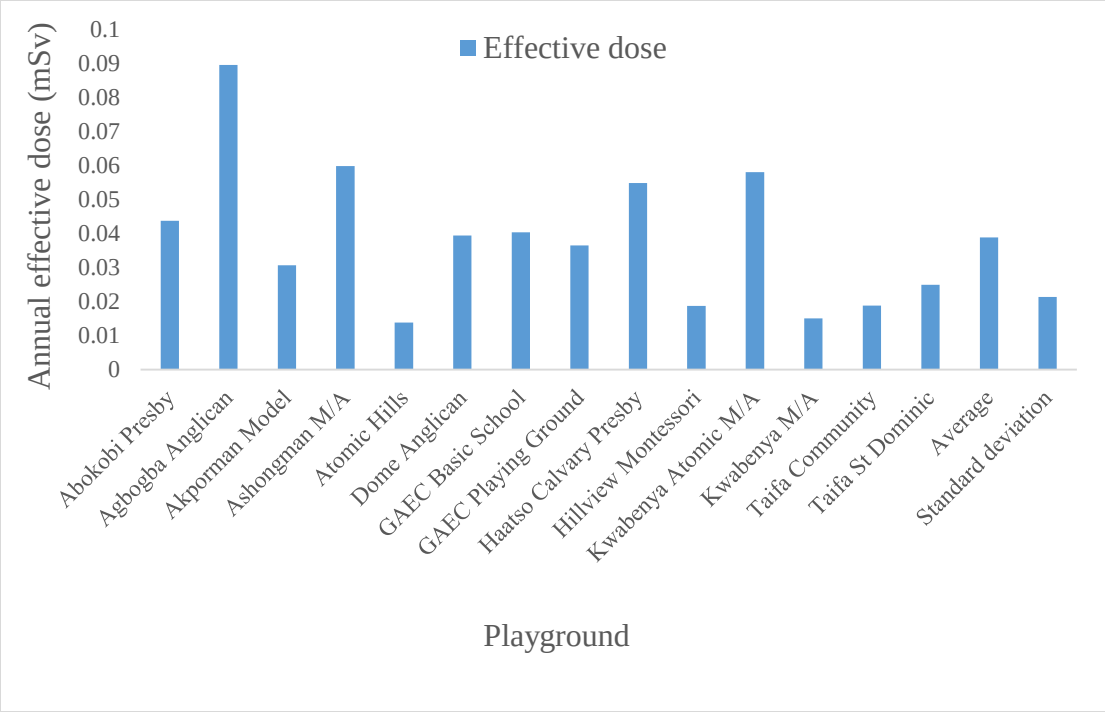

Figure 4.3: Comparison of annual effective dose in different playing grounds

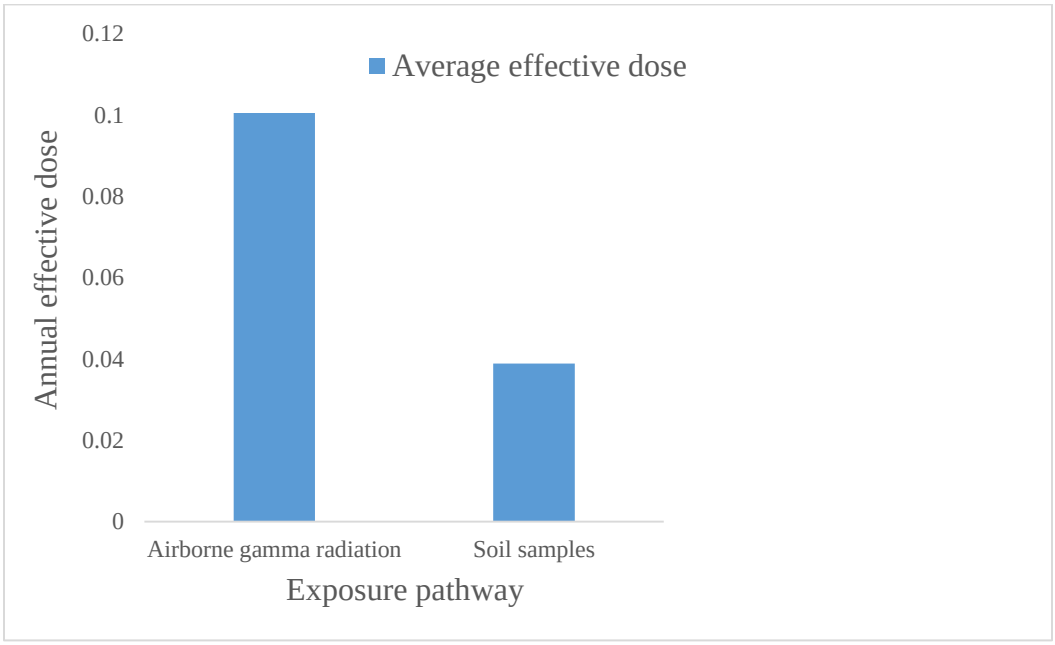

Figure 4.4: Comparison of annual effective doses from different exposure pathways of radiation

4.1.5. Natural Radioactivity Model

The naturally occurring radionuclides activity concentration was predicted using the Forward Differential Approach and a written MATLAB script in Appendix V, based on their current measured concentrations. A difference of 2 years was chosen between successive years. From the predicted results in Appendix VI, it is observed that there is no great variance in activity concentrations of ^{238}U and ^{232}Th whilst activity concentration of ^{40}K is uniform up to the chosen period of time. However, as a result of numerical analysis used, there is a decrease in the data. This decrease in exposure is observed from estimated annual effective dose in the study areas (Figure 4.5).

4.1.6. Radiological Hazard Assessment

The ICRP Risk Assessment Technique was employed in the estimation of the radiological fatality cancer risks for the whole population as well as severe hereditary effects (ICRP, 2007). The practical scheme of radiological risk recommended by ICRP is established on the assumption that at doses below 100 mSv, a specified increment in dose will yield a directly proportionate in the probability of incurring cancer of hereditary effects attributable to ionizing radiation. The model is commonly known as Linear-Non-Threshold (LNT) dose-response for which any dose greater than zero has an optimistic probability of producing an effect (ICRP, 2007).

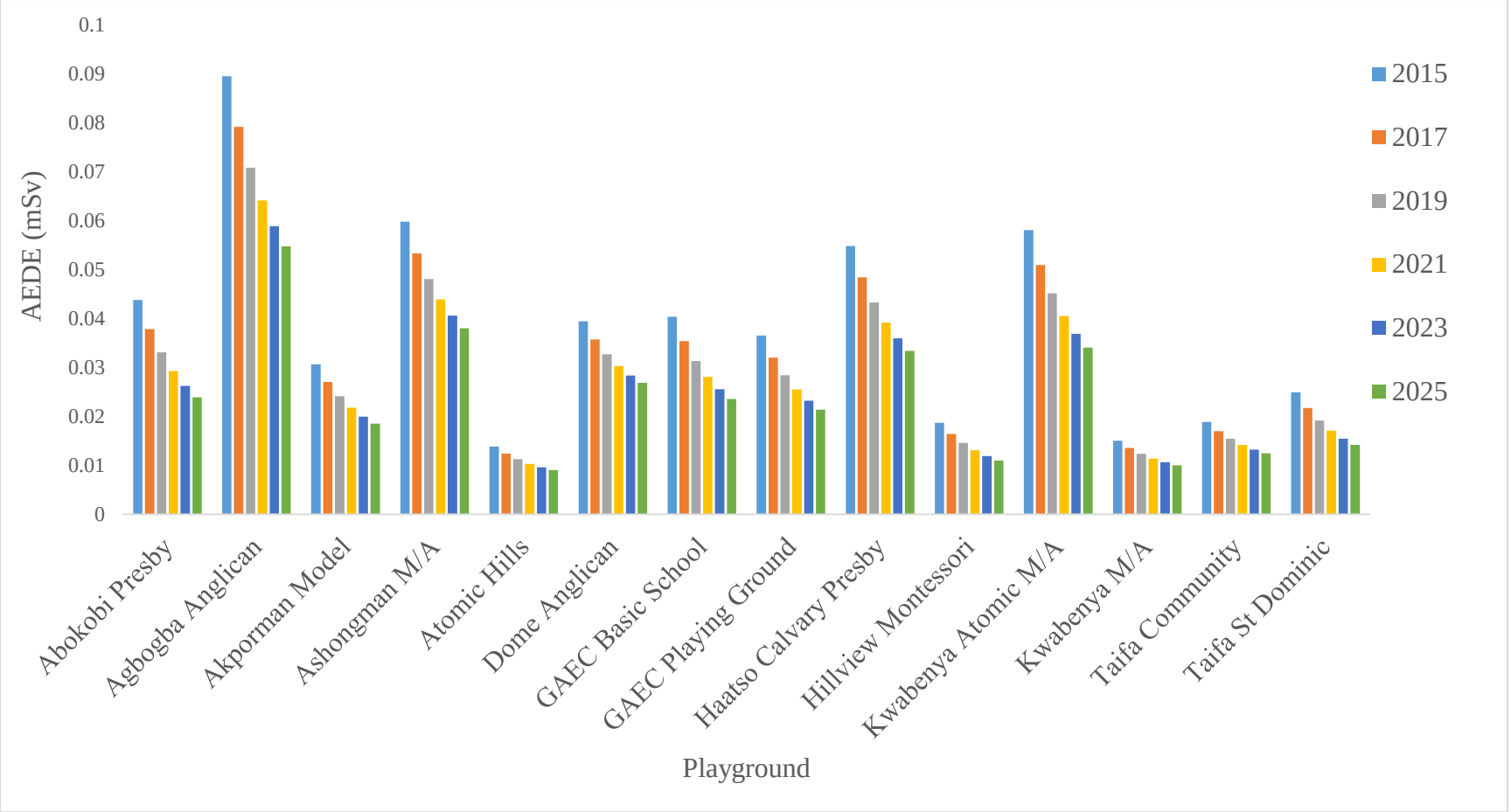

Figure 4.5: Predicted annual effective dose in study areas

The appraisal of risk covered the exposure pathway considered in this study. Table 4.4 shows the average annual effective dose from soils and the estimated risk components. The risk of exposure of low doses and dose rates of radiation was estimated using the 2007 recommended risk coefficients (ICRP, 2007) and an assumed 70 years lifetime of continuous exposure of the population to low level radiation.

Table 4.4: Estimated cancer risk components for external irradiation of ^{238}U, ^{232}Th and ^{40}K in soil

Sample ID	Annual effective dose (Sv)	Fatality cancer risk to population per year	Life time fatality cancer risk to population	Severe hereditary effect per year	Estimated lifetime hereditary effects
Abokobi Presby	4.38E-05	2.41E-06	1.68E-04	8.75E-08	6.13E-06
Agbogba Anglican	8.95E-05	4.92E-06	3.45E-04	1.79E-07	1.25E-05
Akporman Model	3.07E-05	1.69E-06	1.18E-04	6.13E-08	4.29E-06
Ashongman M/A	5.98E-05	3.29E-06	2.30E-04	1.20E-07	8.37E-06
Atomic Hills	1.38E-05	7.62E-07	5.33E-05	2.77E-08	1.94E-06
Dome Anglican	3.94E-05	2.17E-06	1.52E-04	7.89E-08	5.52E-06
GAEC Basic School	4.04E-05	2.22E-06	1.55E-04	8.08E-08	5.65E-06
GAEC Playing Ground	3.65E-05	2.01E-06	1.41E-04	7.30E-08	5.11E-06
Haatso Calvary Presby	5.48E-05	3.01E-06	2.11E-04	1.10E-07	7.67E-06
Hillview Montessori	1.87E-05	1.03E-06	7.20E-05	3.74E-08	2.62E-06
Kwabenya Atomic M/A	5.81E-05	3.19E-06	2.24E-04	1.16E-07	8.13E-06
Kwabenya M/A	1.50E-05	8.27E-07	5.79E-05	3.01E-08	2.10E-06
Taifa Community	1.89E-05	1.04E-06	7.26E-05	3.77E-08	2.64E-06
Taifa St. Dominic	2.49E-05	1.37E-06	9.60E-05	4.99E-08	3.49E-06
Average	3.89E-05	2.14E-06	1.50E-04	7.78E-08	5.44E-06
Standard deviation	2.13E-05	1.17E-06	8.22E-05	4.27E-08	2.99E-06
Min	1.38E-05	7.62E-07	5.33E-05	2.77E-08	1.94E-06
Max	8.95E-05	4.92E-06	3.45E-04	1.79E-07	1.25E-05

The average fatality cancer risks for all playgrounds were in a range of 7.62E-07 - 4.92E-06 with the average of 2.14E-06. This suggests that approximately 2 persons out of a 1 000 000 people are likely to suffer from cancer as a result of external irradiation from soil and this is considered to be insignificant. The lifetime fatality cancer risk for all were in a range of 5.33E-05 - 3.45E-04 with the average of 1.50E-04 which suggests that approximately 1 person out of a 10 000 is likely to suffer from cancer. On the other hand, severe hereditary effects per year and estimated lifetime hereditary effects were in a range of 2.77E-08 - 1.79E-07 and 1.94E-06 - 1.25E-05 with average of 7.78E-08 and 5.44E-06 respectively. Similarly, this proposes that approximately none out of 100 000 000 people is likely to suffer from hereditary diseases per year and approximately 5 persons out of 100 000 are likely to suffer from hereditary related diseases due to low background radiation exposure. The lifetime fatality cancer risk for the population in the study area is slightly above the USEPA acceptable range of risks of 1×10^{-6} to 1×10^{-4} values for the population of the study area (Faanu et al., 2012; USEPA, 1993). However, a risk value of 1×10^{-6} (that is, 1 case out of a million people dying from cancer) is considered as trivial.

4.2. Assessment of Elemental Concentrations

4.2.1. Validation of Results

4.2.1.1. INAA Results

For INAA, the reference materials SAMPLE 4 (114ISE4) of International Soil-analytical Exchange 2011 and SAMPLE 4 (131ISE4) of International Soil-analytical Exchange 2013 were used to validate the short-lived elemental concentration for quality control. Also, SAMPLE 2 (114ISE2) of International Soil-analytical Exchange 2011 was used in

order to validate the INAA method for the determination of medium lived elemental concentration. These reference materials were prepared, irradiated in the inner pneumatic irradiation sites of the GHARR-1 facility. Irradiation duration ranged from 10 s to 1 h depending on the half-life of element of interest and counted in the similar way as that of samples. The results measured were compared with the reference values in Tables 4.5, 4.6 and 4.7.

Table 4.5: Comparison of measured values of SAMPLE4 (114ISE4) as analyzed by INAA with its reference values

Element	Measured value ($mgkg^{-1}$)	Reference values ($mgkg^{-1}$)
Al	6.35×10^4	$6.05 \times 10^4 – 6.7 \times 10^4$
Ti	3.75×10^3	$3.370 \times 10^3 – 4.380 \times 10^3$
V	1.031×10^2	$8.40 \times 10^1 – 1.07 \times 10^2$
Mn	1.047×10^3	$1.02 \times 10^3 – 1.192 \times 10^3$

Table 4.6: Comparison of measured values of SAMPLE 4 (131ISE4) as analyzed by INAA with its reference values

Element	Measured value ($mgkg^{-1}$)	Reference value ($mgkg^{-1}$)
Al	3.881×10^4	$3.74 \times 10^4 – 4.46 \times 10^4$
Ti	4.253×10^3	$3.974 \times 10^3 – 4.693 \times 10^3$
V	4.968×10^1	$4.6 \times 10^1 – 5.69 \times 10^1$
Mn	6.025×10^2	$5.42 \times 10^2 – 6.54 \times 10^2$

Table 4.7: Comparison of measured values of SAMPLE 2 (114ISE2) as analyzed by INAA with its reference values

Element	Measured value ($mgkg^{-1}$)	Reference value ($mgkg^{-1}$)
Na	7.076×10^3	$6.440 \times 10^3 – 7.675 \times 10^3$
K	1.4750×10^4	$1.3900 \times 10^4 – 1.5400 \times 10^4$
La	2.560×10^1	$2.27 \times 10^1 – 2.87 \times 10^1$

From the observation, all the measured values are within the range of the reference values and that indicates the high degree of accuracy and precision of the analytical technique.

4.2.1.2. AAS Results

The two reference materials 114 ISE4 of International analytical soil exchange 2011 and the NIST Standard Reference Material 16469a (Estuarine sediment) were analyzed by means of AAS in order to validate analytical method. The results obtained were compared with the NIST certified values (Table 4.8). The measured values are observed to compare well with the certified/non-certified values and the calculated percentage recoveries show that the experiment was conducted well and there is accuracy in the procedures.

Table 4.8: Comparison of measured values of two reference materials with their respective certified/reference values (mg.kg^{-1})

	NIST Standard Reference Material 16469a (Estuarine sediments)			114 ISE4 of International analytical soil exchange 2011		
	Measured values	Certified values	Percentage recovery (%)	Measured values	Reference values	Percentage recovery (%)
Co	4.848 ± 0.24	5*	97.0	21.411	21.7	98.7
Cr	39.8 ± 2.0	40.9 ± 1.9	97.3	270.968	271.4	99.8
Fe	19939 ± 996.97	20080 ± 0.039	99.3	40342.742	40000.34	100.9
Cd	0.151 ± 0.007	0.148 ± 0.007	102.4	8.558	8.567	99.9
Cu	10.21 ± 0.51	10.01 ± 0.34	102.0	160.131	159.5	100.4
Zn	4851.5 ± 242.6	48.9 ± 1.6	101.1	1046.371	1045	100.1
Pb	12.1 ± 0.6	11.7 ± 1.2	103.3	299.395	299.8	99.9
Ni	22.3 ± 1.12	23*	97.4	60.907	61.31	99.3
As	6.06 ± 0.30	6.23 ± 0.21	97.3	45.968	46.18	99.5
Hg	0.0313 ± 0.0015	0.048*	78.3	3.129	3.925	79.7

*Non-certified values

4.2.2. Analytical Results

Figure 4.6 shows graphical presentation of the elemental concentrations of the metals of environmental interest (As, Cd, Cr, Hg, Ni, Pb and Zn). The elemental concentrations of As, Cd, Cr, Cu, Hg, Ni, Pb and Zn are (in ranges) of 0.075 – 1.45 mg.kg^{-1}, 0.06 – 0.225 mg.kg^{-1}, 3.42 – 15.72 mg.kg^{-1}, 7.44 –30.84 mg.kg^{-1}, 0.01 – 0.05 mg.kg^{-1}, 7.335 – 31.785 mg.kg^{-1}, 0.15 – 11.85 mg.kg^{-1} and 58.5 – 81.5 mg.kg^{-1}. The elemental concentration of As, Cd, Cr, Cu, Hg, Ni, Pb and Zn are 0.64 mg.kg^{-1}, 0.12 mg.kg^{-1}, 9.62 mg.kg^{-1}, 14.87 mg.kg^{-1}, 0.02 mg.kg^{-1}, 16.06 mg.kg^{-1}, 5.60 mg.kg^{-1} and 233.89 mg.kg^{-1} respectively. It is observed that As has low concentration in Kwabenya M/A and high concentration in Ashongman. Cd has low concentration in Taifa community and high concentration in Haatso Calvary Presby. Cr has low concentration in Hillview Montessori and high concentration in Abokobi Presby. Cu has low concentration in Taifa community and high concentration in Dome Anglican. Hg has low concentration in Akporman Model and high

in Ashongman. Pb has low concentration in Ashongman and high concentration in Abokobi Presby. Zn has low concentration in Hillview Montessori and high concentration in Ashongman.

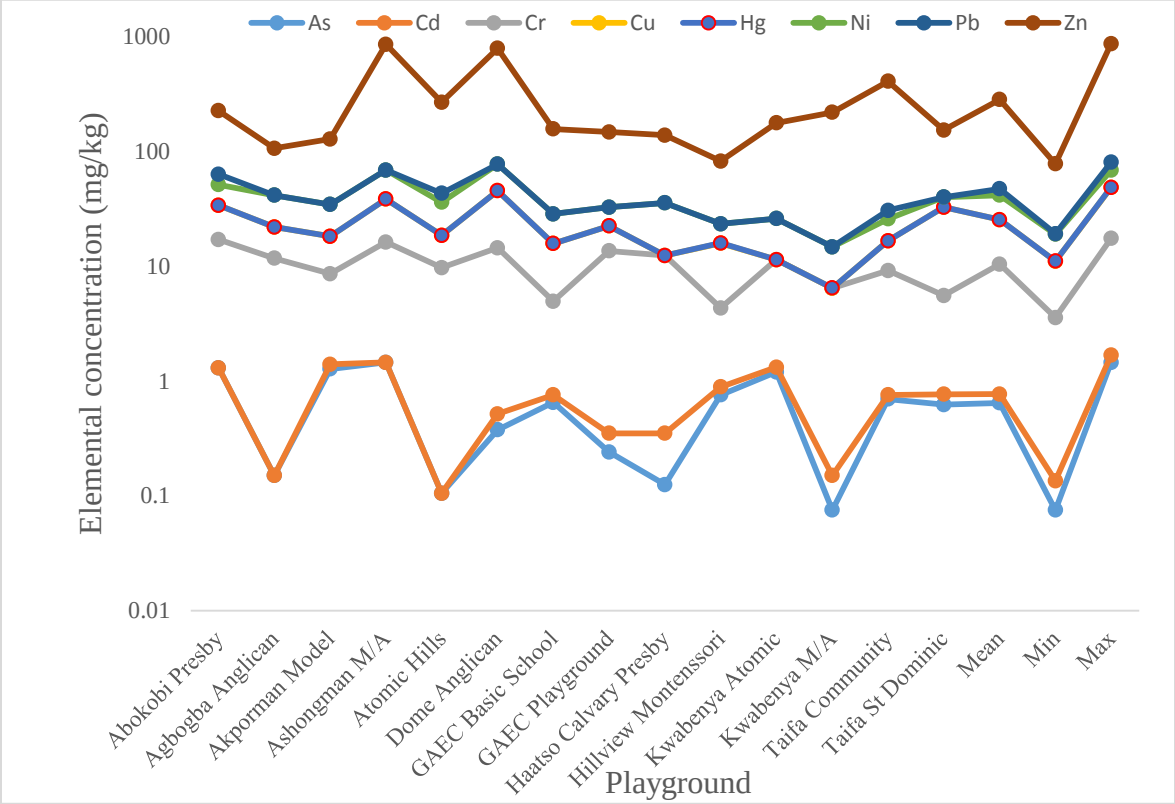

Figure 4.6: Elemental concentrations of As, Cd, Cr, Cu, Hg, Pb and Zn in soil samples

The main descriptive statistic of the comprehensive analysis results are shown in Table 4.10 which is a combination of results obtained by INAA and AAS. Even though straight comparisons of the results of other investigations done in other playgrounds are different by the disparity of playgrounds construction, sampling protocol and sample preparation procedures, the levels of trace elements in the playground soils of basic schools in the Ga East Assembly (with the exception of the common natural trace elements such as Al, Fe, K, Na, Ni, Zn and Ti) are very much lower than those found by other researchers (e.g., De Miguel et al., 2007). This is because in most European developed countries such as Spain, there is a general expectation of heavy traffic emissions as well as industrial activities compared to African country including Ghana (Table 4.9). In this study, the results obtained for all trace elements compare well with the world average concentration in shale (Ebenezer, 2011).

Table 4.9: Comparison of elemental concentrations of the As, Cd, Cr, Cu, Hg, Ni, Pb and Zn from this study with published data

Study	Elemental concentration(mg/kg)								Reference
	As	Cd	Cr	Cu	Hg	Ni	Pb	Zn	
Ghana	0.64	0.12	9.62	14.87	0.02	16.06	5.60	233.89	This study
Spain (2002)	7.30	0.19	20	20	0.24	6.9	38	78	(De Miguel et al., 2007)
Spain (2003)	6.90	0.14	17	14	0.070	5.7	22	50	(De Miguel et al., 2007)
Word average (Shale)	13	0.3	90	45	0.17	68	20	95	(Ebenezer, 2011)

Table 4.10: Summary statistic of the analytical results ($mg.kg^{-1}$)

	Sample Identity (playground)																
	AP	AG	AM	AS	AH	DA	GS	GP	HC	HM	KA	KW	TC	TD	Mean	St.Dev	95% UCL
Al[a]	28010	31080	21305	30610	17240	25770	12790	9761	29840	10970	27860	18730	22040	41150	23368.29	8915.594	27588.053
As[b]	2.3	1.15	2.27	2.45	1.105	1.375	1.65	1.24	0.225	1.755	2.195	1.075	1.695	1.62	1.578929	0.610117	1.8676982
Cd[b]	<0.002	<0.002	0.125	<0.002	<0.002	0.14	0.105	0.11	0.225	0.13	0.12	0.075	0.06	0.145	0.1235	0.044724	0.1446682
Co[b]	0.75	8.7	3.3	7.5	12.45	12.6	12.3	6.3	13.5	5.7	4.65	6.9	7.05	4.8	7.607143	3.869896	9.4387721
Cr[b]	15.72	11.52	7.17	14.67	9.57	13.87	4.17	13.17	11.97	3.42	10.02	6.27	8.37	4.77	9.62	4.048979	11.536389
Cu[b]	16.74	10.14	9.54	22.14	8.79	30.84	10.74	8.79	<0.003	11.49	<0.003	<0.003	7.44	26.94	14.87182	8.157673	18.73286
Fe[b]	23560.7	21575.4	22080.6	24957.6	22676.0	24653.1	21077.6	23813.6	21512.1	20436.0	23558.9	22340.0	22340.0	21704.7	22591.9	1345.5	23228.7
Hg[b]	0.04	0.02	0.01	0.05	0.035	0.012	0.025	0.019	0.025	0.018	0.024	0.019			0.02475	0.011639	0.030259
K[a]	2152	14170	3153	8149	975.3	6773	1054	1381	11290	483.2	7540	1749	4081	1621	4612.25	4302.78	6648.7638
La[a]	18.22	21.47	21.35	22.28	9.89	16.71	4.32	4.73	22.14	3.63	30.27	864	8.4	15.24	75.90357	226.9739	183.33072
Mn[a]	189.8	254.7	193.6	274.7	107.3	278.1	80.45	117.3	239.5	49.63	111.1	165.2	230.7	183.2	176.8057	74.17251	211.9117
Na[a]	636.3	1495	368.4	754.4	417.2	3312	703.4	674.4	1313	343.6	763.2	541.4	1997	373.6	978.0643	826.9683	1369.4699
Ni[b]	17.235	19.485	16.185	29.985	17.385	31.785	12.735	10.185	23.085	7.485	14.535	8.235	9.135	7.335	16.05643	7.904009	19.797411
Pb[b]	11.85	<0.001	<0.001	0.15	7.05	<0.001	<0.001	<0.001	<0.001	<0.001	<0.001	<0.001	4.8	<0.001	5.6	5.890883	8.3881658
Ti[a]	3010	2829	2475	3409	3116	3089	733.9	2173	4957	978	3008	2554	4044	4851	2944.779	1205.868	3515.518
V[a]	75.75	36.21	40.41	34.53	25.66	86.48	66.89	32.45	31.93	20.53	55.01	35.87	33.13	48.98	44.55929	19.59591	53.834067
Zn[b]	162	64.5	93	781.5	223.5	708	127.5	114	102	58.5	150	202.5	375	112.5	233.8929	231.2168	343.32819

[a]Elements analyzed by INAA

[b]Elements analyzed by AAS

4.2.2. Cancer Risk-based Assessment

The risk assessment results of 10 environmental elements of interest are presented in Table 4.11. Arsenic appears to be the largest single contributor to the overall risk, with a value of carcinogenic risk of 3.48E-06. However, this value is below the 1.00E-05 level considered undesirable by most regulatory agencies. Moreover, for non-cancer risk, all the trace elements exhibit a Hazard Index below the threshold value of 1.0. Vanadium is the second largest contributor after aluminum, followed by chromium, manganese, arsenic, lead, nickel, zinc, copper, cadmium and mercury. The hazard indices contributed by these elements are nearly five times the magnitude lower than the regulatory level of 1 (USEPA, 2015). The exposure pathway that scored the highest contribution to the overall figure of risk is found to be ingestion of substrate soil particles followed by dermal absorption of trace elements in these particles. Similar results were obtained by De Miguel et al.,(2007), in a study of risk-based evaluation of the exposure of children in Spain to trace elements.

Table 4.11: Exposure point concentration term (C, mg/kg), reference dose (mg/kg per day) and slope factor (mg/kg per day)$^{-1}$ (from RAIS as of 2015 except Pb, from WHO), and Hazard Quotient and Cancer Risk for each element and exposure route.

Elements	C(95% UCL)	RfD_{ing}	RfD_{inh}	RfD_{der}	HQ_{ing}	HQ_{inh}	HQ_{der}	HQ_{vap}	$HI=\sum HQ_i$	Risk
		SF_{ing}	SF_{inh}	SF_{der}	$Risk_{ing}$	$Risk_{inh}$	$Risk_{der}$			
Al	27588.053	1.00E+00	5.00E-03	1.00E-01	0.071265	1.26E-03	6.98E-03		8.00E-02	
As- non cancer	0.876	3.00E-04	1.50E-05	1.23E-04	7.55E-03	1.33E-05	1.80E-04		7.74E-03	
As-cancer	*0.876*	*1.50E+00*	*1.51E+01*	*3.66E+00*	*3.40E-06*	*3.02E-09*	*8.12E-08*			*3.48E-06*
Cd-non cancer	0.145	1.00E-03	1.00E-05	1.00E-05	3.74E-04	3.30E-06	3.66E-04		7.43E-04	
Cd-cancer	*0.145*		*6.30E+00*			*2.08E-10*				*2.08E-10*
Cr-non cancer	11.536	3.00E-03	1.00E-04	6.00E-05	9.93E-03	2.63E-05	4.87E-03		1.48E-02	
Cr-cancer	*11.536*		*4.20E+01*			*1.10E-07*				*1.10E-07*
Cu	18.733	4.00E-02	4.00E-02	1.20E-02	1.21E-03	1.07E-07	3.95E-05		1.25E-03	
Hg	0.030	1.60E-04	3.00E-05	2.10E-05	4.89E-04	2.30E-07	3.65E-05	1.69E-03	5.25E-04	
Mn	211.912	1.40E-01	5.00E-05	1.84E-03	3.91E-03	9.66E-04	2.92E-03		7.79E-03	
Ni-non cancer	19.797	1.10E-02	1.40E-05	5.40E-03	4.65E-03	3.22E-04	9.28E-05		5.06E-03	
Ni-cancer	*19.797*		*8.40E-01*			*3.79E-09*				*3.79E-09*
Pb	8.388	3.50E-03	3.50E-03	5.25E-04	6.19E-03	5.46E-07	4.04E-04		6.60E-03	
V	53.834	5.04E-03	1.17E-01	7.00E-05	2.76E-02	1.04874E-07	1.95E-02		4.71E-02	
Zn	194.114	3.00E-01	3.00E-01	6.00E-02	1.67E-03	1.47E-07	8.19E-05		1.75E-03	

4.2.3. Pollution Indices

4.2.3.1. Enrichment Factor

The results of the present study show that with the exception of As, Cr, Hg, La, Mn and Ni, most of the trace elements are slightly enriched in the playgrounds soils (Table 4.12 and 4.13). The EF values for Al range from 0.24 to 1.12, Cd from 0.42 to 1.65, Co from 0.08 to 1.56, Cu from 0.35 to 1.31, K from 0.04 to 1.17, Pb from 0.01 to 1.19, Ti from 0.36 to 2.36, V from 0.36 to 1.27 and Zn from 1.31 to 8.34. Overall, the average order of EF values for the elements is Zn (3.24) > Ti (1.33) > Co (0.84) > V (0.71) > Cd (0.62) > Al (0.61) > Cu (0.54) > Ni (0.49) > Mn & Pb (0.43) > K (0.36) > La (0.33) > Cr (0.30) > As (0.10). According to Bhuiyan et al. (2010), EF values between 0.05 and 1.5 specify that the element is totally from crustal materials or natural processes, whereas EF values higher than 1.5 suggest that the sources are likely to be anthropogenic. The authors split the contamination into different categories based on EF values, where EF $\leq$ 2 suggests deficiency to minimal metal enrichment, whereas EF > 2 suggests several degrees of metal enrichment.

4.2.3.2. Geo-accumulation Index

The geo-accumulation index (I_{geo}) was also employed to estimate the degree of metal pollution. The I_{geo} values for the metals of environmental interest are presented in Table 4.11 and 4.12) as -8.02 to -3.75 for As, -2.91 to -1.00 for Cd, -5.30 to -1.60 for Cr, -3.18 to -1.13 for Cu, -5.35 to -3.07 for Hg, -4.68 to -2.20 for Mn, -3.80 to -1.68 for Ni, -3.23 to -0.48 for Ti and -1.28 to 1.40 for Zn. Overall, the average order of I_{geo} values for the metals is Cd (-1.95) > Co (-2.17) > Cu (-2.35) > Ni (-2.83) > Mn (-3.00) > Ti (-3.02) >

Zn (-3.03) > As (-3.22) > Cr (-3.75) > Pb (-3.88) > Hg (-4.23). From observation, the I_{geo} values indicate practically the soils of the investigated schools playgrounds are practically uncontaminated with respect to the measured elements, except Zn which is moderately contaminated. Among the environmentally most toxic metals, Zn is significantly accumulated in the soils, as indicated by their respective average I_{geo} values and its highest value is found in TC (Taifa Community) playground.

4.2.3.3. Contamination Factor

The contamination factors (CFs) of the trace metals of environmental concern are in the following ranges: As (0.006 – 0.112), Cd (0.200 – 0.750), Cr (0.038 – 0.496), Co (0.039 – 0.711), Cu (0.165 – 0.685), Hg (0.059 – 0.294) and Ni (0.108 – 0.467) (Table 4.14). Overall, the average order of CF values for the elements is Cd (0.412) > Co (0.4) > Cu (0.33) > Pb (0.28) > Ni (0.236) > Cr (0.147) > As (0.049). These results indicate that there is no significant contamination found in the soils of playgrounds due to these trace elements.

Table 4.12: Descriptive statistics for enrichment factors and geo-accumulation indices (I_{geo}) of heavy metals for playground soil

Sample ID	Al		As		Cd		Co		Cu		Cr		Fe	
	EF	I_{geo}	EF	I_{geo}	EF	I_{geo}	EF	I_{geo}	EF	I_{geo}	EF	I_{geo}	EF	I_{geo}
AP	0.70	-2.10	0.20	-3.91			0.08	-5.25	0.75	-2.01	0.35	-3.10	1.00	-1.59
AG	0.85	-1.95	0.03	-7.02			1.00	-1.71	0.49	-2.73	0.28	-3.55	1.00	-1.71
AM	0.57	-2.49	0.21	-3.94	0.89	-1.85	0.37	-3.11	0.45	-2.82	0.17	-4.23	1.00	-1.68
AS	0.72	-1.97	0.21	-3.75			0.75	-1.93	0.93	-1.61	0.94	-1.60	1.00	-1.50
AH	0.45	-2.80	0.02	-7.54			1.36	-1.19	0.41	-2.94	0.22	-3.82	1.00	-1.64
DA	0.62	-2.22	0.06	-5.70	0.89	-1.68	1.27	-1.18	1.31	-1.13	0.72	-1.99	1.00	-1.52
GS	0.36	-3.23	0.11	-4.91	0.78	-2.10	1.45	-1.21	0.53	-2.65	0.10	-5.02	1.00	-1.75
GP	0.24	-3.62	0.04	-6.34	0.73	-2.03	0.66	-2.18	0.39	-2.94	0.29	-3.36	1.00	-1.57
HC	0.82	-2.01	0.02	-7.29	1.65	-1.00	1.56	-1.08	0.00		0.29	-3.50	1.00	-1.72
HM	0.32	-3.45	0.13	-4.69	1.00	-1.79	0.69	-2.32	0.59	-2.55	0.09	-5.30	1.00	-1.79
KA	0.70	-2.11	0.18	-4.03	0.80	-1.91	0.49	-2.62			0.22	-3.75	1.00	-1.59
KW	0.49	-2.68	0.01	-8.02	0.53	-2.58	0.77	-2.05			0.15	-4.43	1.00	-1.66
TC	0.58	-2.44	0.11	-4.81	0.42	-2.91	0.78	-2.02	0.35	-3.18	0.20	-4.01	1.00	-1.66
TD	1.12	-1.54	0.10	-4.98	1.05	-1.63	0.55	-2.57	1.30	-1.33	0.12	-4.82	1.00	-1.71
Min	0.24	-3.62	0.01	-8.02	0.42	-2.91	0.08	-5.25	0.35	-3.18	0.09	-5.30	1.00	-1.79
Max	1.12	-1.54	0.21	-3.75	1.65	-1.00	1.56	-1.08	1.31	-1.13	0.94	-1.60	1.00	-1.50
Mean	0.61	-2.47	0.10	-5.49	0.87	-1.95	0.84	-2.17	0.68	-2.35	0.30	-3.75	1.00	-1.65

Table 4.13: Descriptive statistics for enrichment factors and geo-accumulation indices (I_{geo}) of heavy metals for playground soil (continued)

Sample ID	K		La		Mn		Ni		Pb		Ti		V		Zn	
	EF	I_{geo}	EF	I_{geo}	EF	I_{geo}	EF	I_{geo}	EF	I_{geo}	EF	I_{geo}	EF	I_{geo}	EF	I_{geo}
AP	0.16	-4.21	0.40	-2.92	0.45	-2.75	0.51	-2.57	1.19	-1.34	1.31	-1.20	1.17	-1.36	1.31	-1.20
AG	1.17	-1.49	0.51	-2.68	0.66	-2.32	0.63	-2.39			1.35	-1.29	0.61	-2.43	1.49	-1.14
AM	0.25	-3.66	0.50	-2.69	0.49	-2.72	0.51	-2.66			1.15	-1.48	0.66	-2.27	2.09	-0.62
AS	0.58	-2.29	0.46	-2.63	0.61	-2.21	0.83	-1.77	0.01	-7.64	1.40	-1.02	0.50	-2.50	3.61	0.35
AH	0.08	-5.35	0.22	-3.80	0.26	-3.57	0.53	-2.55			1.41	-1.15	0.41	-2.93	4.90	0.65
DA	0.49	-2.56	0.35	-3.05	0.63	-2.20	0.89	-1.68			1.29	-1.16	1.27	-1.17	4.19	0.55
GS	0.09	-5.24	0.11	-5.00	0.21	-3.99	0.42	-3.00			0.36	-3.23	1.15	-1.54	3.01	-0.16
GP	0.10	-4.85	0.10	-4.87	0.27	-3.44	0.30	-3.32			0.94	-1.67	0.49	-2.59	2.38	-0.32
HC	0.93	-1.82	0.53	-2.64	0.62	-2.41	0.74	-2.14			2.36	-0.48	0.54	-2.61	2.36	-0.48
HM	0.04	-6.37	0.09	-5.25	0.13	-4.68	0.25	-3.77			0.49	-2.82	0.36	-3.25	1.42	-1.28
KA	0.57	-2.40	0.66	-2.19	0.26	-3.52	0.43	-2.81			1.31	-1.20	0.85	-1.83	3.16	0.07
KW	0.14	-4.51	0.20	-4.00	0.41	-2.95	0.26	-3.63			1.17	-1.43	0.58	-2.44	4.50	0.51
TC	0.32	-3.29	0.19	-4.04	0.57	-2.47	0.28	-3.48	0.51	-2.64	1.86	-0.77	0.54	-2.56	8.34	1.40
TD	0.13	-4.62	0.36	-3.18	0.47	-2.80	0.23	-3.80			2.29	-0.51	0.82	-1.99	2.58	-0.34
Min	0.04	-6.37	0.09	-5.25	0.13	-4.68	0.23	-3.80	0.01	-7.64	0.36	-3.23	0.36	-3.25	1.31	-1.28
Max	1.17	-1.49	0.66	-2.19	0.66	-2.20	0.89	-1.68	1.19	-1.34	2.36	-0.48	1.27	-1.17	8.34	1.40
Mean	0.36	-3.76	0.33	-3.50	0.43	-3.00	0.49	-2.83	0.57	-3.88	1.33	-1.39	0.71	-2.25	3.24	-0.14

Table 4.14: Metal contamination factors (CFs) for playground soils

Sample ID	Contamination factors (CFs)															
	Al	As	Cd	Co	Cu	Cr	Fe	Hg	K	La	Mn	Ni	Pb	Ti	V	Zn
AP	0.350	0.100		0.039	0.372	0.175	0.499	0.235	0.081	0.198	0.223	0.253	0.593	0.654	0.583	0.653
AG	0.389	0.012		0.458	0.225	0.128	0.457	0.118	0.533	0.233	0.300	0.287		0.615	0.279	0.679
AM	0.266	0.098	0.417	0.174	0.212	0.080	0.468	0.059	0.119	0.232	0.228	0.238		0.538	0.311	0.979
AS	0.383	0.112		0.395	0.492	0.496	0.529	0.294	0.306	0.242	0.323	0.441	0.008	0.741	0.266	1.911
AH	0.216	0.008		0.655	0.195	0.106	0.480	0.206	0.037	0.108	0.126	0.256		0.677	0.197	2.353
DA	0.322	0.029	0.467	0.663	0.685	0.376	0.522	0.071	0.255	0.182	0.327	0.467		0.672	0.665	2.189
GS	0.160	0.050	0.350	0.647	0.239	0.046	0.447	0.147	0.040	0.047	0.095	0.187		0.160	0.515	1.342
GP	0.122	0.018	0.367	0.332	0.195	0.146	0.505	0.112	0.052	0.051	0.138	0.150		0.472	0.250	1.200
HC	0.373	0.010	0.750	0.711		0.133	0.456	0.147	0.424	0.241	0.282	0.339		1.078	0.246	1.074
HM	0.137	0.058	0.433	0.300	0.255	0.038	0.433	0.106	0.018	0.039	0.058	0.110		0.213	0.158	0.616
KA	0.348	0.092	0.400	0.245		0.111	0.499	0.141	0.283	0.329	0.131	0.214		0.654	0.423	1.579
KW	0.234	0.006	0.250	0.363		0.070	0.473	0.112	0.066	0.094	0.194	0.121		0.555	0.276	2.132
TC	0.276	0.053	0.200	0.371	0.165	0.093	0.473		0.153	0.091	0.271	0.134	0.240	0.879	0.255	3.947
TD	0.514	0.048	0.483	0.253	0.599	0.053	0.460		0.061	0.166	0.216	0.108		1.055	0.377	1.184
Min	0.122	0.006	0.200	0.039	0.165	0.038	0.433	0.059	0.018	0.039	0.058	0.108	0.008	0.160	0.158	0.616
Max	0.514	0.112	0.750	0.711	0.685	0.496	0.529	0.294	0.533	0.329	0.327	0.467	0.593	1.078	0.665	3.947
Mean	0.292	0.049	0.412	0.400	0.330	0.147	0.479	0.146	0.173	0.161	0.208	0.236	0.280	0.640	0.343	1.560

4.2.4. Pollution Source Identification

Further evaluation of scope of trace element contamination in the study area and source identification was performed using the Multivariate Statistical Analysis to allow rigorous inspection and evaluation of variability present in voluminous data (Ayivor et al., 2012). Principal Component Analysis (PCA) was used following standard procedures reported in literature (Bhuiyan et al., 2010, 2011). PCA was performed on the logarithmic form of the data. The Varimax Rotation was used to exploit the sum of the variance of the factor coefficients. This technique clusters variables into groups, such that variables going to one group are greatly correlated with one another. The results of the PCA of trace elements contents are shown in Table 4.15.

Table 4.15: Rotated component matrix of six-factor model with moderate to strong loadings in bold typeface

Parameters	PC 1	PC 2	PC 3	PC 4	PC 5	PC 6	Communalities
Al	**0.890**	-0.122	0.065	0.123	-0.212	0.111	0.884
As	-0.062	**0.860**	0.325	0.084	-0.180	0.145	0.91
Cd	-0.390	-0.403	-0.210	0.238	0.402	**0.510**	0.838
Co	-0.055	0.021	0.037	0.039	**0.888**	-0.197	0.833
Cr	0.488	0.467	**0.676**	-0.112	0.087	-0.001	0.934
Cu	-0.081	-0.090	0.218	***-0.884***	-0.205	0.007	0.885
Fe	0.217	0.332	**0.851**	0.016	-0.119	0.124	0.911
Hg	-0.296	**0.874**	-0.020	0.240	0.121	-0.021	0.925
K	**0.852**	0.300	0.074	0.145	0.277	0.120	0.934
La	0.245	0.064	0.175	**0.856**	-0.192	-0.021	0.865
Mn	**0.859**	0.030	0.361	0.058	0.038	0.091	0.882
Na	**0.518**	0.123	0.270	-0.128	**0.592**	0.346	0.843
Ni	0.444	**0.783**	0.243	-0.138	0.184	0.073	0.927
Ti	**0.797**	-0.255	0.308	0.222	-0.066	-0.166	0.876
V	0.206	0.188	0.213	-0.071	-0.214	**0.873**	0.936
Zn	0.194	0.029	**0.915**	-0.030	0.171	0.075	0.911
Eigenvalues	4.037	2.843	2.659	1.78	1.684	1.292	
% of variance	25.23	17.769	16.617	11.123	10.528	8.073	
Cumulative %	25.23	42.998	59.616	70.739	81.267	89.34	

Six variation factors (Vfs) or (PCs) with eigenvalues greater than 1 were extracted. PCA leads to a reduction of the initial dimension of the dataset to six components which explain 89 % of the data variation. Therefore, these six factors play a significant role in explaining trace element contamination in the study area.

Principal component 1 (PC1), which has the highest loadings of Al, K, Mn, Na and Ti and accounts for 25 % of variance (Table 4.15) can be a measure of leaching of crustal components. PC 2, which has positive loadings of As, Hg and Ni, accounts for 17 % of variance and these elements may have originated from both natural sources through weathering of minerals and ores, and anthropogenic sources through industrial processes as byproducts of the smelting process. Also, the level of mercury in the environment can increase due to incineration of municipal and medical waste as well as from a global reservoir of airborne mercury. To the best knowledge of the student or author, there has not been any report of mineral deposits in the study area and, therefore, natural sources for As, Hg and Ni may be ruled out. PC 3 has positive loadings of Cr, Fe and Zn and account for 16 % of variance. PC 4 is positively loaded with La and negatively loaded with Cu and account for 11 % of variance. PC 5 accounts for 10 % of variance and has a positive loading of Co and Na whereas PC 6 has a positive loading of Cd and V and accounts for 8 % of variance. The concentrations of these elements in soils result from natural sources and from vehicular emissions, especially Cr and Zn. Chromium comes from emissions of chromium-based automotive catalytic converters and cement dust, and high Zn content in the soils may come from gasoline, car components, oil lubricants, industrial emissions, and traffic sources particularly vehicle tyres.

Based on information evaluated from Principal Component Analysis, hierarchical cluster analysis was executed (Ayivor et al., 2012; Bhuiyan et al., 2010, 2011). Cluster analysis (CA) was performed on the analyzed parameters with Ward's method and the squared Euclidean distance as a similarity measure. Figure 4.7 shows that four main clusters can be distinguished in the dendrogram acquired from the CA. Cluster 1 includes elements Al, K, La, Mn and Ti, which in the previous discussion were recognized as natural elements from crustal origin. Cluster 2 comprises As, Hg and Ni which are identified as result of atmospheric pollution. Cluster 3 involves elements Cd, Co and Na which previously identified as a result of particulate matters emitted from the geologic media. Cluster 4 consists of elements Cr, Cu, Fe, V and Zn which are said to be derived from both natural and traffic sources as most of the playgrounds are close to the road.

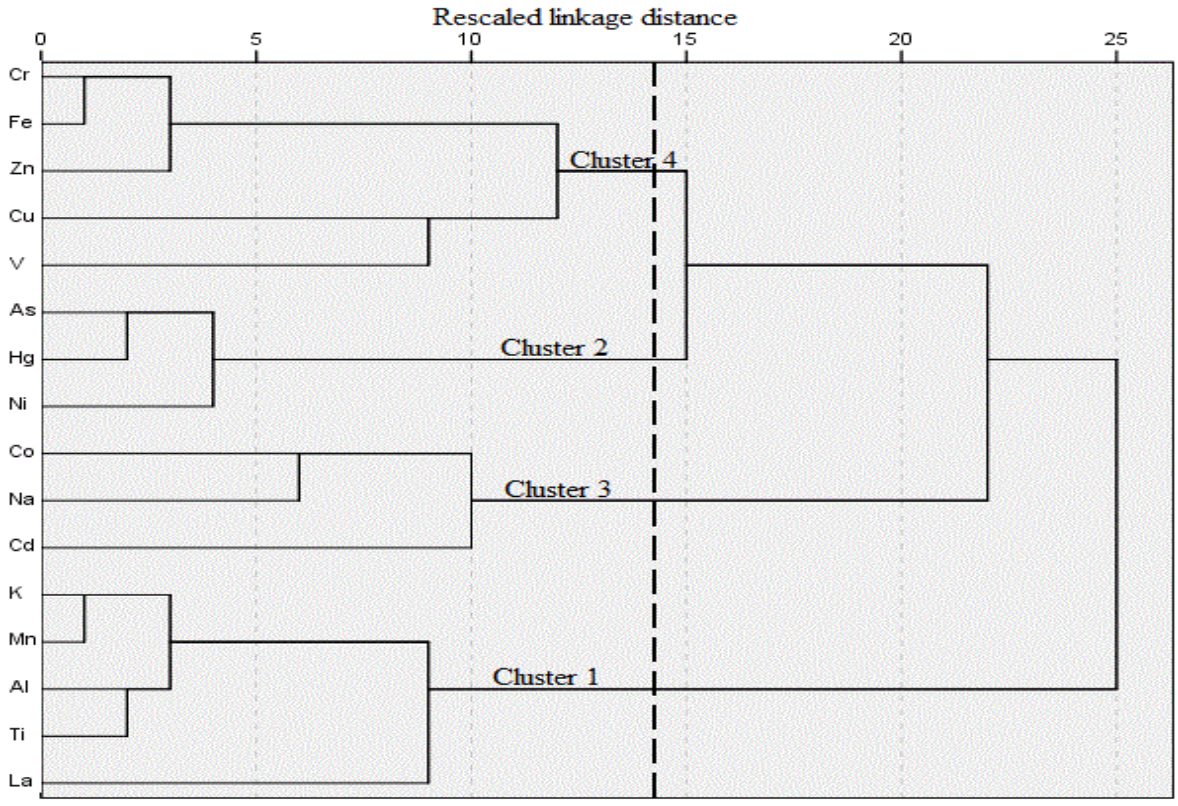

Figure 4.7: Dendogram acquired by hierarchical clustering analysis for parameters

Similarly, sampling points were also analyzed by clustering methods using factor analysis (FA) to determine the structure in the data set and to investigate the relationship between the sampling points and their elemental concentration (Table 4.16). This was organized in the dendrogram to identify the identical geochemical groups (Figure 4.8).

The sampling points AG, AH, AM, AP, GP, HC, KA and KW are clustered in Group 1. Group 2 contains As and DA. The sampling points GS and HM are included in Group 3, whereas Group 4 contains TC and TD.

Table 4.16: Scores for the six-factor model for sampling sites relatively high scores in bold typeface

Sample ID	PC 1	PC 2	PC 3	PC 4	PC 5	PC 6
AP	0.482	0.650	0.143	-0.570	-2.489	0.744
AG	**1.558**	**1.004**	-1.447	-0.658	0.203	-0.628
AM	0.010	0.400	-0.669	0.067	-0.790	0.311
AS	0.608	0.742	**1.770**	-0.367	-0.126	-1.197
AH	-0.532	0.443	0.510	-0.433	-0.049	-1.957
DA	0.339	0.422	**1.588**	-0.446	**1.255**	**1.741**
GS	-1.407	0.550	-0.822	-0.799	0.651	**1.402**
GP	-1.234	0.253	0.606	-0.366	0.290	-0.129
HC	**1.271**	0.156	-1.163	**0.944**	**1.494**	-0.289
HM	-1.776	-0.603	-1.156	-0.560	0.165	-0.824
KA	0.129	0.545	-0.234	**1.286**	-0.150	**0.831**
KW	-0.702	-0.264	0.516	**2.760**	-0.323	-0.257
TC	0.661	-1.893	0.630	-0.653	**0.842**	-0.126
TD	0.593	-2.405	-0.273	-0.206	-0.973	0.378

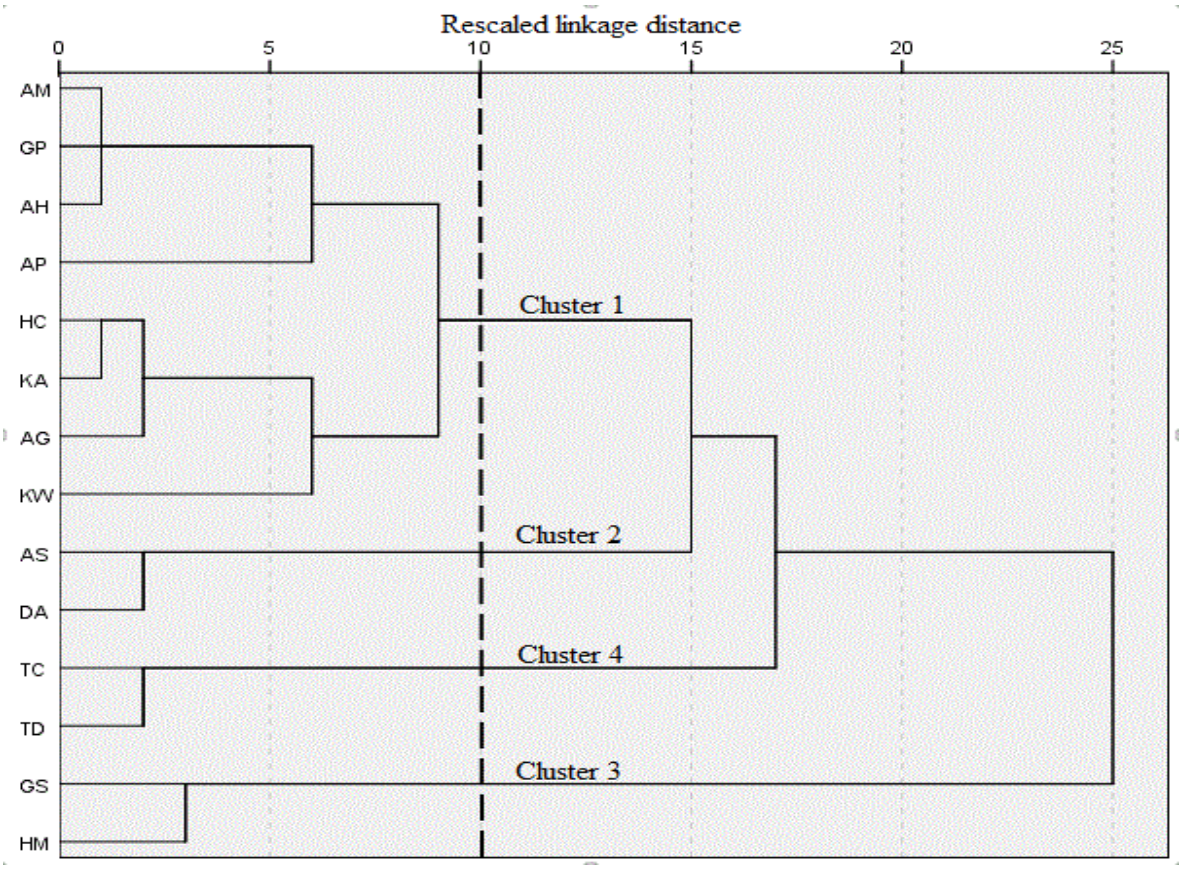

Figure 4.8: Tree diagram acquired by clustering of sampling sites

Table 4.17: Elemental characteristics of the analyzed soils from playgrounds as depicted by and R-mode principal component

AG	AP	AS	AH	DA	GS	GP	HC	KA	KW	TC	TD
Al	As	Al	Cr	Cr	As	Cr	Al	As	Cr	Al	Al
K	Hg	K	Fe	Fe	Hg	Fe	K	Hg	Fe	K	K
Mn	Ni	Mn	Zn	Zn	Ni	Zn	Mn	Ni	Zn	Mn	Mn
Na		Na		Co	Co		Na	La	La	Na	Na
Ti		Ti		Na	Na		Ti	Cd		Ti	Ti
As		As		Cd	Cd		La	V		Cr	
Hg		Hg		V	V		Co			Fe	
Ni		Ni					Na			Zn	
		Cr								Co	
		Fe								Na	
		Zn									

The following elemental associations obtained from PCA and CA are Al-K-Mn-Na-Ti, which could be linked to geogenic source, appear to be common markers for sampling points such as AG, AS, HC, TC and TD (Table 4.17). Also, As-Hg-Ni associations are common markers for AG, AP, AS, GS and KA. The association of Cr-Fe-Zn which may have resulted from traffic emissions are observed to be common markers for the sampling points AS, AH, DA, GP, KW and TC. These observations suggest that most of these sampling points (playgrounds) share same characteristics, as it is clearly illustrated in the tree diagram (Figure 4.8).

CHAPTER 5

CONCLUSIONS AND RECOMENDATIONS

In this chapter, the general conclusions are drawn from the results obtained in this study and necessary recommendations to the next relevant researchers are made.

5.1. Conclusions

The study considered the evaluation of NORMs and trace elements in the playgrounds of basic schools in the Ga East District of the Greater Accra Region of Ghana in terms of exposure of children and the whole public to NORMs and trace elements. In this study, the cancer risk assessments, soil pollution indices, pollution identification, estimation of future doses were also carried out.

The mean activity concentrations of ^{238}U, ^{232}Th and ^{40}K, were estimated to be 19.8 $\pm$ 8.7, 29.1 $\pm$ 16.3 and119.4 $\pm$ 97.9 $Bq.kg^{-1}$ respectively. The results in this study compared well with the worldwide average activity concentrations [35 $Bq.kg^{-1}$ for ^{238}U; 30 $Bq.kg^{-1}$ for ^{232}Th and 400 $Bq.kg^{-1}$ for ^{40}K] (UNSCEAR, 2000). The mean annual effective dose estimated from direct external gamma ray exposure from natural radioactivity concentrations in soil is estimated to be 0.039 mSv/year. This value is lower than the 1 mSv/year dose limit recommended by the ICRP for public radiation exposure control (ICRP, 2007) and indicates that there is no significant radiological hazard to the public. The decrease in exposure is observed from estimated future annual effective doses in the study areas. The results obtained from cancer risk assessment performed according to ICRP method shows no significant hazard to the whole public. The activity concentration

of ^{222}Rn in soil in the absence of transportation and the exhalation rate were estimated and they compared well with the world average values suggested by UNSCEAR (2000).

The levels of trace elements in the soils from playgrounds are lower than the world average concentrations in shales, and are significantly lower than the concentrations found in similar studies in other cities of other countries, such as Spain (De Miguel et al., 2007). The results of a risk assessment indicate that the amount of carcinogenic risk is below the level deemed unacceptable by most regulatory agencies and the aggregate of non-cancer risk is below the unit 1. Although the figures of risk could be affected by the estimation of exposure factors and the toxicity data used, the risk assessment has proven to be a very useful means to explain the exact meaning and significance of the concentrations of trace elements found in urban media.

Several useful tools, methods and indices have been used for evaluation of soil pollution in the playgrounds soils. The metal enrichment factor (EF) and geo-accumulation index (I_{geo}) of most of the metals (As, Cd, Cr, Mn, Ni, Pb, Ti and Zn) show that the soils in the study area are uncontaminated to moderately contaminated (Zn), whereas other (Cr, La, Mn and Ni) indicate crustal origin. Contamination factors of all trace elements suggest no contamination except Ti and Zn that suggest none to medium contamination. Multivariate analysis (PCA, CA) used in this study offered essential tools for better understanding of the source identification and dynamics of pollutant. The PCA applied on the investigated heavy metals identified six components. Among them, PC1 loaded with Al, K, Mn, Na and Ti are derived from crustal origin. The others PC2, PC3, PC4, PC5 and PC6 are loaded with metals that are from either crustal origin or anthropogenic activities. Four main clusters of elements are acquired by CA. The first cluster is considered to be of

geogenic sources, which contains Al, K, La, Mn and Ti. Second, third and fourth clusters which are loaded with As, Cd, Cu, Co, Cr, Fe, Hg, Na, Ni, V and Zn are mainly attributed to anthropogenic sources with some contributions from natural sources.

5.2. Recommendations

Based on the research findings from this study, the concluding comments underlined some aspects in order to improve on future studies. Therefore, the following recommendations are made.

5.2.1. Researchers

- The annual effective dose in basic school playing ground was found to be below the recommended dose limit per year. There is a need to follow up on future annual effective dose in order to validate the model used.
- Children's background exposures such as dietary intake, inhalation of dust at home were not accounted for in this study. Therefore it should be considered to enable calculation of overall risk to children.
- Scientific community should consider sampling at monthly to yearly interval in order to observe the seasonal trend of potentially toxic trace elements in the soils of schools playgrounds.
- Researchers should also consider other part of Greater Accra especially Ga West which was not covered in this study.

5.2.2. Basic School Managements (Ga East district)

- Basic School Managements should consider proper constructions of their play grounds. This involves introducing grass playing fields in order to avoid dust inhalable by children during their games at schools.

5.2.3. Regulators

- Regulatory bodies of Ghana should use results from this study for authorities' regulation purposes.

REFERENCES

Adriano, D. C. (2001). *Trace elements in terrestrial environments: biogeochemistry, bioavailability, and risks of metals*. Springer. Retrieved from http://books.google.com/books?hl=en&lr=&id=H17Tw8NujfYC&oi=fnd&pg=PR7&dq=trace+elements&ots=zCMuCa2QTe&sig=KZXwJMXSSu4YG3KZ3pp1HSbU6XA

Adriano, D. C. (n.d.). Trace elements in the terrestrial environment, 1986. *Spring-Verlag, New York*.

Aguko, W. (2013). Assessment of radiation exposure levels associated with gold mining in Sakwa Wagusu, Bondo district, Kenya. In *Scientific Conference Proceedings*. Retrieved from http://elearning.jkuat.ac.ke/journals/ojs/index.php/jscp/article/view/1047

Al-Kinani, A., Al Dosari, M., Amr, M. A., Al-Saad, K. A., & Helal, A. I. (2012). Radioactivity measurements and risk assessments in soil samples at south and middle of Qatar.

Almeida, S. M., Canha, N., Silva, A., Freitas, M. do C., Pegas, P., Alves, C., … Pio, C. A. (2011). Children exposure to atmospheric particles in indoor of Lisbon primary schools. *Atmospheric Environment*, *45*(40), 7594–7599.

Ayivor, J. E., Okine, L. K. N., Dampare, S. B., Nyarko, B. J. B., & Debrah, S. K. (2012). The application of Westcott Formalism k 0 NAA method to estimate short and medium lived elements in some Ghanaian herbal medicines complemented by AAS. *Radiation Physics and Chemistry*, *81*(4), 403–409.

Baba, A., Bassari, A., Erees, F., & Cam, S. (2004). Natural radioactivity and metal concentrations in soil samples taken along the Izmir-Ankara E-023 highway, Turkey. Retrieved from http://inis.iaea.org.sci-hub.org/search/search.aspx?orig_q=RN:35106161

Bhuiyan, M. A., Parvez, L., Islam, M. A., Dampare, S. B., & Suzuki, S. (2010). Heavy metal pollution of coal mine-affected agricultural soils in the northern part of Bangladesh. *Journal of Hazardous Materials*, *173*(1), 384–392.

Bhuiyan, M. A., Rakib, M. A., Dampare, S. B., Ganyaglo, S., & Suzuki, S. (2011). Surface water quality assessment in the central part of Bangladesh using multivariate analysis. *KSCE Journal of Civil Engineering*, *15*(6), 995–1003.

Boamponsem, L. K., Adam, J. I., Dampare, S. B., Nyarko, B. J. B., & Essumang, D. K. (2010). Assessment of atmospheric heavy metal deposition in the Tarkwa gold mining area of Ghana using epiphytic lichens. *Nuclear Instruments and Methods in Physics Research Section B: Beam Interactions with Materials and Atoms*, *268*(9), 1492–1501.

Cember, H., & Johnson, T. E. (2009). *Introduction to health physics*. New York: McGraw-Hill Medical. Retrieved from http://search.ebscohost.com/login.aspx?direct=true&scope=site&db=nlebk&db=nlabk&AN=268784

Cember, H., & Thomas, E. J. (2009). *Introduction to Health Physics* (4th ed.). McGraw-Hill Companies, Inc.

Choppin, G. R., Liljenzin, J.-O., & Rydberg, J. (2002). *Radiochemistry and nuclear chemistry*. Butterworth-Heinemann. Retrieved from

http://books.google.com/books?hl=en&lr=&id=IsAEjPpvyrkC&oi=fnd&pg=PP2&dq=Radioch,+emistry++and++Nuclear+Chemistry&ots=ZR-Yudqfwp&sig=M-i3uLggwJB0ZdhebnGVXvSmxbY

Darko, E. O., & Faanu, A. (2008). Baseline radioactivity measurements in the vicinity of a gold processing plant. *Journal of Applied Science and Technology*, *12*(1), 18–24.

Darko, E. O., Tetteh, G. K., & Akaho, E. H. K. (2005). Occupational radiation exposure to norms in a gold mine. *Radiation Protection Dosimetry*, *114*(4), 538–545.

De Miguel, E., Iribarren, I., Chacon, E., Ordonez, A., & Charlesworth, S. (2007). Risk-based evaluation of the exposure of children to trace elements in playgrounds in Madrid (Spain). *Chemosphere*, *66*(3), 505–513.

Diab, H. M., Nouh, S. A., Hamdy, A., & El-Fiki, S. A. (2008). Evaluation of natural radioactivity in a cultivated area around a fertilizer factory. *J Nucl Radiat Phys*, *3*(1), 53–62.

Ebdon, L., & Evans, E. H. (Eds.). (1998). *An introduction to analytical atomic spectrometry*. Chichester ; New York: John Wiley.

Ebenezer, K. . (2011). *Pesticide Residues and Levels of Some Metals In Soils and Cocoa Beans in Selected Farms in the Kade Area of the Eastern Region of Ghana*. Kwame Nkrumah University of Science and Technology (M.Sc Thesis, June 2011), Kumasi.

EPA, U. (2002). *Child-specific exposure factors handbook*. US Environmental Protection Agency Washington.

Evans E.H., Ebdon L., Fisher A.S., & Hill S.J. (1998). *An Introduction to Analytical Atomic Spectrometry*. Baffins Lane, Chichester, West Sussex PO19UD, England: John Wiley & Sons Ltd.

Faanu, A. (2011). *Assessment of Public Exposure to Naturally Occurring Radioactive MaterialsFrom Mining and Mineral Processing Activities Of Tarkwa Goldmine in Ghana*. Kwame Nkrumah University of Science and Technology (Ph.D Thesis, Febbruary 2011), Kumasi.

Faanu, A., Darko, E. O., & Ephraim, J. H. (2012). Determination of Natural Radioactivity and Hazard in Soil and Rock Samples in a Mining Area in Ghana. *West African Journal of Applied Ecology*, *19*(1). Retrieved from http://www.ajol.info/index.php/wajae/article/download/77568/68009

Faanu, A., Ephraim, J. H., & Darko, E. O. (2010). Assessment of public exposure to naturally occurring radioactive materials from mining and mineral processing activities of Tarkwa Goldmine in Ghana. *Environmental Monitoring and Assessment*, *180*(1-4), 15–29.

Faweya, E. B., Alabi, F. O., & Adewumi, T. (2014). Determination of radioactivity level and hazard assessment of unconsolidated sand and shale soil samples from petroleum oil field at Oredo (Benin, Niger Delta-Nigeria). *Archives of Applied Science Research*, *6*(2), 76–81.

Gbadago, J. K., Faanu, A., Darko, E. O., & Schandorf, C. (2011). Investigation of the environmental impacts of naturally occurring radionuclides in the processing of sulfide ores for gold using gamma spectrometry. *Journal of Radiological Protection*, *31*(3), 337–352. http://doi.org/10.1088/0952-4746/31/3/003

Gupta, M., Chauhan, R. P., Garg, A., Kumar, S., & Sonkawade, R. G. (2010). Estimation of radioactivity in some sand and soil samples. *Indian Journal of Pure and Applied Physics*, *48*(7), 482–485.

Hagedorn, B., Harwart, S., van der Loeff, M. M. R., & Melles, M. (1999). Lead-210 dating and heavy metal concentration in recent sediments of Lama Lake (Norilsk Area, Siberia). In *Land-Ocean Systems in the Siberian Arctic* (pp. 361–376). Springer. Retrieved from http://link.springer.com.sci-hub.org/chapter/10.1007/978-3-642-60134-7_31

Hamdy, A., Diab, H. M., El-Fiki, S. A., & Nouh, S. A. (2008). Natural radioactivity in the cultivated land around a fertilizer factory.

Harvey, D. (2000). *Modern analytical chemistry*. Boston: McGraw-Hill.

IAEA. (2003). *Extent of Environmental Contamination by Naturally Occurring Radioactive Material (NORM) and Technological Options for Mitigation* (IAEA-TECDOC No. 419). Vienna, Austria.

IAEA. (2011). *Radiation Protection and Safety of Radiation Sources: International Basic Safety Standards* (General Safety Requirements Part 3 No. GSR Part 3 (Interim)). Vienna, Austria.

ICRP. (2007). *Recommendations for a System of Radiological Protection* (No. 103).

International Atomic Energy Agency. (2011). *Exposure of the Public from Large Deposits of Mineral Residues* (IAEA-TECDOC-1660). Vienna.

IPCS. (2002). *Principles and Methods for the Assement of Risk from essential trace Elements* (INTERNATIONAL PROGRAMME ON CHEMICAL SAFETY No. 228).

James Martin. (2006). *Physics for Radiation Protection: A Handbook* (2nd ed.). Weinheim: WILEY-VCH Verlag GmbH & Co. KGaA.

Jolliffe, I. (2002). *Principal component analysis*. Wiley Online Library.

Kabata-Pendias, A. (2010). *Trace elements in soils and plants*. CRC press. Retrieved from http://books.google.com/books?hl=en&lr=&id=Nowwb0xl9fYC&oi=fnd&pg=PA1&dq=trace+elements&ots=JHbMf9bbwp&sig=t627SvEKCRecx5ME8YaJxL5fjWI

Khandaker, M. U. (2011). High purity germanium detector in gamma-ray spectrometry. *International Journal of Fundamental Physical Sciences*, *1*(2).

Knoll, G. F. (2010). *Radiation detection and measurement*. John Wiley & Sons.

Landsberger, S. (1994). *Delayed instrumental neutron activation analysis*. John Wiley, Chichester.

Li, X., Poon, C., & Liu, P. S. (2001). Heavy metal contamination of urban soils and street dusts in Hong Kong. *Applied Geochemistry*, *16*(11), 1361–1368.

Meza-Figueroa, D. (2007). Heavy metal distribution in dust from elementary schools in Hermosillo, Sonora, México. *Atmospheric Environment*, *41*(2), 276–288.

Nichols, A., Aldama, D., & Verpelli, M. (n.d.). *HANDBOOK OF NUCLEAR DATA FOR SAFEGUARDS: DATABASE EXTENSIONS, AUGUST 2008 (International Atomic Energy Agency, International Nuclear Data Committee, 2008)*.

Osvath, L. (2008). *Basic hands-on gamma calibration for low activity environmental levels* (Radiometrics Laboratory). Marine Environment Laboratories, Monaco.

Oyedele, J. A. (2006). Assessment of the natural radioactivity in the soils of Windhoek city, Namibia, Southern Africa. *Radiation Protection Dosimetry*, *121*(3), 337–340. http://doi.org/10.1093/rpd/ncl025

Oyedele, J. A., & Shimboyo, S. (2013). Distribution of radionuclides and radiation hazard assessment in soils of Southern Namibia, Southern Africa. *Radiation Protection Dosimetry*, *156*(3), 343–348. http://doi.org/10.1093/rpd/nct081

Oyedele, J. A., Sitoka, S., & Davids, I. (2008). Radionuclide concentrations in soils of Northern Namibia, Southern Africa. *Radiation Protection Dosimetry*, *131*(4), 482–486. http://doi.org/10.1093/rpd/ncn194

Rubio, B., Nombela, M. A., & Vilas, F. (2000a). Geochemistry of major and trace elements in sediments of the Ria de Vigo (NW Spain): an assessment of metal pollution. *Marine Pollution Bulletin*, *40*(11), 968–980.

Rubio, B., Nombela, M. A., & Vilas, F. (2000b). Geochemistry of major and trace elements in sediments of the Ria de Vigo (NW Spain): an assessment of metal pollution. *Marine Pollution Bulletin*, *40*(11), 968–980.

Sey, M. (2014). *Characteristic of Mine Waste and Radiation Dose Reconstruction of a Historical Mine of Konongo-Odomase in the Ashanti Region, Ghana*. University of Ghana (M.Phil Thesis, June 2014), Accra.

Shakeri, A., Moore, F., & Modabberi, S. (2009). Heavy metal contamination and distribution in the Shiraz industrial complex zone soil, South Shiraz, Iran. *World Applied Sciences Journal*, *6*(3), 413–425.

Shimboyo, S. (2012). *Natural Radioactivity in Soils of The Walvis Bay – Henties Bay Coastal Area, Namibia. University of Namibia, Windhoek*. University of Namibia (M.Sc Thesis, December 2012), Windhoek.

UNSCEAR. (1993). *Sources and effects of Ionizing Radiation*.

UNSCEAR. (2000a). *Biological effects at low radiation doses* (No. 2).

UNSCEAR. (2000b). *Exposures from natural radiation sources, 2000 Report to General Assembly*. Annex B, Ney York.

US EPA. (2002). *Calculating Upper Confidence Limits for Exposure Point Concentration at Hazardous Waste Sites*. Washington, D.C. 20460: Office of Emergency and Remedial Response.

US EPA, O. (n.d.). Cadmium Compounds | Technology Transfer Network Air Toxics Web site | US EPA. Retrieved December 4, 2014, from http://www.epa.gov/ttnatw01/hlthef/cadmium.html

USEPA. (1993). *Diffuse NORM waste characterisation and preliminary risk assessment*. US Environmental Protection Agency. Office of Radiation and Indoor Air.

USEPA. (2015). Integrated Risk Information System (IRIS).

USEPA, E. (1997). Exposure factors handbook. *Office of Research and Development, Washington*.

Vanmarcke, H. (2002). UNsCEAR 2000: sources of ionizing radiation. *Annalen van de Belgische Vereniging Voor Stralingsbescherming*, *27*(2), 41–65.

Win, D. (2004). Neutron activation analysis (NAA). *AU J Technol*, *8*(1), 8–14.

WNA. (2011). *Nuclear Radiation and Health Effects*.

Wong, J. W. C., & Mak, N. K. (1997). Heavy metal pollution in children playgrounds in Hong Kong and its health implications. *Environmental Technology*, *18*(1), 109–115.

Yaqin, J. I., Yinchang, F., Jianhui, W. U., Tan, Z. H. U., Zhipeng, B. A. I., & Chiqing, D. (2008). Using geoaccumulation index to study source profiles of soil dust in China. *Journal of Environmental Sciences*, *20*(5), 571–578.

Accra. (2015). In *Wikipedia*. Wikipedia, The Free Encyclopedia. Retrieved from https://en.wikipedia.org/wiki/Accra

APPENDICES

APPENDIX I

A certificate for a standard source used

CZECH METROLOGY INSTITUTE
INSPECTORATE FOR IONIZING RADIATION
Radiová 1, 102 00 Praha 10

CERTIFICATE

Cert. No: 9031 - OL - 146/14 Type: MBSS 2 Prod. No: 050214-1425039

Radionuclide	Half life days	Activity kBq	Combined standard uncertainty, %
Am-241	157800	4,694	1,1
Cd-109	462,6	14,54	1,4
Ce-139	137,5	1,355	1,1
Co-57	271,26	1,156	1,1
Co-60	1925,4	2,697	1,1
Cs-137	11019	2,689	1,3
Sn-113	115,1	4,000	2,2
Sr-85	64,78	4,570	1,5
Y-88	106,6	5,323	1,2

Mass: 980,0 g Density: 0,98 g/cm^3 Volume: 1000 cm^3

Radionuclide inpurities: gamma < 0,1 %

Reference date: 20.3.2014 Homogeneity better than: 1 %

Description:

Radioactive material is homogeneously dispersed in silicone resin. Composition of the matrix: C - 0,324 H - 0,0816 O - 0,216 Si - 0,379 (mass ratio).

Measuring method:

Preparation issues from standard ER solutions whose activities were determined by suitable absolute method. Final control is based on gamma spectrometry on HPGe detector.

Note:

As the criterion of homogeneity standard deviation of the acivity value of 1 cm^3 element was chosen (n=10). The volume is calculated from the mass and the density.

Date of the cetificate issue: 25.2.2014 Validity: 3 years

Customer:
CANBERRA-PACKARD CENTRAL EUROPE
Wienersiedlung 6
A-2432 Schwadorf
Austria

Český metrologický institut

Ing. Jiří Suráň, MBA
director

Control: RNDr. Richard Bluďovský, CSc., RNDr. Pavel Dryák, CSc.

Tel.: +420 266 020 497 Fax: +420 266 020 466

APPENDIX II

Example of a photo peak of ^{238}U acquired by Gennie 2000 software

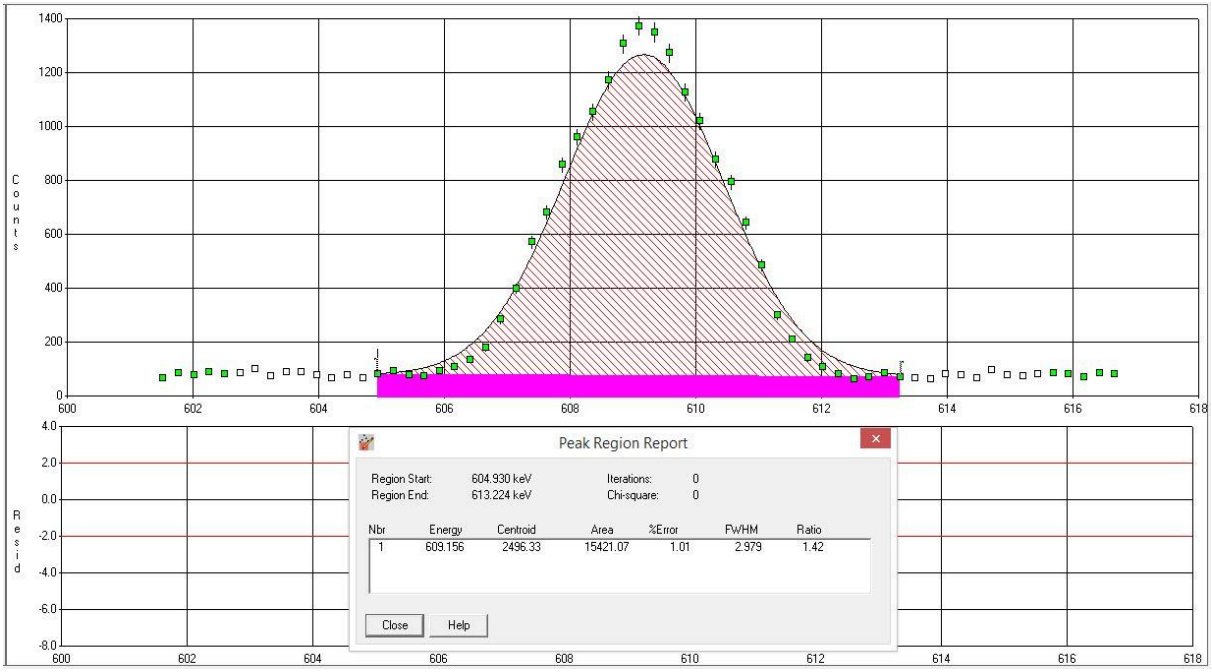

Example of a photo peak of ^{232}Th acquired by Gennie 2000 software

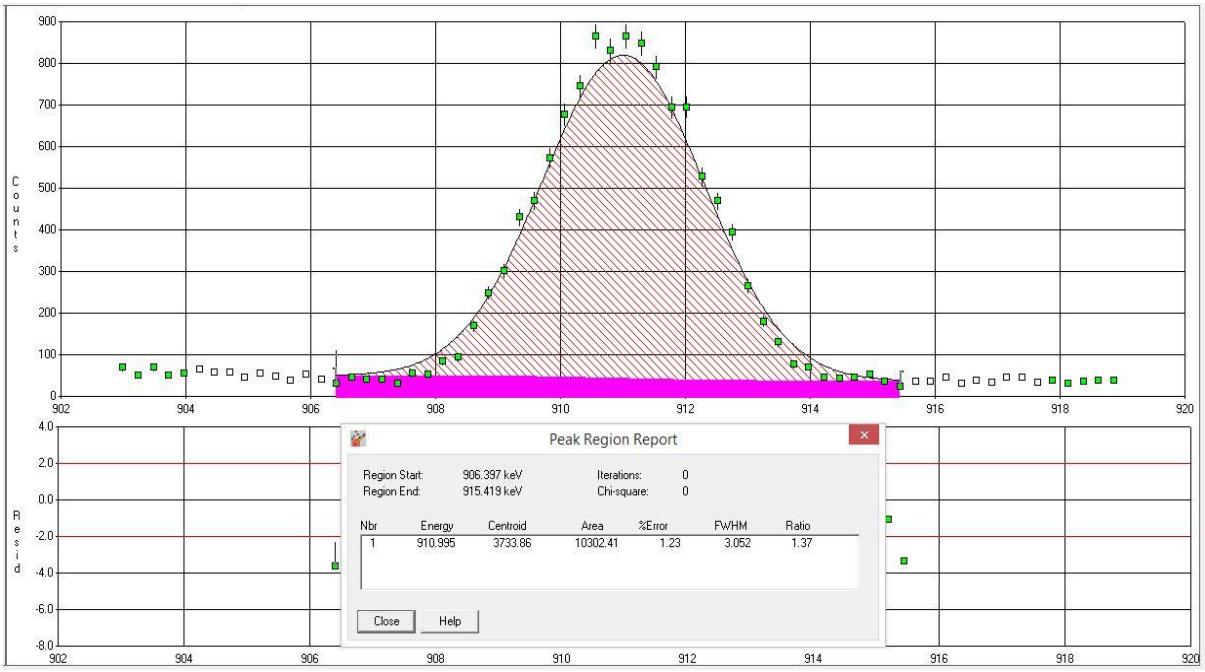

Example of a photo peak of ^{40}K acquired by Gennie 2000 software

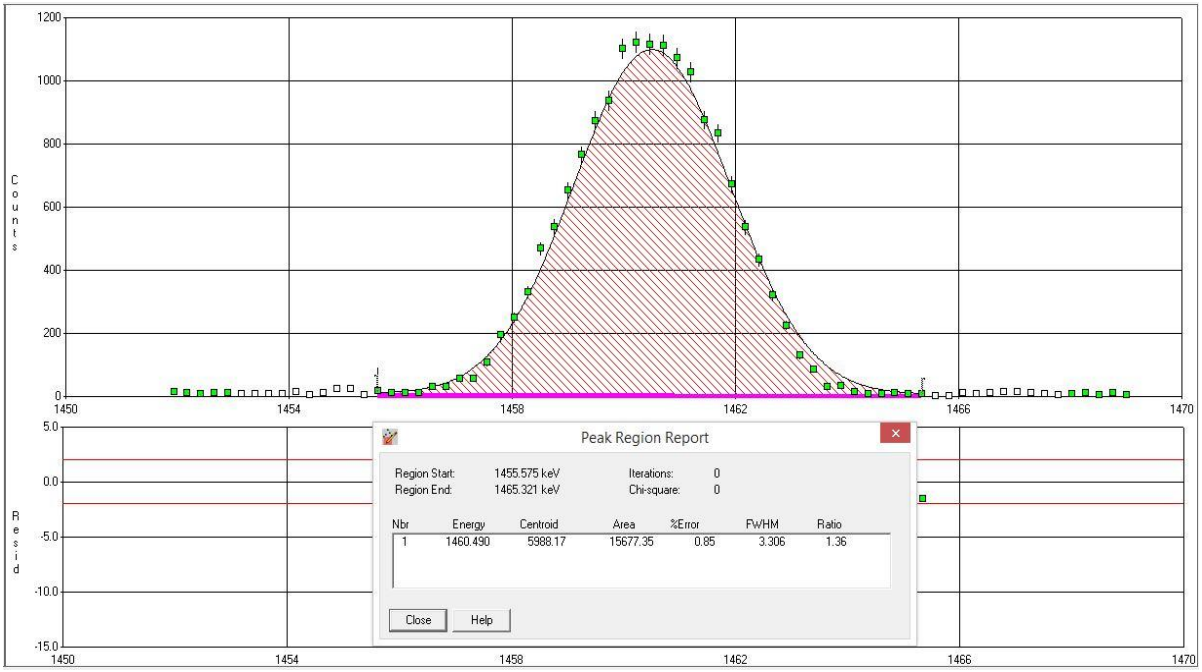

APPENDIX IV

Activity concentration of ^{238}U, ^{232}Th and ^{40}K in soil samples

Sample ID	School	Activity concentration (Bq/kg)		
		^{238}U	^{232}Th	^{40}K
AP	Abokobi Presby	21.9 ± 1.5	37.9 ± 1.4	63.7 ± 6.8
AG	Agbogba Anglican	40.3 ± 3.1	66.4 ± 1.5	342.2 ± 35.6
AP	Akporman Model	16.1 ± 0.5	23.2 ± 1.0	85.2 ± 9.0
AS	Ashongman M/A	26.9 ± 1.5	41.6 ± 3.2	269.1 ± 28.1
AH	Atomic Hills	10.5 ± 0.5	9.2 ± 1.7	20.4 ± 2.3
DA	Dome Anglican	25.5 ± 1.4	23.9 ± 4.1	142.0 ± 14.8
GS	GAEC Basic School	23.2 ± 1.3	32.1 ± 0.3	67.8 ± 7.2
GP	GAEC Playing Ground	17.4 ± 1.3	28.8 ± 0.6	103.5 ± 10.9
HC	Haatso Calvary Presby	23.5 ± 1.1	40.9 ± 2.5	219.5 ± 22.9
HM	Hillview Montessori	11.5 ± 0.6	14.8 ± 1.4	24.4 ± 2.7
KA	Kwabenya Atomic M/A	27.2 ± 1.2	45.8 ± 2.1	170.1 ± 17.8
KW	Kwabenya M/A	9.7 ± 1.5	9.5 ± 1.9	47.9 ± 5.1
TC	Taifa Community	10.2 ± 0.6	12.3 ± 2.4	78.4 ± 8.3
TD	Taifa St Dominic	13.7 ± 0.4	20.6 ± 1.5	37.3 ± 4.0
Average		**19.8**	**29.1**	**119.4**
Standard deviation		8.7	16.3	97.9
Range		9.7 - 40.3	9.2 - 66.4	20.4 - 342.2
World average		**35**	**30**	**400**

Absorbed dose rates, radium equivalent activity, external and internal hazard and annual effective doses due to ^{238}U, ^{232}Th and ^{40}K in soil samples

Sample ID	School	Absorbed Dose rate ($nGyh^{-1}$)	Annual Effective dose (mSv)
AP	Abokobi Presby	35.7	0.044
AG	Agbogba Anglican	73.0	0.090
AM	Akporman Model	25.0	0.031
AS	Ashongman M/A	48.8	0.060
AH	Atomic Hills	11.3	0.014
DA	Dome Anglican	32.2	0.039
GS	GAEC Basic School	32.9	0.040
GP	GAEC Playing Ground	29.8	0.037
HC	Haatso Calvary Presby	44.7	0.055
HM	Hillview Montessori	15.3	0.019
KA	Kwabenya Atomic M/A	47.3	0.058
KW	Kwabenya M/A	12.3	0.015
TC	Taifa Community	15.4	0.019
TD	Taifa St Dominic	20.3	0.025
Average		31.7	0.039
Standard deviation		17.4	0.021
Range		11.3 – 73.0	0.014 – 0.090

APPENDIX V

MATLAB script for calculating future activity concentrations

```
function concentration
%reconstruction of radionuclides activity concentrations
for i=1:14
    initialAU(i)=input('enter initial activity of U-238:');
    initialATh(i)=input('enter initial activity of Th-232:');
    initialAK(i)=input('enter initial activity of K-40:');
    i=i+1;
%exp^-x is estimated with respect to variable time t.
%x=product of decay constant of a specific radionuclide and time.
    for i=1:1
       t(i)=input('enter time ellapsed:');
       i=i+0;
%decay constant calculated w.r.t the half-live of Ra-226, Ra-228 and K-40
       decayRa226=0.000433217;
       decayRa228=0.121604769;
       decayK40=0.000000000541521;
       xU=t*decayRa226;
       xTh=t*decayRa228;
       xK=t*decayK40;
%by using regory-Newton forward difference interpolation formula.
%decay factor of radionuclides is approximated in excel to a polynomial form.
%fourth order polynomial.
        expU=1-0.9560*xU+0.3993*(xU).^2-0.0820*(xU).^3+0.0067*(xU).^4;
        expTh=1-0.9560*xTh+0.3993*(xTh).^2-0.0820*(xTh).^3+0.0067*(xTh).^4;
        expK=1-0.9560*xK+0.3993*(xK).^2-0.0820*(xK).^3+0.0067*(xK).^4;
    end
    finalAU=initialAU*expU;
    finalATh=initialATh*expTh;
    finalAK=initialAK*expK;
end
%print reconstructed data(expected activity concentrations).
finalAU
finalATh
finalAK
```

APPENDIX VI

Predicted activity concentrations ($Bq.kg^{-1}$) in selected schools playgrounds.

Sample ID	2015			2017			2019			2021			2023			2025		
	^{238}U	^{232}Th	^{40}K	^{238}U	^{232}Th	^{40}K	^{238}U	^{232}Th	^{40}K	^{238}U	^{232}Th	^{40}K	^{238}U	^{232}Th	^{40}K	^{238}U	^{232}Th	^{40}K
AP	21.89	37.94	63.66	21.87	29.97	63.66	21.85	23.54	63.66	21.83	18.40	63.66	21.82	14.35	63.66	21.80	11.18	63.66
AG	40.35	66.36	342.21	40.31	52.42	342.21	40.28	41.17	342.21	40.25	32.18	342.21	40.21	25.09	342.21	40.18	19.56	342.21
AM	16.08	23.21	85.22	16.06	18.34	85.22	16.05	14.40	85.22	16.04	11.26	85.22	16.02	8.78	85.22	16.01	6.84	85.22
AS	26.86	41.61	269.08	26.84	32.87	269.08	26.82	25.81	269.08	26.80	20.18	269.08	26.78	15.73	269.08	26.75	12.26	269.08
AH	10.55	9.22	20.36	10.54	7.28	20.36	10.53	5.72	20.36	10.52	4.47	20.36	10.51	3.49	20.36	10.50	2.72	20.36
DA	25.52	23.92	141.97	25.50	18.90	141.97	25.48	14.84	141.97	25.46	11.60	141.97	25.44	9.05	141.97	25.42	7.05	141.97
GS	23.15	32.12	67.81	23.13	25.37	67.81	23.11	19.92	67.81	23.09	15.58	67.81	23.08	12.14	67.81	23.06	9.47	67.81
GP	17.38	28.85	103.54	17.37	22.79	103.54	17.35	17.89	103.54	17.34	13.99	103.54	17.33	10.91	103.54	17.31	8.50	103.54
HC	23.48	40.87	219.55	23.46	32.29	219.55	23.44	25.35	219.55	23.42	19.82	219.55	23.40	15.45	219.55	23.38	12.04	219.55
HM	11.52	14.76	24.37	11.51	11.66	24.37	11.50	9.16	24.37	11.49	7.16	24.37	11.49	5.58	24.37	11.48	4.35	24.37
KA	27.20	45.82	170.12	27.17	36.20	170.12	27.15	28.43	170.12	27.13	22.22	170.12	27.11	17.33	170.12	27.08	13.50	170.12
KW	9.75	9.53	47.92	9.74	7.53	47.92	9.73	5.91	47.92	9.72	4.62	47.92	9.71	3.60	47.92	9.71	2.81	47.92
TC	10.18	12.27	78.42	10.17	9.69	78.42	10.17	7.61	78.42	10.16	5.95	78.42	10.15	4.64	78.42	10.14	3.61	78.42
TD	13.74	20.57	37.34	13.73	16.25	37.34	13.72	12.76	37.34	13.71	9.98	37.34	13.70	7.78	37.34	13.69	6.06	37.34

APPENDIX VII

Preparation of calibration standards and calibration curves

Iron (Fe): Standards for the determination of Fe were prepared to a maximum concentration of 10.00 mg/L as follows:

Standard Concentration (mg/L)	Mean Absorbance
0.00	0.0000
2.00	0.1579
5.00	0.3975
10.00	0.7478

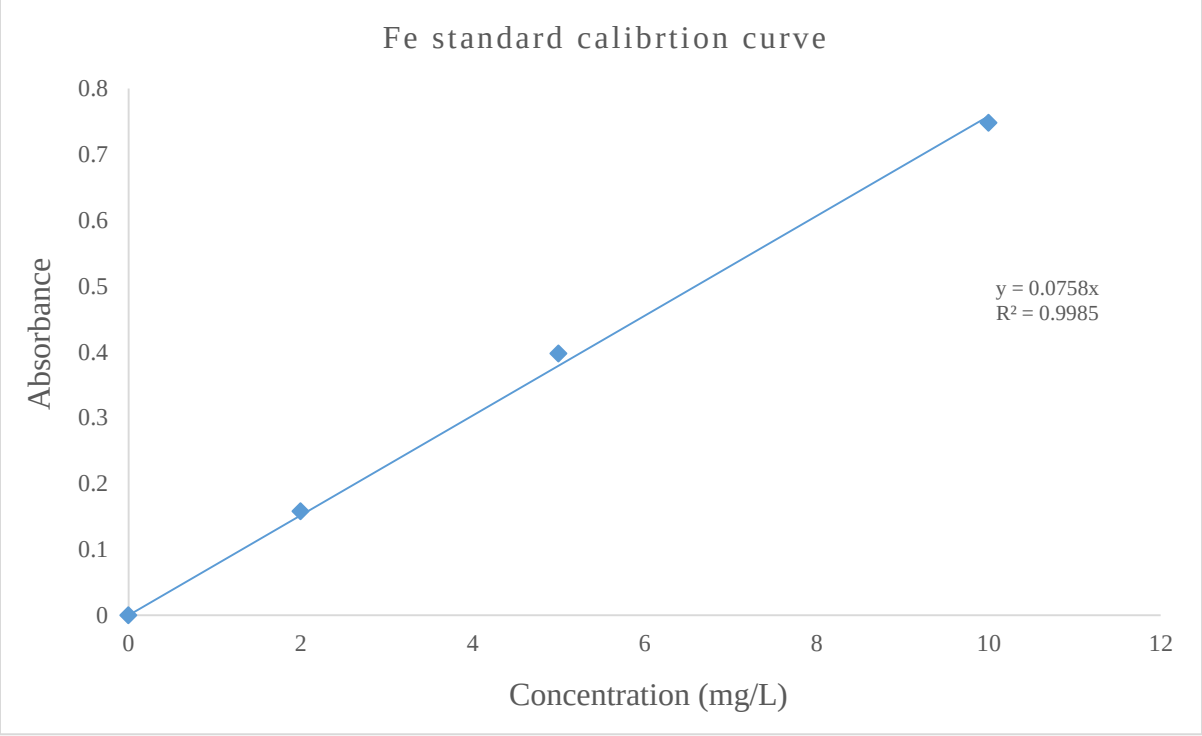

Copper (Cu): Standards for the determination of Cu were prepared to a maximum concentration of 8.000 mg/L as follows:

Standard Concentration (mg/L)	Mean Absorbance
0.000	0.0000
2.000	0.2597
5.000	0.7396
8.000	1.0889

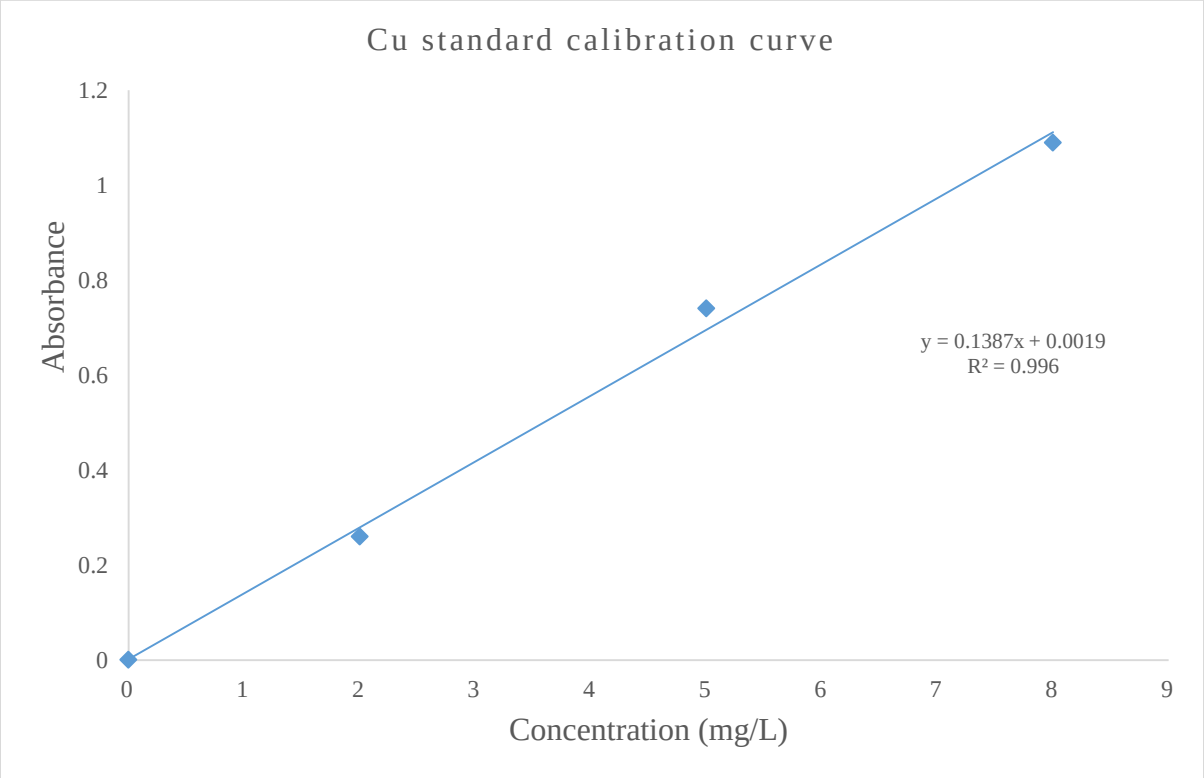

Lead (Pb): Standards for the determination of Pb were prepared to a maximum concentration of 10.0 mg/L as follows:

Standard Concentration (mg/L)	Mean Absorbance
0.0	0.0000
2.0	0.0803
5.0	0.2005
10.0	0.4011

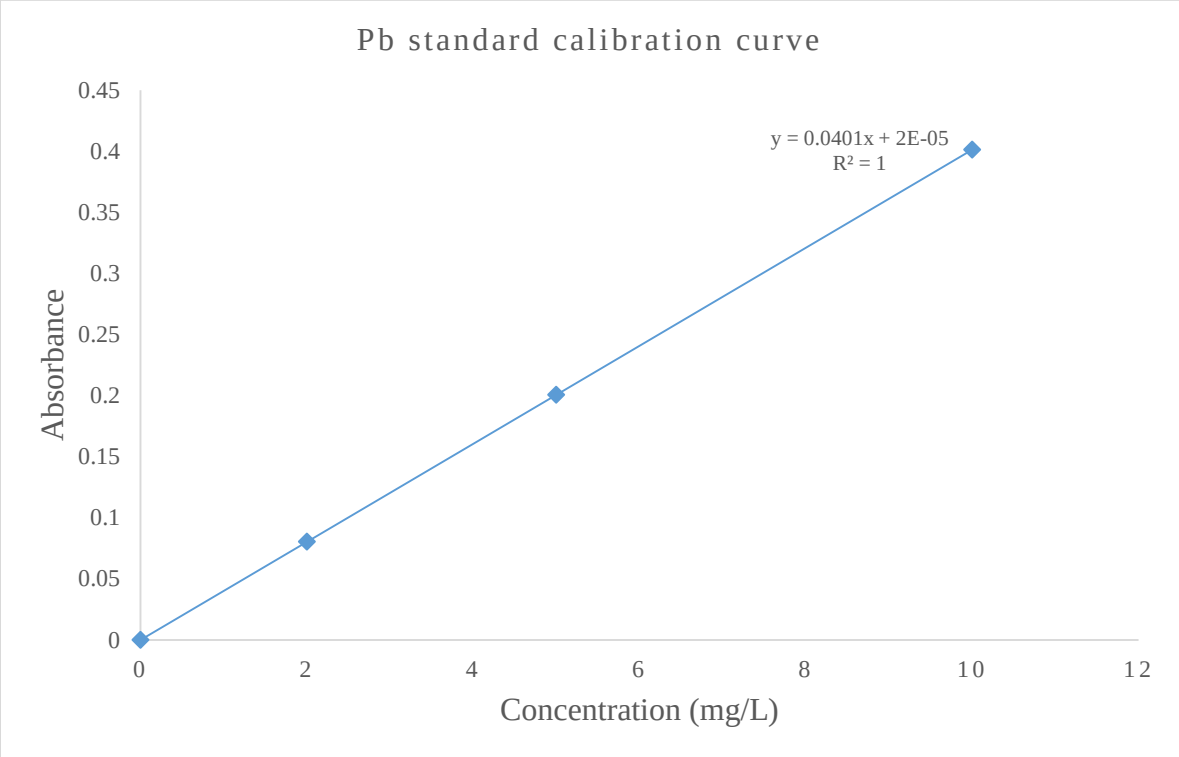

Cobalt (Co): Standards for the determination of Co were prepared to a maximum concentration of 8.000 mg/L as follows:

Standard Concentration (mg/L)	Mean Absorbance
0.000	0.0000
2.000	0.1435
5.000	0.3705
8.000	0.6019

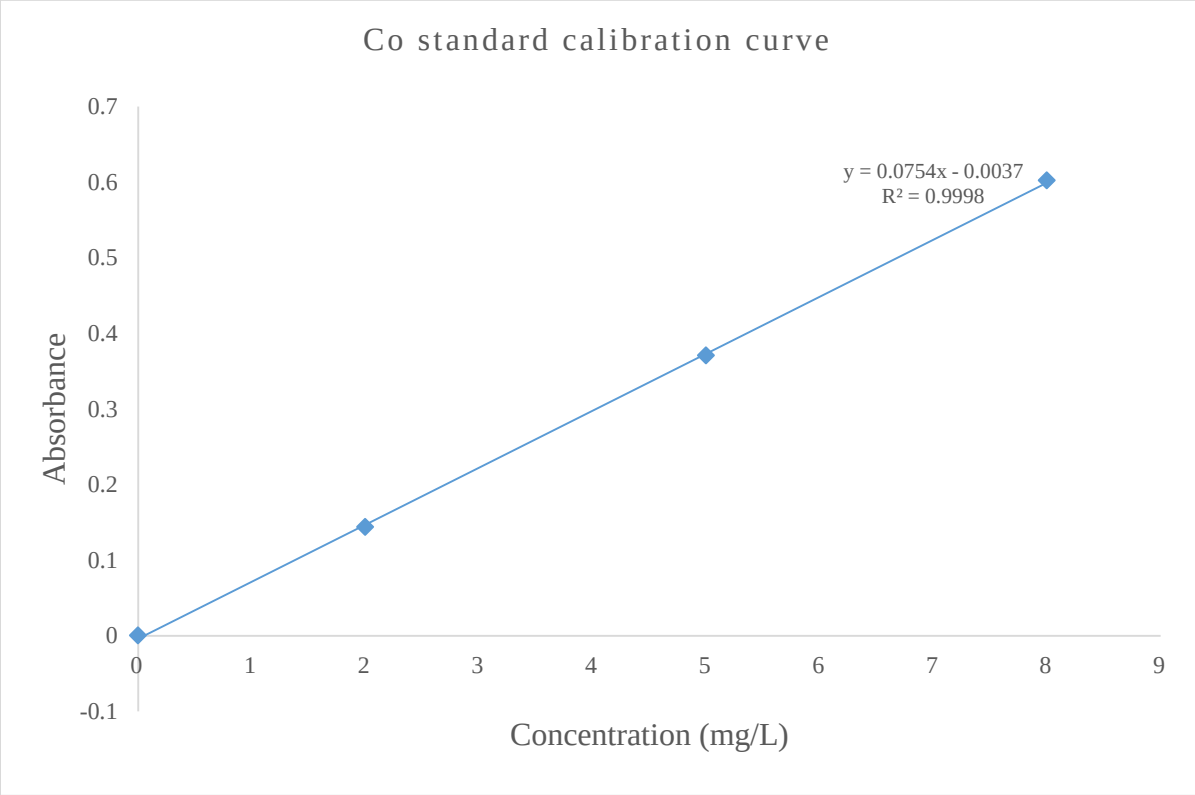

Zinc (Zn): Standards for the determination of Zn were prepared to a maximum concentration of 1.000 mg/L as follows:

Standard Concentration (mg/L)	Mean Absorbance
0.000	0.0000
0.250	0.1437
0.500	0.3213
1.000	0.6464

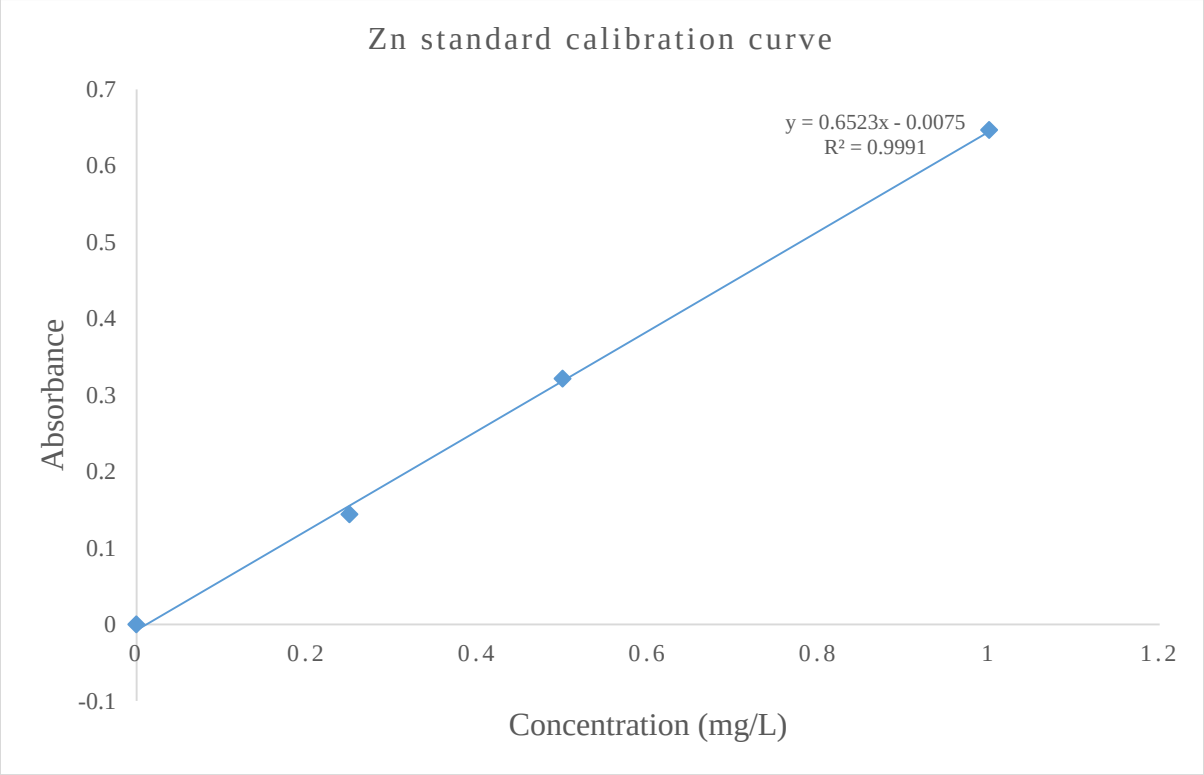

Chromium (Cr): Standards for the determination of Cr were prepared to a maximum concentration of 5.000 mg/L as follows:

Standard Concentration (mg/L)	Mean Absorbance
0.000	0.0000
1.000	0.0844
2.000	0.1679
5.000	0.4364

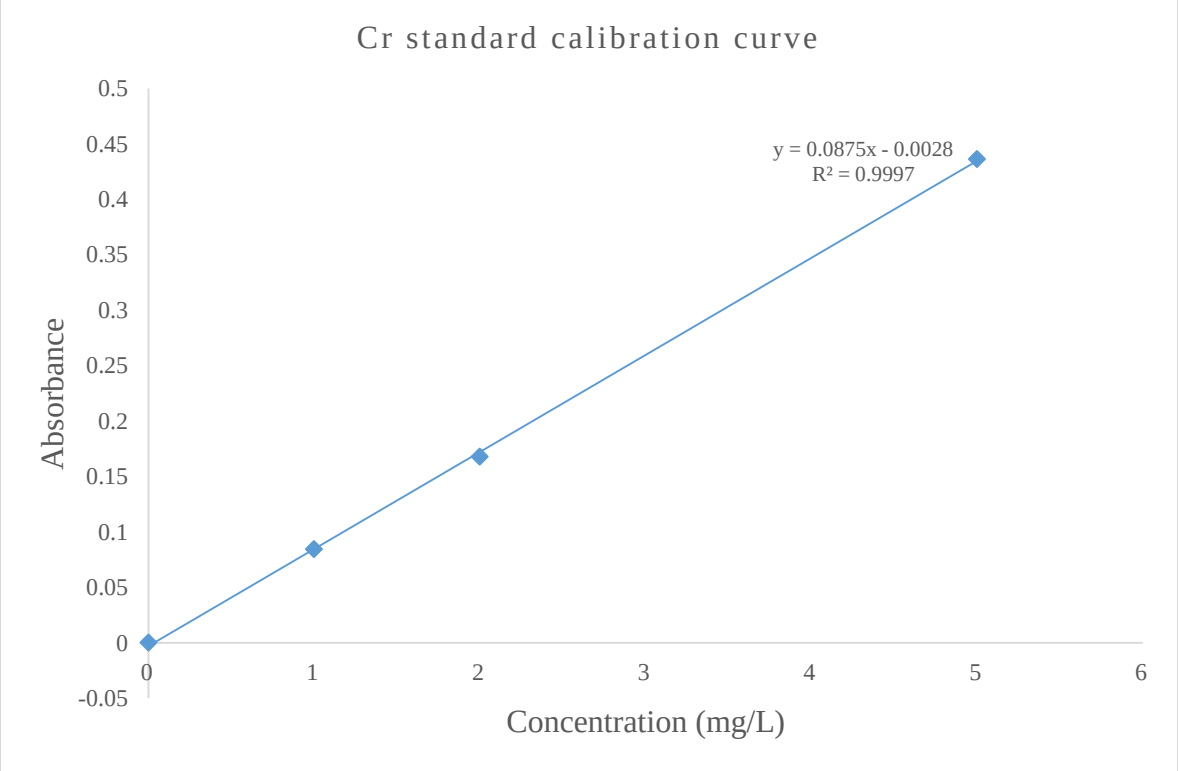

Nickel (Ni): Standards for the determination of Ni were prepared to a maximum concentration of 10.000 mg/L as follows:

Standard Concentration (mg/L)	Mean Absorbance
0.000	0.0000
2.000	0.1860
5.000	0.4625
10.000	0.9656

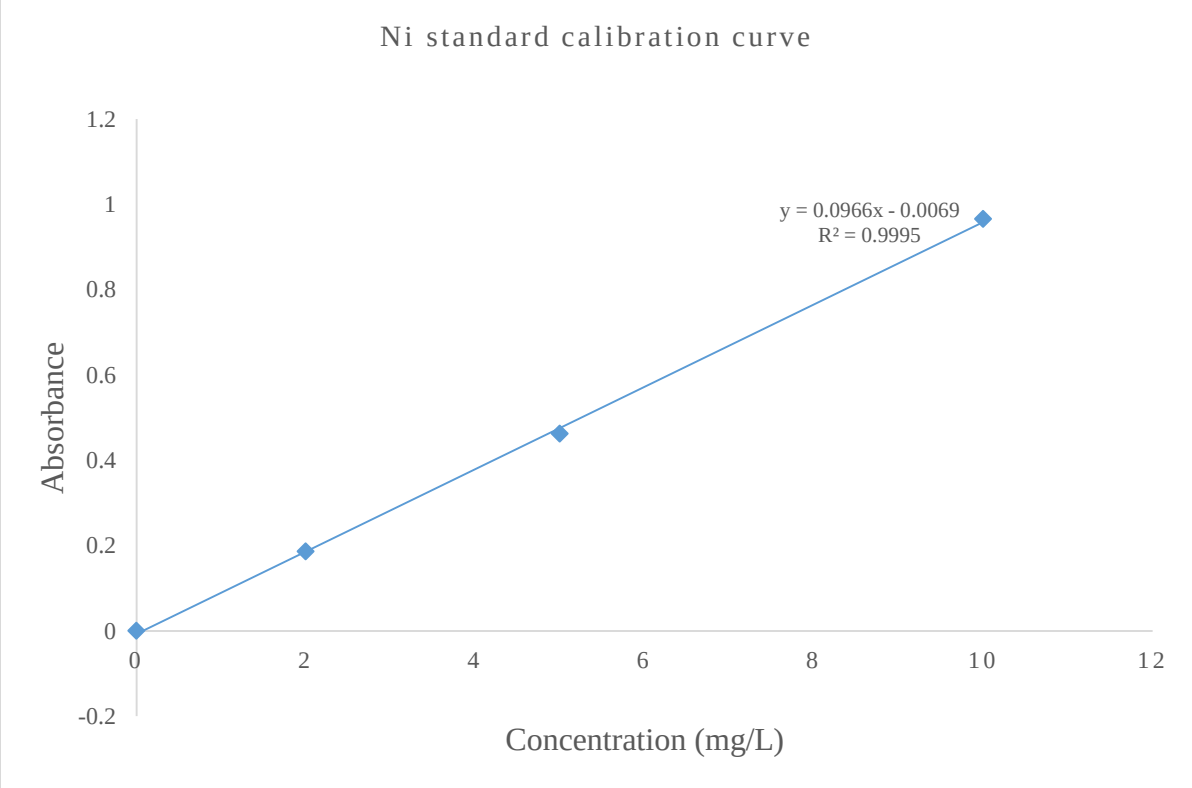

Mercury (Hg): Standards for the determination of Hg were prepared to a maximum concentration of 1.000 mg/L as follows:

Standard Concentration (mg/L)	Mean Absorbance
0.000	0.000
0.200	0.057
0.400	0.114
0.800	0.229
1.000	0.288

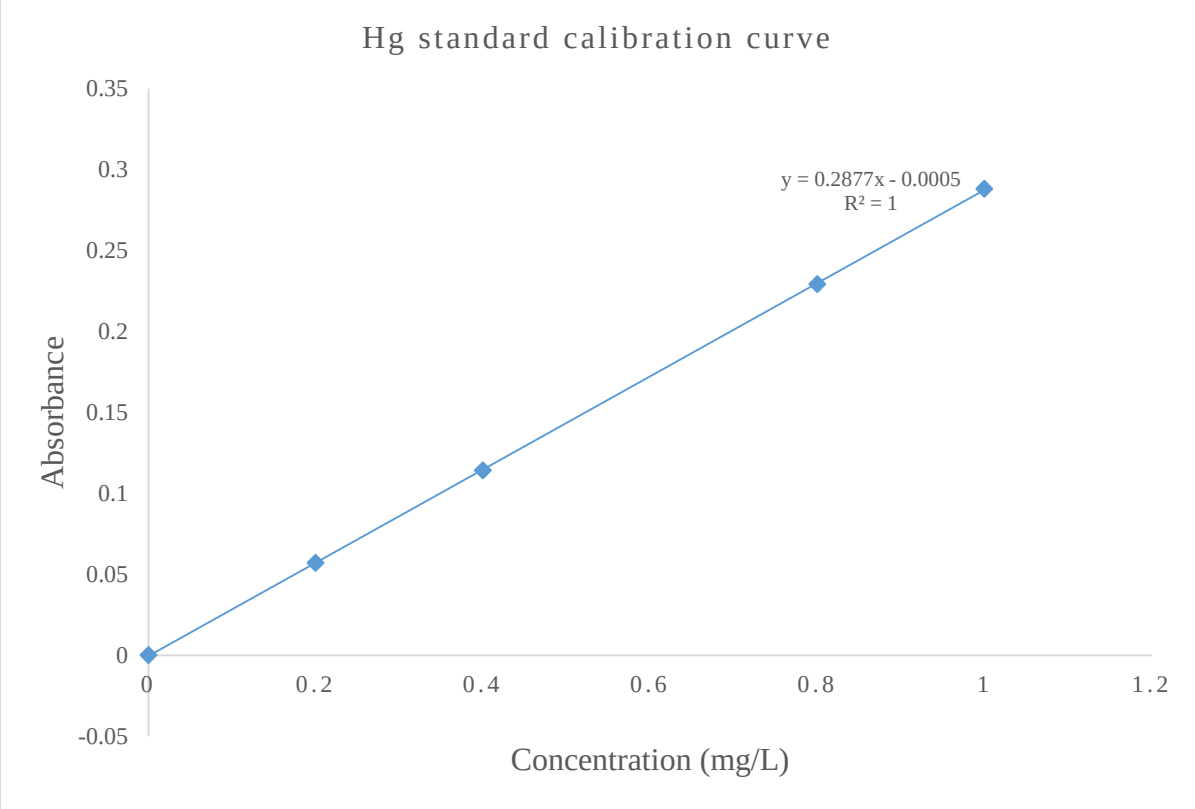

Cadmium (Cd): Standards for the determination of Cd were prepared to a maximum concentration of 3.000 mg/L as follows:

Standard Concentration (mg/L)	Mean Absorbance
0.000	0.0000
0.500	0.1589
2.000	0.6126
3.000	1.0344

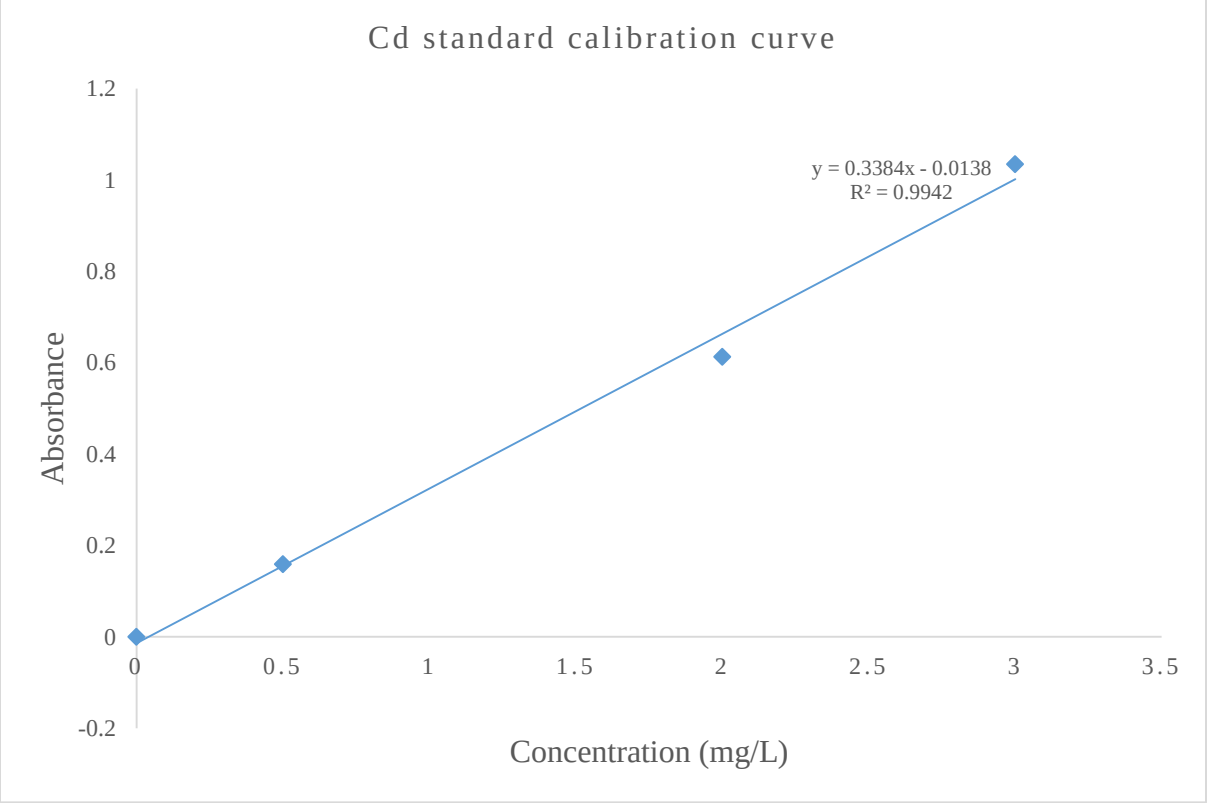

Arsenic (As): Standards for the determination of As were prepared to a maximum concentration of 0.08 mg/L as follows:

Standard Concentration (mg/l)	Mean Absorbance
0.00	0.0000
0.02	0.1070
0.04	0.2223
0.08	0.4470

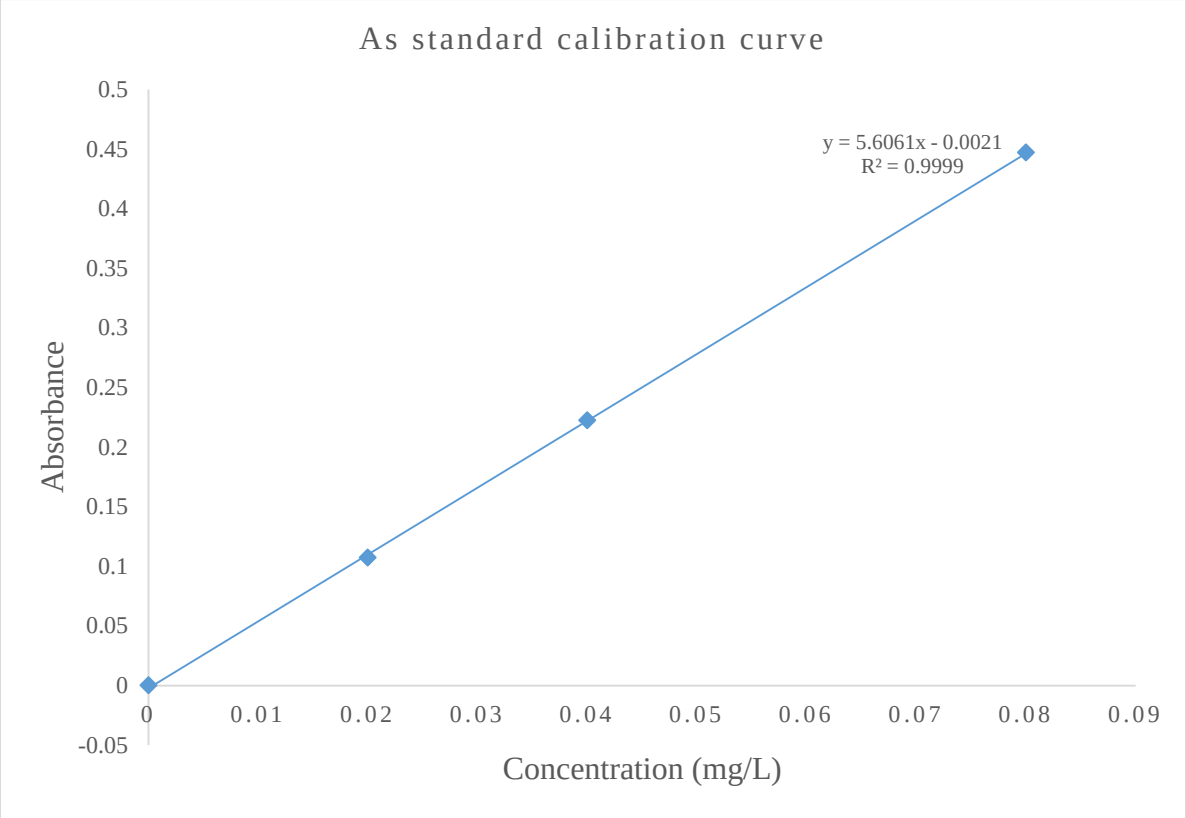

APPENDIX VIII

Procedure for computing the UCL of the mean when the underlying distribution is normal

Exhibit 1: Directions for Computing UCL for the Mean of a Normal Distribution — Student's *t*

Let $X_1, X_2, \ldots, X_n$ represent the n randomly sampled concentrations.

STEP 1: Compute the sample mean $\overline{X} = \frac{1}{n}\sum_{i=1}^{n} X_i$.

STEP 2: Compute the sample standard deviation $s = \sqrt{\frac{1}{n-1}\sum_{i=1}^{n}\left(X_i - \overline{X}\right)^2}$.

STEP 3: Use a table of quantiles of the Student's t distribution to find the $(1-\alpha)^{th}$ quantile of the Student's t distribution with n-1 degrees of freedom. For example, the value at the 0.05 level with 40 degrees of freedom is 1.684. A table of Student's t values can be found in Gilbert (1987, page 255, where the values are indexed by p=1-α, rather than α level). The t value appropriate for computing the 95% UCL can be obtained in Microsoft Excel® with the formula TINV((1-0.95)*2, n-1).

STEP 4: Compute the one-sided (1-α) upper confidence limit on the mean

$$UCL_{1-\alpha} = \overline{X} + t_{\alpha,n-1}\, s / \sqrt{n}$$

APPENDIX IV

Trace elements determined by Instrumental Neutron Activation Analysis (INAA)

		Elemental concentration (mg/kg)						
Sample ID	School	Al	K	La	Mn	Na	Ti	V
AG	Agbbogba	31080±404	14170±481	21.47±1.29	254.7±12.99	1495±17.94	2829±421	36.21±1.71
AP	Abokobi Presby	28010±221	2152±178	18.22±1.08	189.8±6.84	636.3±9.55	3010±415	75.75±1.97
AS	Ashongman M/A	30610±367	8149±415	22.28±1.27	274.7±10.44	754.4±11.32	3409±456	34.53±1.35
HC	Haatso Calvary Presby	29840±358	11290±406	22.14±1.36	239.5±9.11	1313±17.07	4957±634	31.93±1.25
AH	Atomic Hills	17240±206	975.3±73.15	9.89±0.62	107.3±7.84	417.2±5.01	3116±405	25.66±1.01
AM	Akporman Model	21305±136	3153±126	21.35±0.88	193.6±0.12	368.4±4.79	2475±1.71	40.41±0.03
DA	Dome Anglican	25770±309	6773±162	16.71±1.19	278.1±10.57	3312±1.21	3089±441	86.48±1.65
KA	Kwabenya Atomic	27860±334	7540±180	30.27±1.03	111.1±9.89	763.2±7.64	3008±406	55.01±1.44
KW	Kwabenya M/A	18730±243	1749±1.32	864±1.74	165.2±11.9	541.4±0.31	2554±375	35.87±1.8
TC	Taifa Community	22040±264	4081±163.24	8.4±0.81	230.7±9.69	1997±15	4044±525	33.13±1.13
TD	Taifa St Dominic	41150±534	1621±81.05	15.24±0.86	183.2±13.2	373.6±4.49	4851±664.59	48.98±2.21
GP	GAEC Playground	9761±126	1381±111	4.73±0.41	117.3±11.97	674.4±8.1	2173±306	32.45±1.11
GS	GAEC Basic School	12790±166	1054±113	4.32±0.45	80.45±7.81	703.4±8.45	733.9±199.63	66.89±1.68
HM	Hillview Montessori	10970±109	483.2±99.06	3.63±0.33	49.63±0.11	343.6±5.16	978±0.01	20.53±0.02

Trace elements determined by Atomic Absorption Spectroscopy (AAS)

	Elemental concentration (mg/kg)									
Sample ID	As	Cd	Cr	Co	Cu	Fe	Hg	Ni	Pb	Zn
Abokobi Pressby	3.3	< 0.002*	15.72	0.75	16.74	235606.7	0.9	17.24	11.85	162
Agbogba Anglican	3.15	< 0.002*	11.52	8.7	10.14	215758.4	0.6	19.49	< 0.001*	64.5
Akporman Model	3.27	0.225	7.17	3.3	9.54	220804.5	1.2	16.19	< 0.001*	93
Ashongman M/A	3.45	< 0.002*	44.67	7.5	22.14	249577.6	1.95	29.99	0.15	781.5
Atomic Hills	3.105	< 0.002*	9.57	12.45	8.79	226761	1.35	17.39	7.05	223.5
Dome Anglican	3.375	0.24	33.87	12.6	30.84	246530.1	2.55	31.79	< 0.001*	708
GAEC Playground	3.165	0.255	4.17	12.3	10.74	210771.6	1.65	12.74	< 0.001*	127.5
GAEC School	3.24	0.27	13.17	6.3	8.79	238139.6	1.95	10.19	< 0.001*	114
Haatso Calvary Pressby	2.04	0.225	11.97	13.5	< 0.003*	215125.1	2.25	23.09	< 0.001*	102
Hillview Montessori	1.755	0.3	3.42	5.7	11.49	204360	1.8	7.49	< 0.001*	58.5
Kwabenya Atomic	3.195	0.12	10.02	4.65	< 0.003*	235586.9	2.4	14.54	< 0.001*	150
Kwabenya M/A	3.075	0.075	6.27	6.9	< 0.003*	223396.9	1.95	8.24	< 0.001*	202.5
Taifa Community	1.695	0.06	8.37	7.05	7.44	223396.9	< 0.001*	9.14	4.8	375
Taifa St Dominic	1.62	0.225	4.77	4.8	26.94	217044.7	< 0.001*	7.34	< 0.001*	112.5

*Detection Limit